AD-A181 902 THE DESIGN OF A FOUR SQUARE GEAR TESTER FOR NOISE AND VIBRATION MEASUREME (U) PENNSYLVANIA STATE UNIV STATE COLLEGE APPLIED RESEARCH LAB S V VILANILAM ET AL 1/2

UNCLASSIFIED DEC 86 ARL/PSU/TR-87-002 F/G 14/2 NL

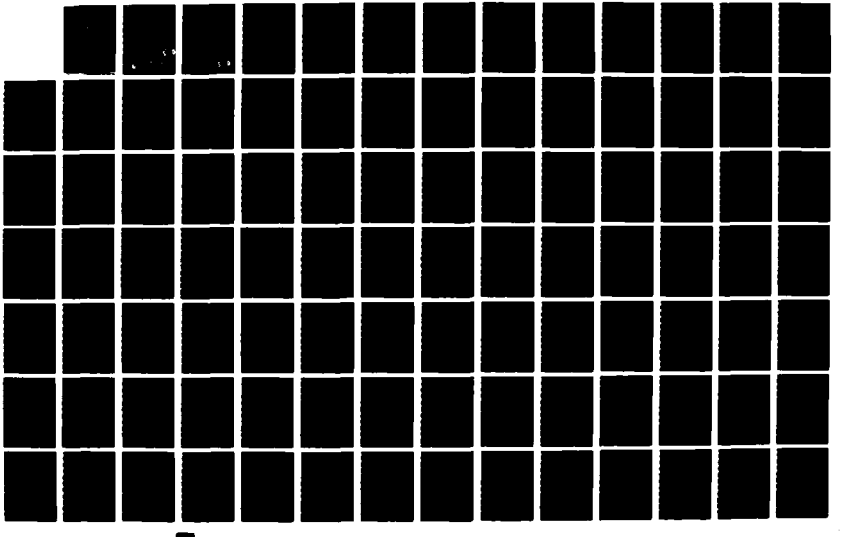

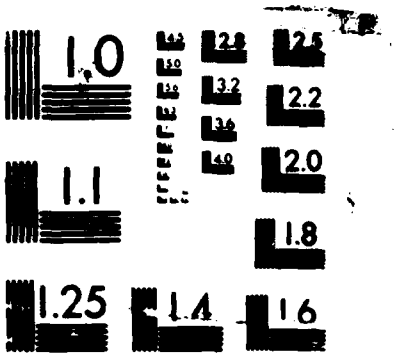

MICROCOPY RESOLUTION TEST CHART

(12)

Applied Research Laboratory

Technical Report

THE DESIGN OF A FOUR SQUARE GEAR TESTER
FOR NOISE AND VIBRATION MEASUREMENTS

by

S. V. Vilanilam, M. J. Pechersky

PENNSTATE

1855

12

The Pennsylvania State University
APPLIED RESEARCH LABORATORY
P. O. Box 30
State College, PA 16804

THE DESIGN OF A FOUR SQUARE GEAR TESTER FOR NOISE AND VIBRATION MEASUREMENTS

by

S. V. Vilanilam, M. J. Pechersky

Technical Report TR 87-002
December 1986

Supported by:
Naval Sea Systems Command

L. R. Hettche, Director
Applied Research Laboratory

Approved for public release; distribution unlimited

UNCLASSIFIED

SECURITY CLASSIFICATION OF THIS PAGE

ARL-TM-1902

REPORT DOCUMENTATION PAGE

1a. REPORT SECURITY CLASSIFICATION	1b. RESTRICTIVE MARKINGS
2a. SECURITY CLASSIFICATION AUTHORITY	3. DISTRIBUTION / AVAILABILITY OF REPORT Approved for public release; distribution unlimited.
2b. DECLASSIFICATION / DOWNGRADING SCHEDULE	
4 PERFORMING ORGANIZATION REPORT NUMBER(S)	5. MONITORING ORGANIZATION REPORT NUMBER(S)
6a NAME OF PERFORMING ORGANIZATION Applied Research Laboratory The Pennsylvania State University	6b OFFICE SYMBOL (If applicable) ARL
	7a. NAME OF MONITORING ORGANIZATION Naval Sea Systems Command Department of the Navy
6c ADDRESS (City, State, and ZIP Code) P. O. Box 30 State College, PA 16804	7b. ADDRESS (City, State, and ZIP Code) Washington, DC 20362
8a. NAME OF FUNDING / SPONSORING ORGANIZATION Naval Sea Systems Command	8b. OFFICE SYMBOL (If applicable) NAVSEA
	9. PROCUREMENT INSTRUMENT IDENTIFICATION NUMBER
8c ADDRESS (City, State, and ZIP Code) Department of the Navy Washington, DC 20362	10. SOURCE OF FUNDING NUMBERS PROGRAM ELEMENT NO. / PROJECT NO. / TASK NO. / WORK UNIT ACCESSION NO.

11 TITLE (Include Security Classification)
The Design of a Four Square Gear Tester for Noise and Vibration Measurements

12 PERSONAL AUTHOR(S)
Santosh V. Vilanilam

13a TYPE OF REPORT	13b. TIME COVERED	14. DATE OF REPORT (Year, Month, Day)	15. PAGE COUNT
M.S. Thesis	FROM _____ TO _____	December 1986	161

16 SUPPLEMENTARY NOTATION

17 COSATI CODES			18. SUBJECT TERMS (Continue on reverse if necessary and identify by block number)
FIELD	GROUP	SUB-GROUP	four square, gear tester, noise, spur gears, vibration

19 ABSTRACT (Continue on reverse if necessary and identify by block number)

The following report provides the design procedures for a Four Square Gear Tester. The primary purpose of the tester is to investigate noise generation in spur gears that result from two major sources: 1) Dynamic Loads and 2) Fluid Dynamics.

The tester is designed to operate at 9000 rev/min with an applied shaft load of 301.11 in-lbs. The design includes mechanical components, such as:

1) A dc shunt-wound electric motor (with SCR) which will allow testing to be performed over wide range of loading as well as speed,

2) A speed increasing mechanism consisting of pulleys and V-belts to provide the desired range of speed and torque,

20 DISTRIBUTION / AVAILABILITY OF ABSTRACT	21. ABSTRACT SECURITY CLASSIFICATION
☒ UNCLASSIFIED/UNLIMITED ☐ SAME AS RPT. ☐ DTIC USERS	Unclassified
22a NAME OF RESPONSIBLE INDIVIDUAL	22b. TELEPHONE (Include Area Code) 814/865-6344 / 22c. OFFICE SYMBOL

DD FORM 1473, 84 MAR 83 APR edition may be used until exhausted. All other editions are obsolete.

SECURITY CLASSIFICATION OF THIS PAGE
UNCLASSIFIED

3) Air bearings which are intended to minimize extraneous vibrations and provide good shaft alignment,

4) Flexible shaft couplings, with a low degree of dynamic imbalance and bending force transmission, to accomodate both angular and parallel shaft misalignment,

5) Gear mounts, also with low dynamic imbalance and with the required torque rating, to fasten the gears to the shaft; and

6) Precision ground steel shafts which will provide center-to-center accuracy and therefore minimize vibration.

In addition a pressure-spray lubrication system was also selected to cool and lubricate the mating gear teeth. In order to measure the gear noise and vibration, an instrument system consisting of:

1) A high precision tachometer-generator for recording shaft speed,

2) An accelerometer to measure shaft vibrations,

3) A hydrophone to measure the gear noise; and

4) Strain rosettes coupled with a slip ring to measure shaft torsional strain and bending.

was selected. The report also proposes the use of non-intrusive electro-optical techniques to measure both vibration and hydrodynamic sources of gear noise.

ABSTRACT

The following report provides the design procedures for a Four Square Gear Tester. The primary purpose of the tester is to investigate noise generation in spur gears that result from two major sources: 1) Dynamic Loads and 2) Fluid Dynamics.

The tester is designed to operate at 9000 rev/min with an applied shaft load of 301.11 in-lbs. The design includes mechanical components, such as:

1) A dc shunt-wound electric motor (with SCR) which will allow testing to be performed over wide range of loading as well as speed,

2) A speed increasing mechanism consisting of pulleys and V-belts to provide the desired range of speed and torque,

3) Air bearings which are intended to minimize extraneous vibrations and provide good shaft alignment,

4) Flexible shaft couplings, with a low degree of dynamic imbalance and bending force transmission, to accommodate both angular and parallel shaft misalignment,

5) Gear mounts, also with low dynamic imbalance and with the required torque rating, to fasten the gears to the shaft; and

6) Precision ground steel shafts which will provide center-to-center accuracy and therefore minimize vibration.

In addition a pressure-spray lubrication system was also selected to cool and lubricate the mating gear teeth. In order to measure the gear noise and vibration, an instrumentation system consisting of:

1) A high precision tachometer-generator for recording shaft speed,

2) An accelerometer to measure shaft vibrations,

3) A hydrophone to measure the gear noise; and

4) Strain rosettes coupled with a slip ring to measure shaft torsional strain and bending.

was selected. The report also proposes the use of non-intrusive electro-optical techniques to measure both vibration and hydrodynamic sources of gear noise.

TABLE OF CONTENTS

LIST OF TABLES

LIST OF FIGURES

ACKNOWLEDGMENTS

The author is grateful to his advisor, Dr. Martin Pechersky, for his guidance during the course of this project. The independence and responsibility he has given me, have enabled me to achieve more than I would have thought possible.

Appreciation is expressed to Mr. Ravi Venkatesan for his advice and support through some of the more difficult stages of this project. The author also wishes to thank Mr. Vijay Agarwal and Dr. Akhlesh Lakhtakia for their encouragement and advice during the course of this research.

Finally, the author would like to thank Ms. Gladys Marshall for her skillful typing of the manuscript and for her patience in handling the numerous additions and corrections.

1.0. INTRODUCTION

The following report presents the design of a Four Square Gear Tester and describes the procedures used in the design. The primary purpose of the tester is to investigate noise generation in spur gears that result from two major sources: 1) dynamic forces arising from basic gear geometry and loading (structural dynamics), and 2) pressure and flow fields surrounding the mesh region (fluid dynamics). The test conditions are the following:

1. 31 teeth meshing with 31 teeth
2. 8.5 diametral pitch
3. maximum torque on shaft: 301.11 in-lbs
4. shaft speed: 9000 rpm

when the testing pitch line velocity is 8593.127 fpm and the intensity of tooth loading or K factor is 67.87 psi. The report also contains:

- A brief discussion of gear noise and sources of gear noise,
- A critique of other available methods of testing gears under load,
- The basis for the method selected for gear testing,
- A description of the selected mechanical components and the basis for their selection,
- A description of the selected lubrication system and the basis for its selection,
- A description of the selected standard instrumentation (acoustic, strain, and acceleration) and the basis for their selection,
- A brief discussion of the possible non-intrusive electrooptical (EO) techniques that can be employed to measure both vibration and flow sources of gear noise,

- The mechanical design of the Four Square Gear Tester which includes assembly drawings, and
- A list of equipment along with the cost of the components.

1.1 Gear Noise and Sources of Gear Noise

The subject of gear noise has been a major area of concern for many decades both from an environmental safety point of view and for improving machinery performance. A large component of machinery noise results from the structural vibrations set up as a result of the meshing action of gears. This noise is either tonal or repetitively pulsed and therefore is easily discernible in the area surrounding a particular machine. This noise field can be very unhealthful. The noise signature may also give an indication of excessive wear and imminent failure of machinery components. Figure 1.1 shows the typical noise characteristics of meshing spur gears.

It is obvious from the upper portion of the figure that gear noise occurs primarily in frequency bands that are multiples of the tooth mesh frequency. The lower portion of the figure shows a plot of the output as a function of speed for the total A weighted spectrum and the first two tooth meshing components. Note that the output should be increased by 26 dB to relate it to one micropascal. The white noise or ghost component of the spectrum is thought to result from the tooth surface imperfections created during the gear forming process [1,2]. Hence, it is clear from Figure 1.1 that meshing spur gears operating at fairly high speeds have an intense noise signature with a highly structured spectrum.

The two most important mechanisms involved in the generation of gear noise and vibration are: 1) Dynamic Loads, and 2) Fluid Dynamics. The dynamic effects on gears are due to such factors as:

- load sharing and sliding of gear teeth
- tooth to tooth geometric variability of a given gear

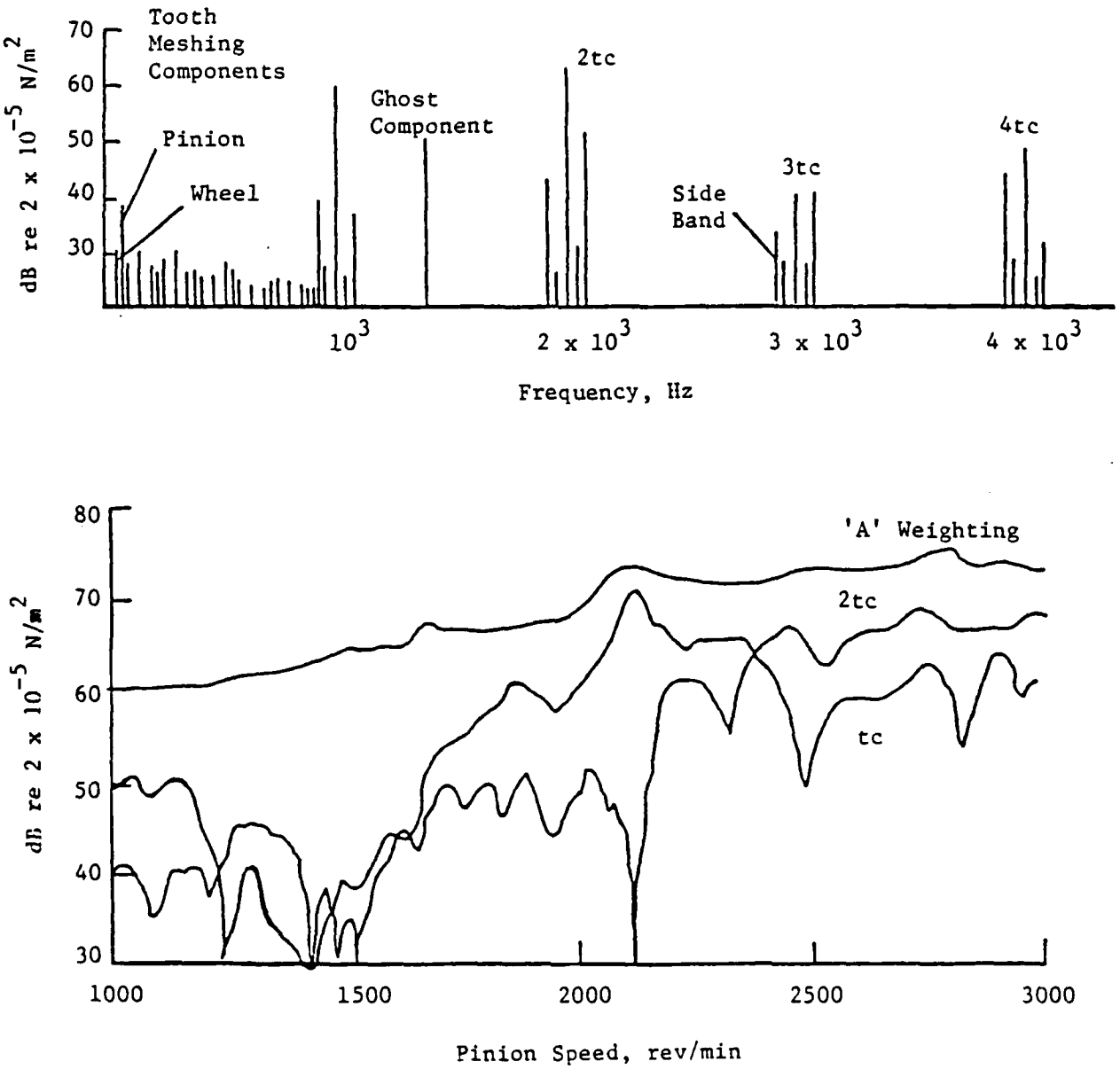

Figure 1.1 Gear Noise Characteristics (Greeves, 1974)

- damping characteristics of the gear material

- machining errors such as:
  - tooth profile error
  - pitch circle run-out
  - lead angle error
  - tooth spacing error

- assembly errors such as:
  - improper mounting of the gears
  - angular shaft misalignment
  - properties of the lubricating oil

These factors set up tooth and gear body vibrations which are transmitted to the gear box via gear shafts and bearings and through airborne radiation. The related noise is subsequently radiated to the surroundings by the gear case. At this point, it is important to realize that the original vibrations which set up the acoustic field in the first place are often masked by the structural dynamics (i.e., transfer function) of the gear case and its mounts [1].

The instantaneous dynamic tooth forces that develop due to load sharing alone is shown in Figure 1.2. Curve a-b-c is the initial loading curve that results in an acceleration and deformation of the driven gears. If the acceleration force is large enough, tooth separation can occur (line c-d). When the teeth regain contact there is a sudden increase in force due to impact (W_d). The force curve then drops to the average load (line f-g) and is further decreased as the teeth disengage [1,3]. Hence, it is this complex variation of force with time that leads to gear body vibration. The dynamic situation is further complicated when factors such as tooth to tooth geometric variability, damping characteristics of the gear material, . . ., etc., are taken into consideration.

The one noise source which has been largely ignored but which is of significant importance is flow-induced noise. Flow-induced noise results

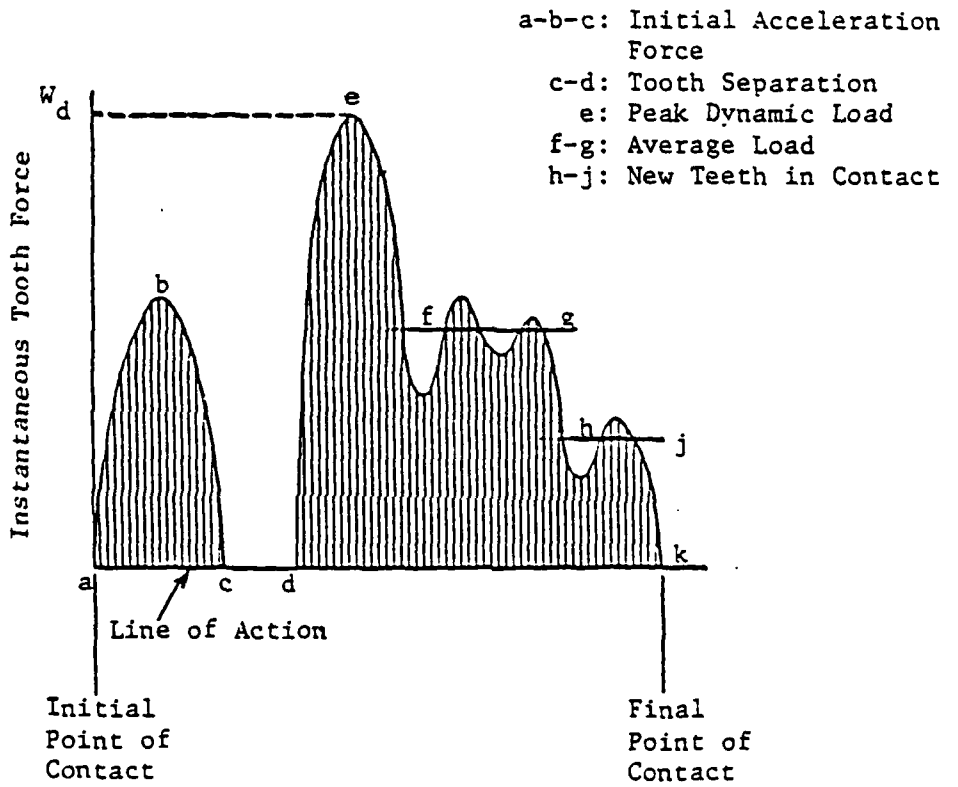

Figure 1.2 Dynamic Force on Tooth Pair During Engagement (Shigley, 1963)

from the compression of the air and oil mixture trapped between the meshing gear teeth. This type of noise source is especially found in high-speed, wide-face, spur gears where the air and oil mixture must travel a relatively large distance in a short period of time [1]. Ignoring the effects of compressibility of the trapped gas, Mach numbers in excess of 0.9 have been attained by past investigators for a pitch line velocity of 4720 fpm [1,4]. If compressibility is considered, a much more complicated situation results. The complexity arises from the build up of shock waves in the intra-tooth region. Shock waves result as the pressure in this region rises above the critical pressure (the critical pressure of air at room temperature is 29 psi). And, if the meshing rate is fast enough a shock tube effect may also be present in which the shock and rarefaction waves are radiated from the intra-tooth region to the gear casing [1].

It is readily apparent from the above discussion that the study of gear noise and vibration does not lend itself to simple analysis. Much of the research done in the past has been of an empirical nature. That is, certain modifications to the gear box transmission are made, and acoustic measurements are compared with similar measurements on an unmodified transmission [1]. Another type of empirical study has been to introduce known errors onto the gear set and measure changes in the acoustic signal as has been done by Yuruzume, Mizutani, and Tsubuku of the Mechanical Engineering Laboratory of Japan. In their study, five kinds of tooth profile errors such as convex, concave, and wavelike, were formed on spur gears by grinding. They found that test gears having concave tooth profile errors contained many harmonics. In particular, it was found that sound levels at the second, third, and fourth harmonics were high [1,5].

While fundamental analytical approaches can be taken, they can only be related indirectly to experimental conditions through acoustic and indirect dynamic measurements. Furthermore, an analytical model may not be sufficiently thorough and complete to account for all the factors affecting the computed data.

As of today there has been no experimental work concerning the gas dynamic effects related to gear noise. A continuing problem has been the difficulty in performing direct measurements of the vibrations which are the ultimate sources of gear noise. With the advent of lasers and other modern electrooptical techniques, it now appears possible to perform direct measurements concerning both the structural and fluid dynamic effects related to gear noise. For instance, an inexpensive laser vibrometer can be used to measure the local velocity of any point on the gear. Speckle Interferometry can be used to study the vibration of the gear set due to the dynamic forces arising from the basic gear geometry and loading; and Laser Doppler Velocimetry (LDV) can be used to characterize the flow fields surrounding the gear, particularly near the gear mesh region [1]. Section 1.3 provides a summary of the possible EO techniques that are being considered. This section also provides a list of selected acoustic, strain, and acceleration instrumentation.

1.2. Methods of Testing Gears Under Load

This section will present the two set-ups most often used to study gear noise and vibration, namely: 1) The standard gear noise testing machine which requires a dynamometer to load the gears, and 2) The Four Square Gear Tester. Section 1.2.1 will describe the standard testing machine; Section 1.2.2 provides the advantages of using the Four Square

Method; and Section 2.2.1 provides a general description of the Four Square Gear Tester.

1.2.1. The Standard Gear Testing Machine

The standard gear testing machine requires a large dynamometer to load the gears. A similar machine was used by Yuruzume, Mizutani, and Tsubuku to study transmission errors and noise of spur gears having uneven tooth profiles. As shown in Figure 1.3, a motor drives the test gears through an intermediate flywheel which stabilizes the rotation of the test gears. An electric dynamometer loads the master gear through another flywheel. This flywheel eliminates the influence of the dynamometer on the transmission to the gears. The test section is placed in an anechoic chamber and covered with glass wool to reduce or eliminate noise and vibration that are not under investigation. The microphone measuring the noise is mounted on a spring and placed at a distance of eight inches from the test gears [5].

This type of machine is not only very expensive but can be highly inaccurate. The dynamic imbalance of the large flywheels could cause dynamic tooth loads to such an extent that premature failure of the gears is unavoidable. The imbalance could also be the source of extraneous noise and vibration.

Unlike the standard gear testing machine, the Four Square Gear Tester is highly accurate due to the simplicity of the four square arrangement. The gears are loaded by means of a split coupling and driven by a variable speed electric motor. An automatic and continuous pressure-spray lubrication system cools and lubricates the mating teeth surfaces. The test section is acoustically and vibrationally isolated

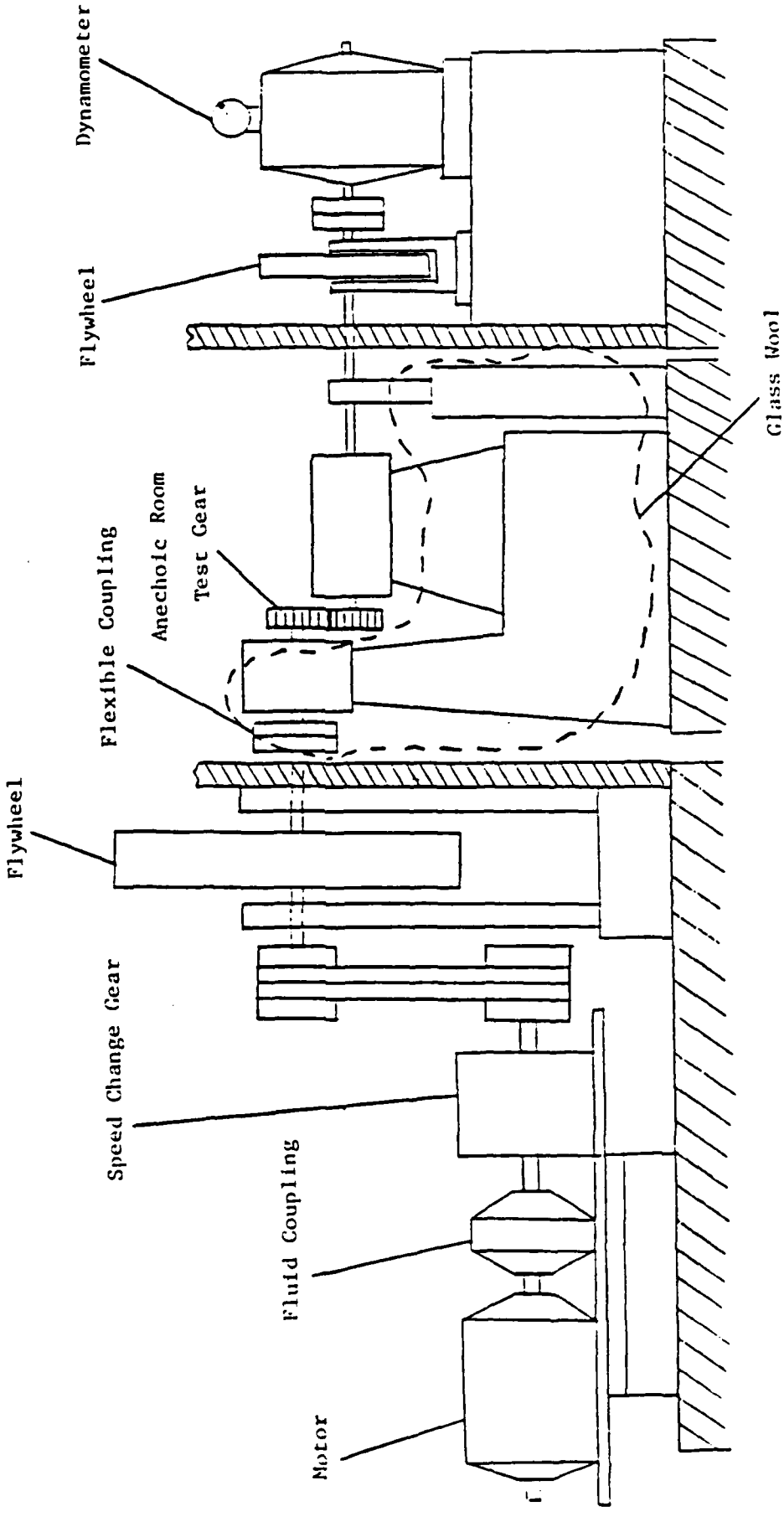

Figure 1.3 The Transmission Layout for Gear Noise Tests (Using a Dynamometer to Load the Gears) (Yuruzume, 1979)

from the drive section via an acoustic barrier, shaft seals, and flexible shaft couplings. And, air bearings keep extraneous noise and vibration to a minimum.

Strain rosettes and a slip ring are mounted on one of the test section shafts to measure the shaft torsional strain. These rosettes are also capable of measuring shaft bending. Hydrophones and accelerometers measure the gear noise and shock and vibration of the system, respectively.

1.2.2. The Four Square Gear Tester

The Four Square Method of testing gears was selected for the following primary reasons:

- Accuracy:
  Due to the simplicity of the four square arrangement it is possible to construct such a device with a high degree of accuracy, thereby reducing or eliminating extraneous noise and vibration [1].

- Economical:
  The power source need only overcome the frictional losses in the set-up and therefore a small size motor can be employed to drive the gears. In addition, the gears are loaded by means of a split coupling (torque flanges) hence, eliminating the need for a large and expensive dynamometer.

- Efficiency:
  The power transmitted by the gear box is effectively recirculated.

1.3. Instrumentation

A recurring problem with experimental work has been the difficulty in performing direct measurement of gear noise and vibration. We propose to measure both the vibration and flow sources of gear noise using modern electrooptical techniques coupled with the standard acoustic, strain, and

acceleration instruments. The selected standard instruments are the following:

1) **Strain Rosettes and a Slip Ring:** To measure shaft torsional strain and bending.

2) **Accelerometer:** To measure shock and vibration of the system.

3) **High Precision Tachometer:** To monitor shaft velocity.

4) **Hydrophone:** To measure the gear noise.

The possible EO techniques that can be employed to investigate gear vibrations due to structural and fluid dynamics are the following:

1) **Speckle Interferometery:** A whole field measuring technique for structural dynamics that allows for the measurement of gear body deformations (in the plane of the gear) that result from the time varying tooth loads in the basic gear geometry and machining errors such as tooth profile error, pitch circle runout, and tooth spacing error [1].

2) **Laser Vibrometry:** A point to point measuring technique for structural dynamics. It is a non-intrusive measuring technique to study gear noise due to dynamic forces arising from basic gear geometry and loading.

3) **Laser Inferoferometry.** A whole field measuring technique that can be used to characterize the flow field surrounding the gear mesh. In particular, a Mach Zehnder interferometer can measure the mass density field in a plane parallel to the axis of gear rotation and detect the presence of shock waves [1].

4) **Laser Doppler Velocimetry (LDV)/Laser Doppler Anamometry (LDA):** This is a technique for point-to-point measurement of fluid velocity. It is non-intrusive and can be used to measure the velocity of air and oil mixture escaping from the mesh region.

2.0. DESIGN OF THE FOUR SQUARE GEAR TESTER

This section will describe the mechanical design of the Four Square Gear Tester. Also included in this section are: 1) Design of the test and drive gears and their mechanical and thermal properties, 2) A general description and layout of the tester, 3) Description of the selected mechanical components, such as, the motor, pulleys, bearings, gear mounts, couplings, and shafts, and their basis of selection, and 4) Description of the selected lubrication system, and the basis of its selection.

2.1. Gear Design

The symbols defined below are used in the calculations for this section.

A	exposed surface area of gear case $A = 2.977\ ft^2$
b	gear face width $b = 1.333$ in
C_f	surface condition factor $C_f = 1.0$ [6]
C_H	hardness ratio factor $C_H = 1.0$ [6]
C_L	life factor $C_L = 1.0$ [6]
C_m	load distribution factor $C_m = 2.5$ [6]
C_O	over load factor $C_O = 1.01$ [6]
C_P	elastic properties coefficient $C_P = 2300$ [6]

C_R safety factor
$C_R = 1.25$ [6]

C_S size factor
$C_S = 1.0$ [6]

C_T temperature factor
$C_T = 1.0$ [6]

C_V dynamic factor
$C_V = 0.70$ [6]

C_1 standard center distance
$C_1 = 3.6471$ in

C_2 non-standard center distance

d pitch diameter
$d = 3.6471$ in

D gear diameter
$D = 3.883$ in

E Youngs Modulus of Steel
$E = 30 \times 10^6$ psi

f average coefficient of friction
$f = 0.038$

F_b allowable load based on bending

F_d dynamic tooth load

F_n tooth load
$F_n = 177.94$ lbs (see Low Friction Bearings)

F_t tangential load on gear tooth
$F_t = 164.98$ lbs (see Low Friction Bearings)

F_w wear load that arises from compressive stresses between meshing gear teeth

h_p horsepower

I geometry factor
$I = 0.85$ [6]

K_ℓ an approximate wear load factor
$K_\ell = 300$ [6]

L length of beam or the whole depth of the gear tooth
$L = 0.2647$ in

M_G gear teeth ratio
$M_G = 1$ [6]

N — number of teeth
$N = 31$

n — gear speed
$n = 9000$ rpm

P — diametral pitch
$P = 8.5$ teeth/in

Q — temperature rise of gear case

r_o — outside radius
$r_o = 1.9415$ in

r — pitch radius
$r = 1.8235$ in

S_{ac} — allowable contact stress number
$S_{ac} = 145{,}000$ psi [6]

t_1 — estimated operating temperature of the gear set (with oil cooling)
$t_1 = 250°F$

t_2 — initial temperature of gear set
$t_2 = 80°F$

T — arc tooth thickness at pitch radius
$T = 0.1831$ in

U_L — unit load (psi)

V_P — pitch line velocity

Y — Lewis form factor
$Y = 0.611$ [6]

σ_b — an approximate bending stress of 9310 steel
$\sigma_b = 32{,}000$ psi [9]

σ_c — calculated contact stress number (psi)

ϕ — pressure angle
$\phi = 22$ degrees

ϕ_1 — pressure angle at pitch radius

ϕ_2 — pressure angle at meshing position

δ — tooth expansion

α — coefficient of linear thermal expansion of 9310 steel
$\alpha = 6.5 \times 10^{-6}/°F$ [8]

The test and drive gears used in our study are typical of high speed turbomachinery gears. Both the test and drive gears are 9310 steel spur gears of the same size. The gear drawing is shown in Figure 2.1. The basic dimensions and other pertinent data of the gears are given below (Table 2.1).

Table 2.1. Test and Drive Gear Data (Dimensions in Inches).

pitch diameter	3.6471	base circle diameter	3.3815
number of teeth	31	diametral pitch	8.50 teeth/inch
pressure angle	22°	finished circular	0.1831
face width	1.3330	tooth thickness (honed)	0.1821
outside diameter	3.8830	tooth circle diameter	3.3510 3.3450
circular pitch	0.3696	root radius	0.0570

Approximate values for the working depth, whole depth, and clearance of the gears are calculated below. The working depth is the depth of the engagement of two gears, that is, the sum of their addendums. The working depth is given by [6]

$$\text{working depth} = \frac{2}{P} = \frac{2}{8.5} = 0.2353 \text{ in.}$$

The whole depth is the total depth of a tooth space, and is equal to the addendum plus dedendum. The whole depth is given by [6]

$$\text{whole depth} = \frac{2.25}{P} = \frac{2.25}{8.5} = 0.2647 \text{ in.}$$

The clearance of a given gear is the amount by which the dedendum exceeds the addendum of its mating gear. The clearance is given by [6]

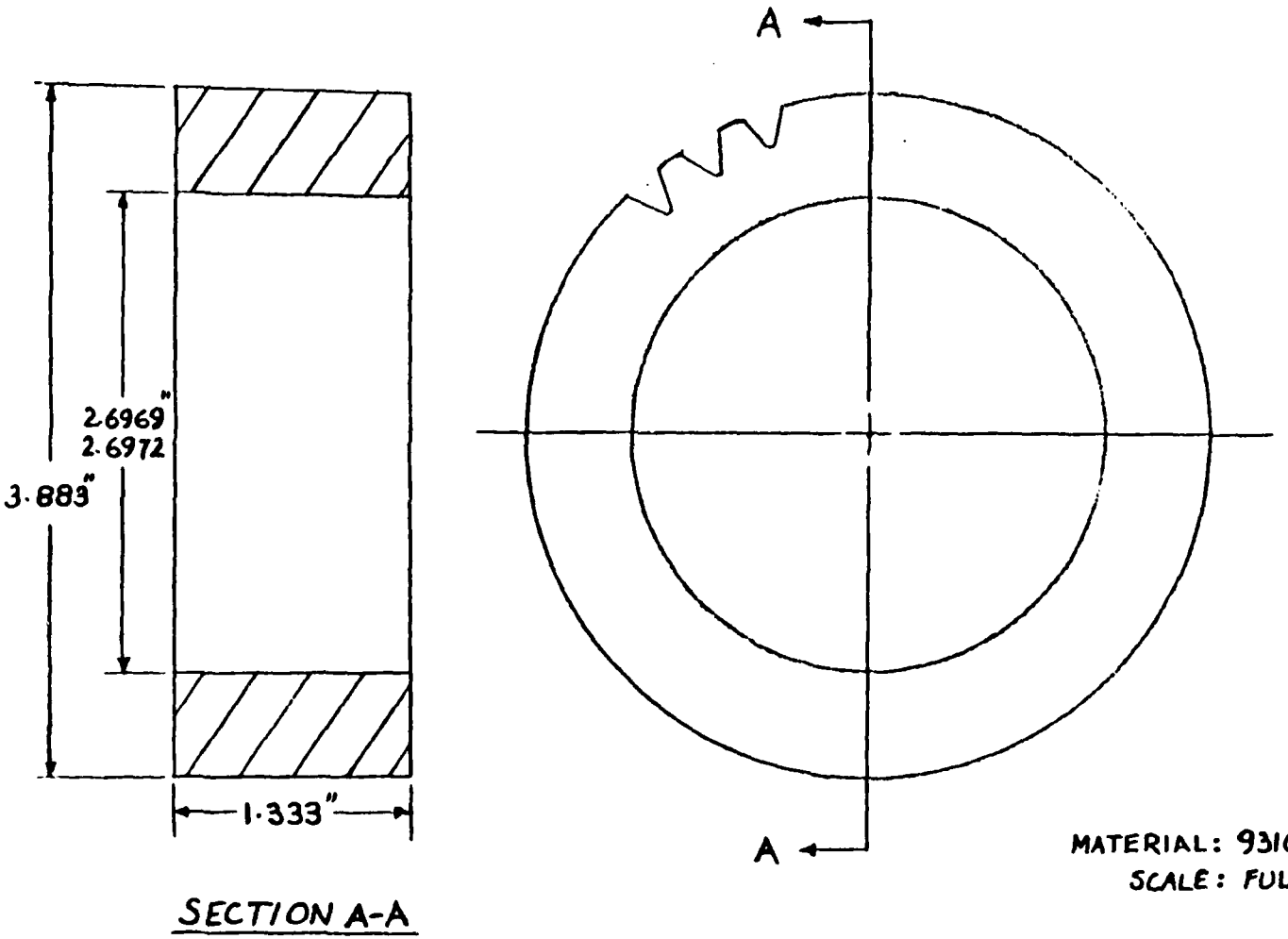

Figure 2.1 Test and Drive Gear

$$\text{clearance} = \frac{0.25}{P} = \frac{0.25}{8.5} = 0.02941 \text{ in}$$

The mechanical properties and the chemical composition of 9310 steel are given in Tables 2.2 and 2.3, respectively.

Table 2.2. Mechanical Properties of AISI E9310 Steel [7].

Tensile Strength (psi)	Yield Strength (psi)	Elongation in 2 inches (%)	Reduction in Area (%)	Hardness BHN
174,500	139,000	15.3	62.1	363

The coefficient of linear thermal expansion, thermal conductivity, Youngs modulus, and density of E9310 steel are 11 x 10^{-6}/°C, 21.791 BTU/hr-ft °C, 30 x 10^6 psi, and 0.283 lbm/in^3 respectively [8].

Beam Strength of the Gear Tooth and Dynamic Load on the Gear

The following calculations determine the beam strength of the gear tooth and the dynamic load on the gear. The beam strength of the gear tooth is the ability of the gear tooth to resist tooth breakage and is determined by the Lewis equation. This equation treats the gear tooth as a cantilever beam, and is given by [6]

$$F_b = \frac{\sigma_b \, b \, Y}{P} = \frac{(32000)(1.333)(0.611)}{8.5} = 3066.213 \text{ lbs.}$$

The dynamic effects which act upon the gear tooth are created from inaccuracies of tooth forming and spacing, combined with inertia of the rotating masses. In order to calculate the dynamic load on the gear

Table 2.3. Chemical Composition of AISI E9310 Steel [7].

C (%)	Mn (%)	P (%)	S (%)	Si (%)	Ni (%)	Cr (%)	Mo (%)
0.08-0.13	0.45-0.65	0.025 max	0.025 max	0.20-0.35	3.0-3.5	1.00-1.40	0.08-0.15

tooth, the pitch line velocity of the gears must be known. The pitch line velocity of the gears is given by [6]

$$V_p = \frac{\pi\ d\ n}{12} = \frac{(\pi)(3.6471)(9000)}{12} = 8593.271 \text{ fpm}$$

For a pitch line velocity that is greater than 4000 fpm, the dynamic tooth load is given by [6]

$$F_d = \left(\frac{78 + \sqrt{V_p}}{78}\right) F_t = \left(\frac{78 + \sqrt{8593.271}}{78}\right)(164.98) = 361.052 \text{ lbs.}$$

Since F_b is greater than F_d, the design for beam strength of the gear tooth is safe [6].

Surface Wear Strength of the Gear

Two similar equations are used to determine the surface wear strength of the gear. The first of these is the Buckingham equation and the second is the AGMA (American Gear Manufacturers Association) formula. The Buckingham equation is given by [6]

$$F_w = d\ b\ M_G\ K_\ell = (3.6471)(1.333)(1)(300) = 1458.475 \text{ lbs.}$$

The AGMA formula for determining gear safety as far as wear is concerned is given below. AGMA specifies that the calculated stress number, σ_c, must be less than or equal to an allowable contact stress number, S_{ac}, which has been modified by several correction factors or [6]

$$\sigma_c \leq \frac{C_L\ C_H}{C_T\ C_R}\ S_{ac}$$

where

$$\sigma_c = C_P \sqrt{\frac{F_t\ C_o\ C_s\ C_m\ C_f}{C_v\ d\ b\ I}} = 2300 \sqrt{\frac{(164.98)(1.01)(1.0)(2.5)(1.0)}{(0.70)(3.6471)(1.333)(0.85)}}$$

$$= 27{,}600$$

and

$$\left(\frac{C_L\ C_H}{C_T\ C_R}\right) S_{ac} = \left(\frac{(1.0)(1.0)}{(1.0)(1.25)}\right)(145{,}000) = 116{,}000$$

Since the left side of the equation is less than the right side (27,600 < 116,000), the gears are safe as far as wear is concerned [6].

Indices of Tooth Loading

The indices that are most important in gear design are the unit load, from the standpoint of tooth strength, and K-factor, from the standpoint of tooth surface durability. The higher the unit load index, the more risk of tooth breakage, and the higher the K-factor, the more risk of tooth pitting (a fatigue phenomenon caused by stresses exceeding the endurance limit of the gear material). Furthermore, the load indices show the intensity of loading that the gear teeth are trying to carry. The unit load index is derived from the Lewis equation for beam strength, and K-factor is based on the Hertz equation (or contact stress formula). The unit load is determined by [10]

$$U_L = \left(\frac{P}{b}\right) F_t = \left(\frac{8.5}{1.333}\right)(164.98) = 1052 \text{ psi.}$$

The K-factor is given by [10]

$$K = \left(\frac{F_t}{db}\right)\left(\frac{M_G + 1}{M_G}\right) = \left(\frac{164.98}{(3.6471)\ (1.333)}\right)\left(\frac{1 + 1}{1}\right) = 67.87 \text{ psi}$$

The contact stress number, σ_c, can also be determined by using the K-factor, as follows [10]:

$$\sigma_c = \sqrt{\frac{(0.70)(E)}{2\ (\cos\phi)(\sin\phi)}}\sqrt{K} = \sqrt{\frac{(0.70)\ (30 \times 10^6)}{2\ (\cos 22)(\sin 22)}}\sqrt{67.87}$$

$$= 45{,}300 \text{ psi}$$

Note that this value is greater than the contact stress number calculated earlier. Nevertheless, the gear design is still safe as far as wear is concerned.

Center Distance

The gear chosen for our study is a planet gear that is not intended to mesh with itself. It is used in an epicyclic gear train. On one side the planet meshes with the sun, while on the other side (180 degrees away) it meshes with the ring gear. A center distance based on drawing pitch diameter would be too tight or too loose. Therefore, the center distance had to be made non-standard. The non-standard center distance is given by [11]

$$C_2 = \left(\frac{\cos \phi_1}{\cos \phi_2}\right) C_1$$

where the pressure angle at meshing position (ϕ_2) can be determined by the following equation [11]:

$$\text{inv } \phi_2 = \frac{2(NT - \pi r)}{4\ Nr} + \text{inv } \phi_1$$

where

$$\text{inv } \phi_1 = \tan \phi_1 - \phi_1 = 0.020053 \text{ radians.}$$

Hence, inv ϕ_2 = 0.019587 and ϕ_2 = 21.835 degrees. Substituting the value of ϕ_2 into the equation for non-standard center distance yields, C_2 = 3.64288 inches. If an arc tooth thickness (T) of 0.1821 in is used, then the non-standard center distance is 3.64036 inches.

Efficiency of the Gears

The over-all efficiency of the gears are dependent on three types

of losses: 1) gear-mesh losses, 2) bearing losses, and 3) windage losses. Since air bearings are employed in our test rig, torque loss, and therefore bearing loss, will be very small and hence, neglected. The percent efficiency for the gears based upon the losses of the gear mesh is given by [12]

$$E = 100 - P_L$$

where P_L = percent power loss. The percent power loss is determined by the following equation [12]:

$$P_L = \left(\frac{(50)(f)}{\cos \phi}\right)\left(\frac{(H_s^2 + H_t^2)}{H_s + H_t}\right) = \left(\frac{(50)(0.038)}{\cos 22}\right)\left(\frac{H_s^2 + H_t^2}{H_s + H_t}\right)$$

where

H_s = specific sliding velocity at start of approach action

and

H_t = specific sliding velocity at end of recess action

The specific sliding velocities can be determined by [12]

$$H_s = \left(\frac{M_G + 1}{M_G}\right)\left(\sqrt{\left(\frac{r_o}{r}\right)^2 - \cos^2 \phi} - \sin \phi\right)$$

$$H_t = (M_G + 1)\left(\sqrt{\left(\frac{r_o}{r}\right)^2 - \cos^2 \phi} - \sin \phi\right)$$

Since the gear ratio, M_G, is unity, $H_s = H_t = 0.2975$. Hence, $P_L = 0.609\%$. Therefore, $E = 99.39\%$.

A crude estimation of the windage losses of the gear box is given by [12]

$$P_w = \frac{n^3 D^5 b^{0.7}}{100 \times 10^{15}} = \frac{(9000)^3 (3.883)^5 (1.333)^{0.7}}{100 \times 10^{15}} = 0.007869 \text{ hp.}$$

Rise in Temperature of Gear Case and Thermal Expansion of Gear Tooth

In high speed gears, the heat developed from frictional losses can be very high. Although the actual temperature of the gears is considerably higher than that of the case, the temperature of the gear case is an indication of the temperature of the gears [11]. The rise in temperature of the gear case is strongly dependent upon the flow of air around the case. In still air, the temperature rise of the gear case is given by [11]

$$Q = \frac{(0.01)(F_n)(V_p)}{(26)(A)} = \frac{(0.01)\ (177.94)\ (8593.271)}{(26)(2.977)} = 197.55°F$$

When there is free natural circulation of air around the case, the temperature rise is given by [11]

$$Q = \frac{(0.01)(F_n)(V_p)}{(35)(A)} = \frac{(0.01)(177.94)(8593.271)}{(35)(2.977)} = 146.75\ °F$$

High speed gears are often made with sufficient backlash so that the teeth will not bind when the gears expand from frictional heat [11]. The tooth expansion of the gear can be estimated by treating the gear tooth as a cantilever beam. In equation form, the tooth expansion is determined by [13]

$$\delta = \alpha\ L\ (t_1 - t_2) = (6.5 \times 10^{-6})(0.2647)(250-80)$$

$$= 2.9242 \times 10^{-4}\ \text{in}$$

2.2. Mechanical Design of the Tester

The design of our test rig includes purchased mechanical components, such as, the shafts, bearings, couplings, gear mounts, pulleys and belts, and an electric motor. The design also includes a purchased

lubrication system to cool and lubricate the mating gears. Section 2.2.1 provides a general layout and description of the tester; Section 2.2.2 gives a description of the selected mechanical components and the basis for their selection; and Section 2.2.3 describes the selected lubrication system and the basis for its selection.

2.2.1. General Layout and Description of the Four Square Gear Tester

A schematic of the tester is shown in Figure 2.2. As previously mentioned the Four Square Gear Tester makes use of the power recirculating principle whereby a known torque is applied by means of a split coupling or torque flanges. The torque is maintained by pinning the flanges at a specified relative angle corresponding to the desired torque. Hence, tooth loading is achieved by torsional strain energy of the shaft applied through the torque flanges [1]. In our study, the gears will be loaded to a maximum of 301.11 in-lbs.

The gears are driven by a variable speed electric motor which allows testing to be performed over a wide range of loading as well as speed. A speed increasing drive consisting of pulleys and V-belts provide the desired range of speed (the gears will be driven at speeds up to 9000 rpm) and torque. The test gears are acoustically and vibrationally isolated from the drive gears via an acoustic barrier, shaft seals, and flexible shaft couplings. Precision ground shafts transmit the necessary power to the gears. Air bearings keep the extraneous noise level to a minimum. And, the gear mounts fasten the gears to the shafts.

A pressure-spray oil lubrication system with a central reservoir simultaneously serves both test and drive sections. Since the system is

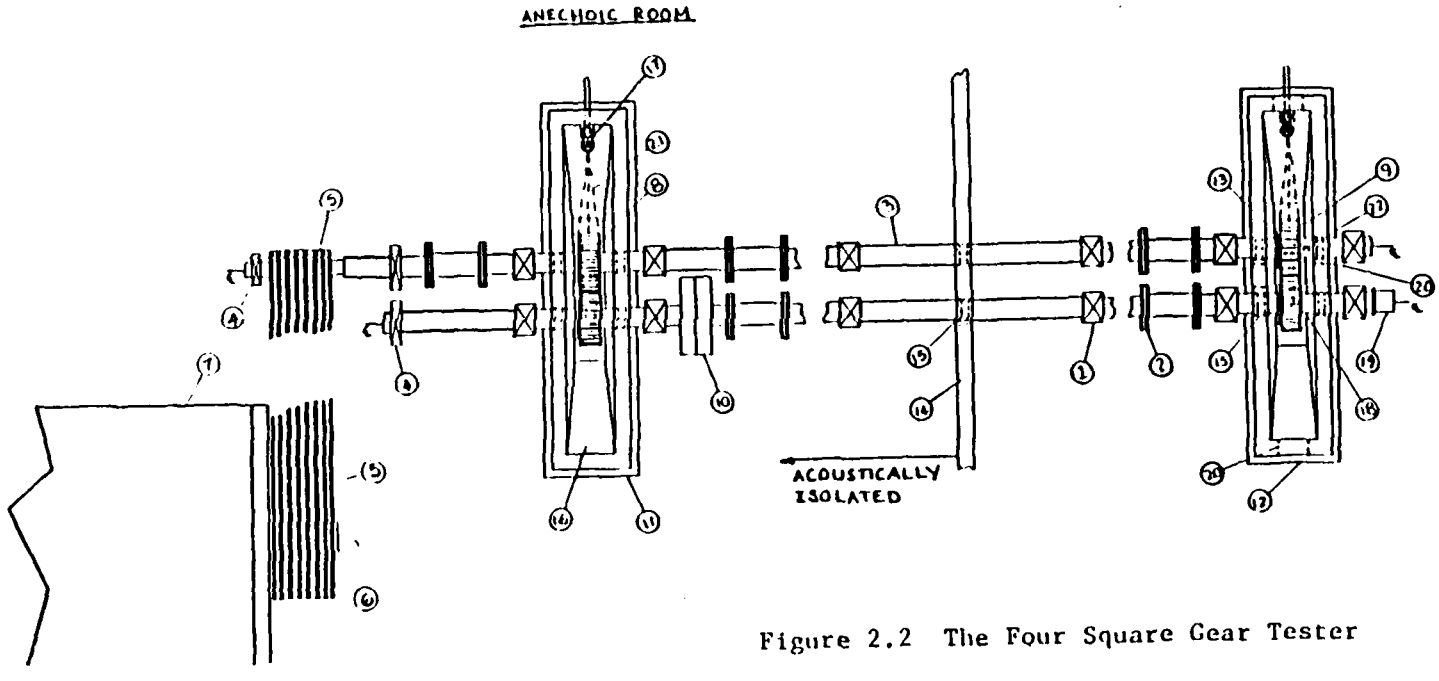

NO	PART
1	AIR BEARING
2	FLEXIBLE COUPLING
3	SHAFT
4	ROLLER BEARING
5	PULLEY
6	BELT
7	MOTOR
8	DRIVE GEAR
9	TEST GEAR
10	TORQUE FLANGE
11	DRIVE SECTION BOX
12	TEST SECTION BOX
13	CLAMP PLATE
14	ACOUSTIC WALL
15	ACOUSTIC SEAL
16	OIL PAN
17	SPRAY NOZZLE
18	STRAIN GAGE
19	SLIP RING
20	VIEW PORT
21	OIL SPRAY
22	ACCELEROMETER

Figure 2.2 The Four Square Gear Tester

SCALE: 1/4
DATE: 9/6/86
DRAWN BY: Santosh V. Anilam

not of an oil re-circulating type, the sprayed oil will be collected in an oil pan located at the bottom of each gear casing.

Because the applied torque is known to vary as the gears wear [1], strain rosettes connected to a slip ring are mounted on the gear shaft to measure shaft bending and twisting. A hydrophone (inserted via the ceiling of the test section casing) is employed to measure the gear noise. It is planned that sound levels will be measured at frequencies which are up to seven times the tooth mesh frequency. Since the tooth mesh frequency will be on the order of 3500 Hz, a minimum hydrophone pick up distance of four inches is required [1]. And an accelerometer mounted on the shaft is used to measure shock and vibration of the set-up. The view ports are specially designed to accommodate the possible non-intrusive EO techniques that were mentioned earlier.

Using the standard measuring techniques described above, the correlation of transmission error and/or gear box strain with sound level over a wide range of speed, load, running time, and lubricant conditions will be made. It is expected that noise waveforms should show a peak related to the strain waveforms and a large change in sound level at the time of transition from engagement of one pair of teeth to another. These acoustic signatures will then be correlated with detailed vibration and flow measurements using electrooptical techniques [1].

A substantial effort is made to reduce or eliminate sound and vibration that are not under investigation. The entire drive section including the drive motor and drive pulley and belt assembly along with the main components of the lubrication system are placed in an anechoic chamber. The drive and test section gear casing and components are mounted on top of their respective fabricated steel stands. These stands

are themselves mounted on isolation pads to reduce any cross influence between the stands and other stands within the laboratory.

2.2.2. Component Selection

The Four Square Gear Tester consists of both fabricated parts and purchased components. The fabricated parts include such items as: the mounting bases and enclosure for the test and drive section, housing for the bearings, the driven pulley, and the gear mounts. The purchased components are:

1) A variable speed electric motor which will allow testing to be performed over a wide range of loading as well as speed,

2) A speed increasing mechanism consisting of pulleys and V-belts to provide the desired range of speed and torque,

3) Low friction bearings which are intended to minimize extraneous vibrations and provide good shaft alignment,

4) Shaft couplings, with a low degree of dynamic imbalance and bending force transmission,

5) Gear mounts, also with low dynamic imbalance, and with the required torque rating,

6) Precision ground steel shafts which will provide center-to-center accuracy and therefore minimize vibration.

This section will describe the selected components and provide the basis for their selection including loading and tolerance requirements and cost. One of the main considerations in selecting these components is that they introduce a minimum of extraneous vibration; since this vibration would act as a noise source in the experiments and tend to mask the basic noise and vibration sources in the gears. The following subsections will describe the individual components in the order listed above.

2.2.2.1. Motor. The primary purpose of the motor is to provide the necessary power to drive the gears over a wide range of rotational speeds and loads. As previously mentioned, one of the main advantages of using the four square arrangement to test gears is that the power source need only supply the frictional losses in the set-up and not the full circulating power. Since these losses are negligible (see Section 2.1) it is possible to use a small size motor (10 hp) to drive the gears. But, since it is our intention to eventually test these gears at higher K-factors (in order to test the gears at its full load carrying capacity, it is necessary to further the test beyond 600 K-factor), it is imperative to use a larger size motor.

The following are the selection criterion for this particular motor:

General Requirements

The general requirements are as follows:

1) The motor should have a high degree of rotational speed constancy; since the collection of data is expected to take on the order of an hour per run.

2) Vibrational levels of the motor should be very low.

3) The maximum speed of the motor should be close to the desired speed of the gears.

4) The motor should be reversible over its entire speed range; in order to study the engagement and disengagement phases of the gear mesh cycle without an extensive effort for set-up between runs.

Based on these requirements and after a preliminary survey of the various types of electric motors commercially available, the following specifications were selected:

1. speed range from 0 to 2500 rpm

2. reversibility over entire speed range

3. 0.1% long term speed stability

4. 43 hp at full speed, corresponding to an applied torque on the gear shafts of 301.11 in-lbs

5. visual and electronic speed read-out

Based on these specifications a d.c. shunt-wound motor with a Silicon Controlled Rectifier (SCR), manufactured by Contraves Corporation, was selected. A direct-current shunt-wound motor with an SCR controller was chosen for the following reasons:

1) Shunt-wound dc motors are most suitable for applications where constant speed is needed at any control setting, or where an appreciable speed range is required [14].

2) Dc motor speed can be controlled smoothly down to zero, immediately followed by acceleration in the opposite direction [14].

3) They respond quickly to changes in control signals due to their high ratio of torque-to-inertia [14].

4) The SCR controller can regulate or switch the dc power of the motor.

The selected motor provides constant torque from 0 to 2500 rpm, 54 hp maximum at 2500 rpm, reversibility, and 0.1% long term speed stability. In addition, the motor system offers the following desirable features:

1) The motor has a rolled steel frame for dimensional stability and cast iron end bells for strength and rigidity. It has additional turns of copper wire in the field windings resulting in the reduction of power dissipation and operating temperatures. A ventilated drip-proof blower mounted on the motor, cools the motor, and enables it to achieve high torques at low speeds. Also, the motor drive is regenerative (motor generated energy is fed back into the dc supply) and therefore contributes to the rapid deceleration of the loads [15].

2) The motor is fitted with a high precision tachometer-generator to achieve the desired 0.1% speed stability. The

temperature compensated tachometer, with a ripple of 0.5%, has an extremely linear voltage-speed relationship throughout its entire speed range, providing accurate regulation for shaft velocity feedback. It also features a two-pole construction with antifriction ball bearings, and a totally enclosed non-ventilated steel frame. The tachometer weighs only 35 lbs [15].

3) The motor system also consists of an isolation transformer to provide impedence and noise isolation. The transformer impedence protects the SCR from in-rush currents and the noise isolation prevents large spikes (from the electrical supply) from entering the SCR.

4) The motor has a 150% overcurrent capability and requires an electrical supply voltage of 230 volts. The acceleration torque of the motor is 1800 in-lbs. The maximum torque output of the motor, at 2500 rpm, is 1356 in-lbs. The motor weighs approximately 775 lbs.

The following paragraphs provide the speed-torque relationship of the selected motor and the corresponding specifications.

Speed-Torque Relationship

The following graphs will provide a better understanding of the speed-torque relationship of the selected blower ventilated motor. The solid and dotted lines in Figures 2.3 and 2.4 represent the speed-torque relationships for the class F and class H insulations, respectively. The letters A, D, and E represent types of controllers. The selected motor has a type C SCR controller and class F insulation, and the solid curve of interest lies somewhere between curves A and D (this selection was made after discussions with Contraves engineers). From Figure 2.3, it is evident that as the speed increases, especially in the 80 to 100% of the base speed range, there is constancy in torque but as the speed decreases there is torque variation. Figure 2.4 shows the speed-torque relationship of a self-ventilated motor or motor without a blower. By comparing the two graphs one can easily see the advantage of using a blower ventilated

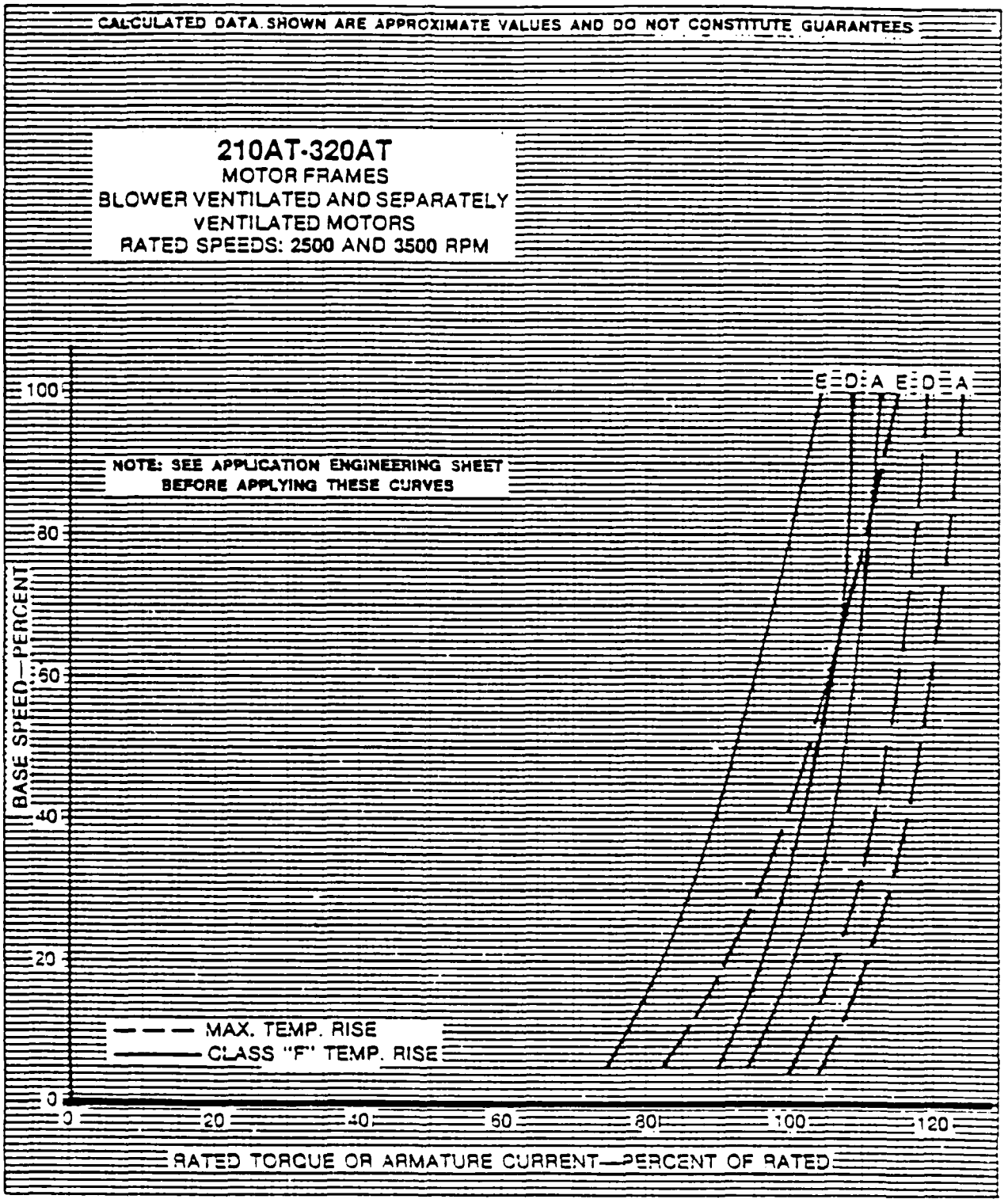

Figure 2.3 The Maximum Continous Speed vs. Torque Relationship of the Contraves Blower Ventilated Motor.

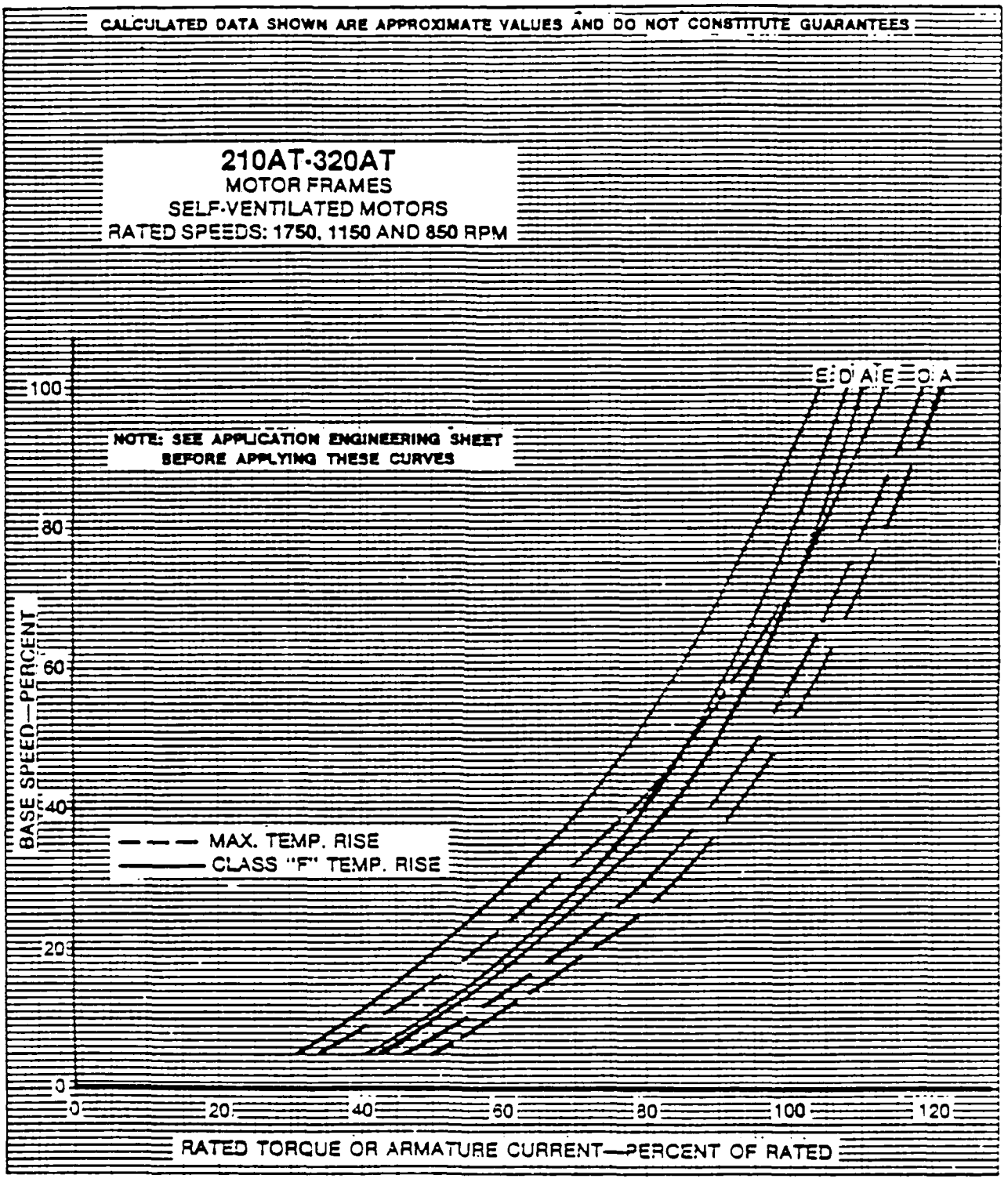

Figure 2.4 The Maximum Continous Speed vs. Torque Relationship of the Contraves Self-Ventilated Motor.

motor in this particular application. Furthermore, the torque output of the self-ventilated motor, at a lower percentage of the base speed, is far less than the torque output of the blower ventilated motor.

Contraves Motor Specifications

The main system components of the Contraves motor are the following:

i) regenerative SCR controller (ADB/F 460.145, 460 V, 145 amps max)

ii) a 60 hp dc shunt wound electric motor with a 2500 rpm base speed includes a 328AT frame, foot mount, ventilated drip proof blower (top mount), thermal switch, and an XC46 high precision tachometer (100 V/1000 rpm)

iii) isolation transformer (75 KVA 230 V input, 460 V secondary) in NEMA 1 enclosure

iv) floor mount (size 48 x 36 x 16 in) in NEMA 12 enclosure with fan ventilation for mounting of panel and controls

The system is also equipped with start/stop pushbuttons, an emergency stop pushbutton (coasts to stop upon activation), a power on light, field economy (lowers the field current when the motor is not in continuous use), a speed potentiometer to control motor velocity, a motor blower starter, and a digital display meter to show motor velocity. In addition, since the power requirement to drive the system is 43 hp at 9000 rpm, Contraves engineers have assumed some inefficiencies associated with the gearing to the load. An eighty-five percent efficiency is assumed by the manufacturer. The total price of the motor package is $20,422.00. Schematics of the motor and the motor mounted blower are shown in Figures 2.5 and 2.6, respectively.

2.2.2.2. Belt-Drive (Pulleys and Belts). The following symbols defined below are used in the calculations for this section.

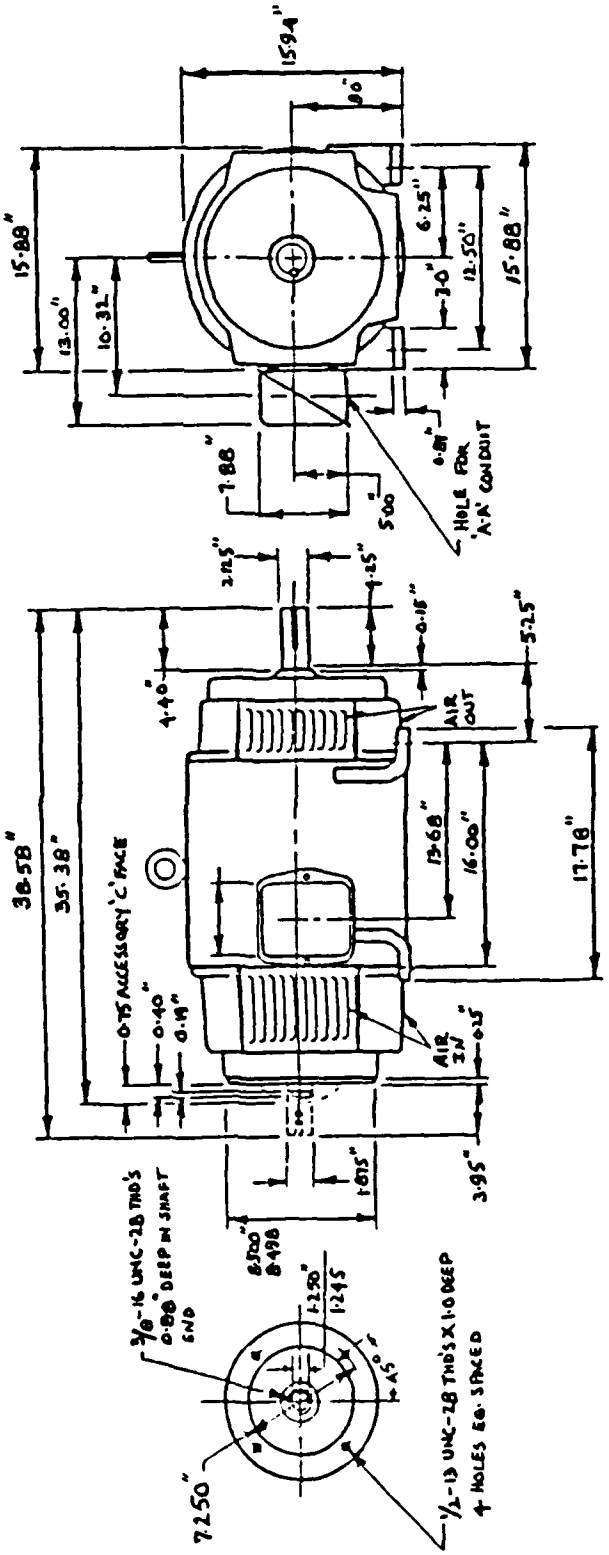

Figure 2.5 Contraves Motor

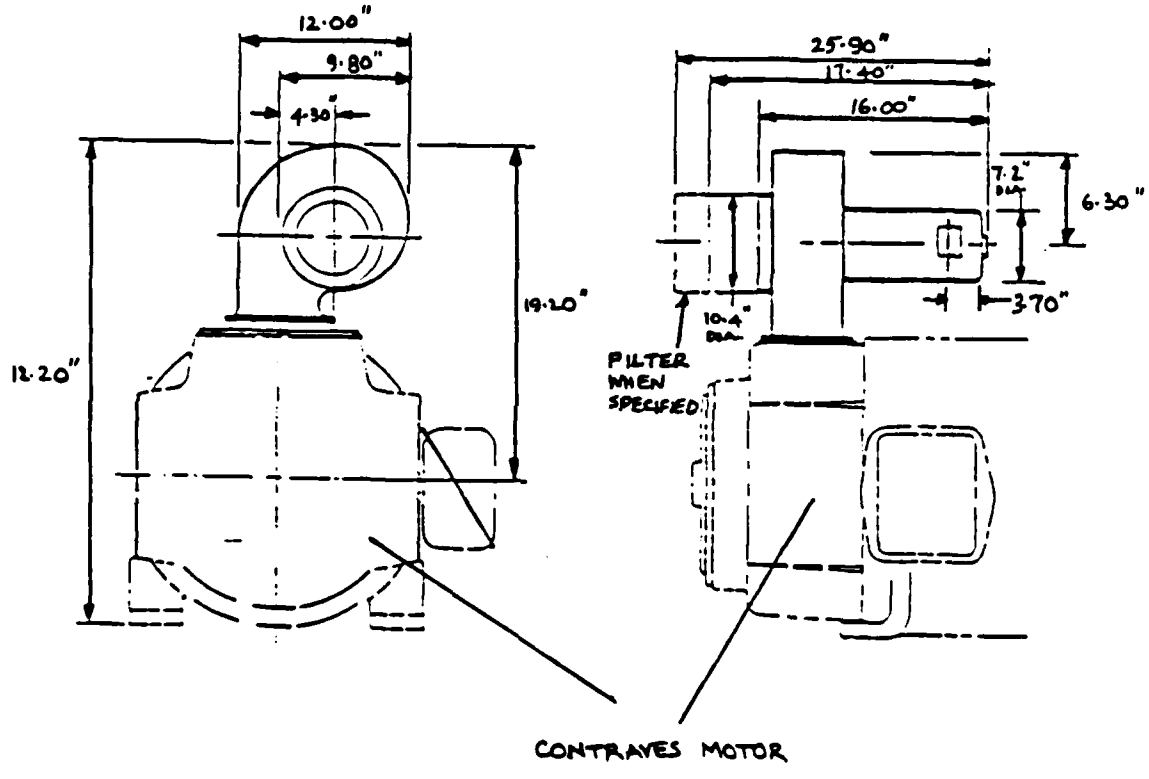

Figure 2.6 The Contraves Motor Mounted Blower

C	center-distance between pulleys
D	pitch diameter of the driver pulley
d	pitch diameter of the driven pulley
e	base of natural logarithm
f	natural fequency
hp	horsepower
k	a constant for V-belt drive design k = 0.51230 [23]
L	belt length
m	mass per unit length of belt $m = 3.238 \times 10^{-5}$ lbs-sec^2/in^2
N	correction factor for the arc of contact N = 1
n	gear speed n = 9000 rpm
T_c	centrifugal force per belt
T_1/T_2	belt tension ratio
T_1	tight side tension
T_2	slack side tension
t_1	tight side tension per belt
V	belt velocity
θ	arc of contact

The purpose of the belt-drive is to provide the desired range of speed and torque. The pulley and belt system was chosen because it is quieter during operation. The general requirements the belt-drive should meet are as follows:

1) It should provide the driving force from the motor to the gears with as little vibration and noise as possible.

2) The drive should have an appreciable service life, as it is expected the test apparatus wil be run continuously for an hour and five such runs per day will be conducted.

3) The drive pulleys should be dynamically balanced to prevent extraneous vibrations.

4) The belts should have a high degree of bend or flexibility to permit operation over the smaller pulley of the belt drive.

5) The belts should also have an appreciable depth-to-width ratio, thereby placing more of the pulley directly under the belts. This arrangement permits better belt force distribution over the pulleys.

6) The belt-drive should be able to operate at a short center-distance, since the motor and the drive section of the test apparatus will be separated by a short center-distance and placed on the same platform.

7) The belt-drive should be lightweight and hence, prevent any sizeable increase in the bearing loads and the lateral deflection of the shafts.

Based on these characteristics and consequent to a survey of various types of belt drives commercially available, the following specifications were chosen:

1. V-belts with dimensions:
   depth = 0.312 in
   top width = 0.375 in

2. Ductile Steel Pulleys with:
   driver pulley diameter = 9 in
   driven pulley diameter = 3 in
   driver rpm = 3000
   driven rpm = 9000

3. center distance: 24.0 in

4. horsepower rating of belts: 43

5. service life: 10,000 hrs

A Dayco Speed Increasing V-Belt drive was selected based on these requirements. A drive with narrow V-belts was selected for the following reasons:

1) Narrow V-belts have greater depth-to-width ratio, thereby placing more of the pulley directly under the reinforcing cords. Loads in the tensile cord are thus transferred more

directly to the sides of the pulley, allowing minimum load shedding and producing better force distributions. For a given width, narrow V-belts, therefore, have power ratings much higher than those of conventional V-belts [22].

2) V-belts are well adapted for use in short-center drives [21].

3) If V-belts are cogged (a cogged belt has molded teeth to allow flexibility) then the allowable degree of bend of the belt can be maximized and operation over small pulleys is made possible [22].

4) A narrow V-belt drive provides the highest power in the smallest package and is well suited for high speed applications.

The following calculations were made to select our V-belt drive.

Center-Distance, Pulley Diameters, and Belt Length

Since a short center drive is required, a center distance of twenty-four inches was assumed. The center-distance between pulleys, pitch diameters of the pulleys, and belt length are related by the following equation [23]

$$C = \frac{b + \sqrt{(b^2 - 32\ (D-d)^2)}}{16}$$

where

$$b = 4\ (L) - 6.28\ (D+d)$$

In order to determine the unknowns D and d, the following assumption was made: The center-distance will be greater than the diameter of the larger pulley and less than three times the sum of the two pulley diameters or [24]

$$D < C < 3\ (D+d)$$

For a speed increasing drive the size of the driver pulley is significantly larger than the size of the driven pulley. Since our

application demands a speed ratio of approximately 4 to 1, it was assumed that the pitch diameter of the driver pulley is four times the pitch diameter of the driven pulley. Based on these assumptions, and after several iterations of the above relation for center-distance, the following values were selected:

$C = 24.0$ in

$D = 9.0$ in

$d = 3.0$ in

$L = 67.2$ in

Belt Velocity

The belt velocity determines two things: 1) the belt material; and 2) whether the pulleys should be dynamically balanced. The belt velocity is determined by [23]

$$V = \frac{\pi d n}{12} = \frac{(\pi)(3)(9000)}{12} = 7068.580 \text{ fpm}$$

Net Belt Tension

Once the belt velocity is known the net belt tension (the difference in tight side and slack side tensions) can be determined by the following equation [23]:

$$\text{net belt tension} = \frac{(33{,}000)\ (\text{design horsepower})}{V}$$

$$= \frac{(33{,}000)\ (\text{design horsepower})}{7068.580}$$

where

$$\text{design horsepower} = (\text{transmitted horsepower})\ (\text{safety factor})$$

Since the test apparatus will not continuously run for more than an hour, the safety factor was taken as unity. Hence,

$$\text{design horsepower} = \text{transmitted horsepower} = 43$$

Therefore,

$$\text{net belt tension} = 200.741 \text{ lbs}$$

Arc of Contact and Arc Length of the Smaller Pulley

The arc of contact or the angle of wrap is defined as the angle subtended by the arc over which the belt contacts the pulley. The arc of contact is given by [23]

$$\theta = 180 - \left(\frac{D-d}{C}\right)(60)$$

$$= 180 - \left(\frac{9-3}{24}\right)(60)$$

$$= 165 \text{ deg}$$

The arc length of the wrap is determined by [23]

$$\text{arc length} = \left(\frac{\pi}{360}\right)(\theta)(d)$$

$$= \left(\frac{\pi}{360}\right)(165)(3)$$

$$= 4.320 \text{ in}$$

Belt Tension Ratio

The proper tension in the belt will result in a belt drive that provides the highest efficiency and longest service life. Inadequate tensions lead to slip and premature wear of the belt. The belt tension ratio is given by [23]

$$\frac{T_1}{T_2} = e^{k\,\theta\,(\text{rad})} = e^{0.51230(2.879)} = 4.810$$

In order to determine the tight side tension, T_1, the following equation was employed [23]:

$$T_1 = \frac{41{,}250 \text{ (design horsepower)}}{(N)(V)}$$

$$= \frac{(41{,}250)(43)}{(1)(7068.580)}$$

$$= 250.930 \text{ lbs}$$

To obtain a more accurate value for the slack side tension, T_2, the following equation was used [23]:

$$T_2 = \frac{33{,}000 \text{ (1.25 - N) (design horsepower)}}{(1) \text{ (7068.580)}} = 50.190 \text{ lbs.}$$

Number of Belts

The number of belts required to transmit 43 hp from the motor to the driven shaft is determined by dividing the design horsepower by the corrected horsepower rating per belt. During the course of a personal correspondence with the Dayco Technical Center a corrected horsepower rating of 9.13 (per belt) was selected for this particular design. Hence, the number of belts required is five.

Centrifugal Force and Dynamic Hub Loading

Because the belts are operating at such high speeds, the centrifugal force of the belts and the dynamic load on the hub of the pulley become important considerations. Again, during personal correspondence with Dayco engineers a centrifugal force (per belt) of 10 lbs (corresponding to a belt speed of 7068.580 fpm) was selected. The

following relation provides an approximate value for the dynamic hub load [23]:

$$\text{dynamic hub load} = (T_1 + T_2) - T_c$$

$$= (250.930 + 50.190) - 10$$

$$= 291.120 \text{ lbs}$$

Belt Natural Frequency

The fixed-fixed end condition (see Figure 2.7) was considered to determine the natural frequency of the belts. Considering each belt as a taut string and assuming small deflections, the natural frequency is given by [20]

$$f_n = n\left(\frac{c}{2C}\right) = n\left(\frac{c}{(2)(24)}\right) = n\left(\frac{c}{48}\right)$$

where n = mode numbers and

$$c = \sqrt{\frac{t_1}{m}} = \sqrt{\frac{50.186}{3.238 \times 10^{-5}}} = 1244.952 \text{ in/sec}$$

Therefore, the natural frequency of the system is now given by

$$f_n = n\left(\frac{1244.952}{48}\right) = n\,(25.936)$$

For n = 1, f_1 = 25.936 cycles/sec; for n = 2, f_2 = 51.872 cycles/sec; and for n = 3. f_3 = 77.808 cycles/sec.

Service Life

Since the belt speed is greater than 6500 fpm, Dayco engineers recommended that the designed pulleys should be made of ductile steel and must be dynamically balanced. Also, based on the calculated tensions and

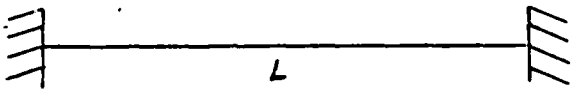

Figure 2.7 Fixed-Fixed

the given horsepower rating per belt, a service life of 10,000 hours was assigned to this designed belt drive.

Based on these calculations a Dayco speed increasing drive system was selected (also considered was the final drive ratio based on maximum motor speed of 2500 rpm). The Dayco drive is a 8-belt drive with the following matching components:

8-3V80 driver pulley

8-3V2.25 driven pulley

8-3VX630 V-belts

Both the driver and driven pulleys are made of cast iron. The deep groove driver pulley (the deep grooves keep the belts aligned and prevent them from rolling) has an eight inch outside diameter and is fitted with a removable hub bushing to allow the desired bore size (see Appendix A). The combined weight of the pulley and the bushing is approximately 23 lbs. The driven pulley is a special order item (Appendix A provides a complete drawing of this pulley) and it weighs approximately 2.6 lbs. The pitch diameter of the pulley is 2.25 in. The Dayco V-belts are cogged, lightweight (0.3 lbs per belt), and have high horsepower ratings.

The Dayco V-belt drive is designed to transmit 41 horsepower and has a service life of 25,000 hrs. If the drive is operated continuously for more than an hour, ten belts should be employed to obtain the above service life. Furthermore, if the transmitted horsepower is increased to 50, the service life of the belt-drive will drop to 10,000 hrs. The following are computer generated values provided by the Dayco Technical Center for the selected drive system. Note the similarities in the designed and selected drive systems. Also note that the use of a smaller pulley results in a lower belt speed.

Dayco 8-Belt Drive Data

pitch diameter of driver pulley, D = 8 in

pitch diameter of driven pulley, d = 2.25 in

design horsepower = 43.26

corrected horsepower rating per belt = 5.22

corrected horsepower rating for 8 belts = 41.73

driver pulley rpm = 2500

driven pulley rpm = 8889

belt speed, V = 5236 fpm

speed ratio = 3.56

belt length, L = 63.06 in

belt depth = 0.312 in

belt top width = 0.375 in

dynamic hub load = 414.920 lbs

centrifugal force per belt, T_c = 5.32 lbs

center distance between pulleys, C = 23.03 in

tension ratio: T_1/T_2 = 5.00

arc of contact (for small pulley), θ = 165.20 deg

tight side tension, T_1 = 340.80 lbs

slack side tension, T_2 = 77.84 lbs

net belt tension = 262.96 lbs

Following the same procedure as for the designed drive, the natural frequency of the selected belt-drive in modes 1, 2, and 3 are f_1 = 24.392 cycles/sec, f_2 = 48.785 cycles/sec, and f_3 = 73.177 cycles/sec, respectively. Since the belt speed is below 6500 fpm, special balancing of the pulleys is not required. As a result of which, the Dayco

belt-drive is more economical than the designed drive. The Dayco price list is as follows:

Part	Cost
8-3V80 driver pulley with bushing	$80.83
8-3V2.25 driven pulley	$91.76
8-3VX630 V-belts	$79.84 ($9.98 per belt)

2.2.2.3. Low Friction Bearings. The symbols defined below are used in the calculations for this section:

d	pitch diameter d = 3.6471 in
F_n	tooth load
F_{n1}	bearing reaction
F_{n2}	bearing reaction
F_r	radial load
F_t	tangential load
T	applied shaft torque T = 301.11 in-lbs
ϕ	pressure angle ϕ = 22 degrees

Low friction bearings are used in this design for the following reasons:

1) To minimize extraneous vibrations.

2) To prevent power loss due to friction.

3) To support the imposed shaft loads.

The general requirements the bearings should meet are as follows:

1) There should be no metal-to-metal contact between the journal and the bearing; this minimizes friction, extraneous noise, and shaft misalignment.

2) The bearings should be able to support the calculated shaft load.

3) They should have the desired internal diameter and operating speed.

4) The bearings should have an appreciable service life.

Based on these requirements, a survey of commercially available low friction bearings was made. The following specifications were then selected:

1. speed range: 0 to 9000 rpm
2. load capacity: 90 to 120 lbs
3. internal diameter: 1.377 ± 0.001 in
4. service life: 10,000 to 20,000 hrs

Either a hydrodynamic bearing (oil is usually the lubricant) or an air lubricated bearing meets the above specifications. Air bearings were chosen over the former for the following reasons:

1) They are quieter during high speed operation.

2) They are more economical and easily available.

3) Simplifies the lubrication system.

The other advantages of using an air bearing are:

1) The elimination of mechanical contact confers upon the bearing an indeterminate life. This type of bearing suffers no wear and, in consequence, can operate for an unlimited period. The fact that there is no degradation of performance with time is of fundamental importance [16].

2) The elimination of mechanical contact also results in exceedingly smooth rotation with very low drag enabling high rotational speeds to be obtained [16].

3) The nature of the load carrying mechanism results in a precise definition of the axis of rotation, achieving maximum stiffness at zero eccentricity [16].

An important consideration in designing systems that make use of gears to transmit power is the proper design of the bearings. This basically means calculating the resultant bearing loads [6]. The bearing loads were determined upon assuming that the effect of the gear mounts, couplings, and shafts are negligible as compared to the tooth loads. As shown in Figure 2.8, the bearing reactions are a direct result of the force F_n that the teeth of one gear exerts on the meshing teeth of the other. This force, which acts normal to the tooth surfaces and along the pressure angle ϕ, can be resolved into components F_t and F_r related by [6]

$$F_t = F_n \cos \phi$$

and

$$F_r = F_n \sin \phi$$

The torque T that the normal force produces with respect to the center of the gears is given by [6]

$$T = F_n \left(\frac{d}{2}\right) \cos \phi = F_t \left(\frac{d}{2}\right)$$

Since torque T is known, F_n, F_t, and F_r can be determined. Hence, F_n = 177.94 lbs, F_t = 164.98 lbs, and F_r = 66.65 lbs.

To determine the bearing reactions, it is necessary to view Figure 2.8 along ϕ (see Figure 2.9) and hence, eliminating the forces F_r and F_t from the picture. Since F_n acts at the mid-point of the shaft, the bearing reactions are equal to one another. From static analysis, F_{n1} = F_{n2} = 88.97 lbs.

Based on these calculations, sleeve type air bearings, manufactured by Masten-Apen Ltd., were selected. The mechanism of load carrying capacity of these bearings is similar to that in aerostatic bearings. The operation of aerostatic bearings is illustrated in Figures 2.10 and 2.11.

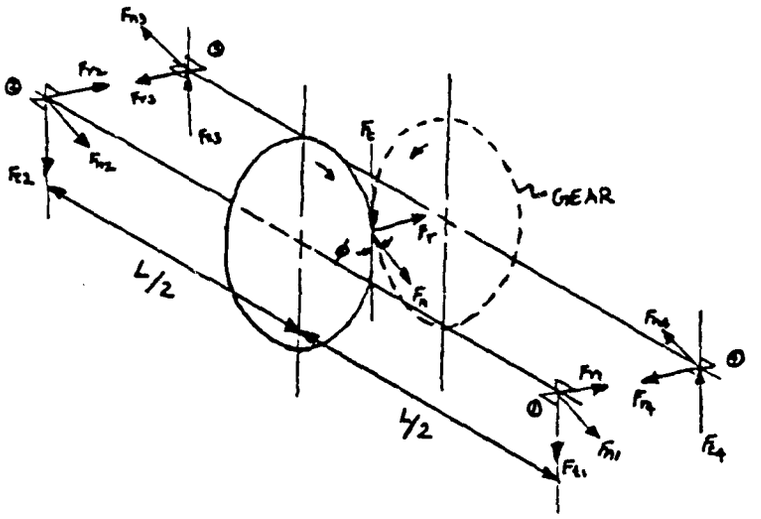

Figure 2.8 Bearing Reactions

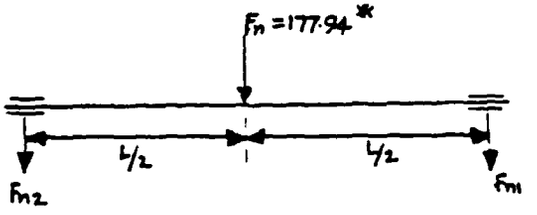

Figure 2.9 Bearing Reactions due to Tooth Load, F_n

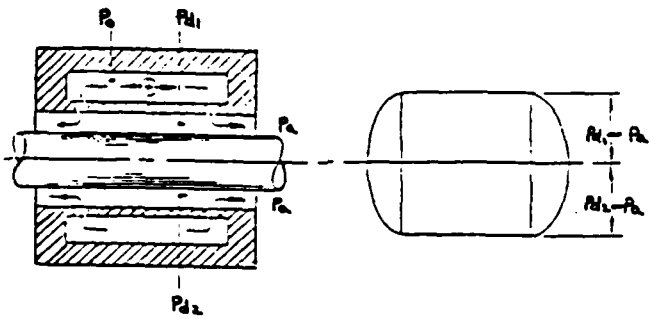

Figure 2.10 Aerostatic Bearing (no load on shaft) (Tempest, 1984)

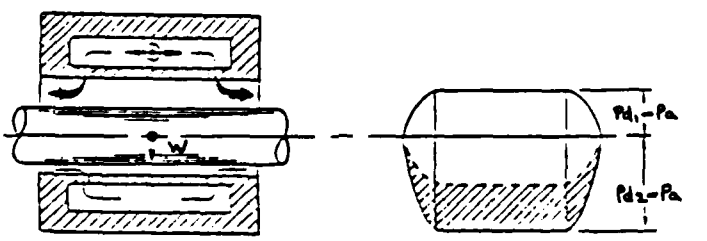

Figure 2.11 Aerostatic Bearing (load on shaft) (Tempest, 1984)

Figure 2.10 shows a cylindrical shaft located concentrically within a cylindrical sleeve. Air under pressure is fed through a series of jets into the annulus between the shaft and the bearing. A pressure drop occurs as the air passes through the jets giving rise to pressures as jet outlets indicated by P_{d1} and P_{d2}. In the concentric condition these pressures are equal and may be designated P_0. Once the air has passed through the jets it escapes through the narrow annulus to the outer ends of the bearing. The basic mechanism of the load carrying capacity is that the radial displacement of the shaft, as shown in Figure 2.11, results in a different resistance to flow between the top and bottom of the bearing. The net result is that P_{d2} increases above P_0, and P_{d1} diminishes below P_0, thereby creating the pressure differential necessary to support the imposed shaft load [16].

In the selected bearings, air under pressure enters through a 1/8 inch hole and into the annulus through several small jets that are randomly spaced throughout the entire inner surface of the bearing. In order to lift and center the shaft, an air flow rate of 5.5 cubic feet per minute is needed (this is a standard value). The bearings are capable of supporting 113.40 lbs of radial load at an air pressure of 100 psi. The shaft speed is limited only by the radial elongation limit of the shaft material. Furthermore, the bearings are made of 660 cast bronze and can operate with commercial grade cold rolled shafts with a 125 RMS finished [17].

Other pertinent design data for the selected bearings are as follows:

inner diameter:	1.3760/1.3755 in
outer diameter:	2.1255/2.1245 in
length:	1.375 in

recommended housing[1] size: 2.1255/2.1245 in
price per bearing: $96.34

The bearing accessories such as the air tank, airline filter, and air compressor were selected from a Compressed Air Products, Inc., catalog. The air tank has the capacity to hold 120 gallons of air at a standard working pressure of 200 psi. The 20 horsepower air compressor has a flow rate of 82 CFM at 100 psi. Furthermore, the compressor is equipped with an air cooled after cooler and dual and modulation controls. The compressor weighs 360 lbs. The price list for the bearing accessories is as follows:

air tank = $480.00
air filter = $ 51.00
air compressor = $5904.00

The following outlines one possible method of switching off the motor (hence, shutting off the test apparatus) when the flow rate to the bearings falls below the required, and therefore, prevent bearing wear and failure.

The Proposed Method

The flow diagram of the proposed electrical system is shown in Figure 2.12. This system will turn the motor off when it detects a change in load current. As shown, the dc current enters a trans-conductance amplifier where it is deamplified. The output current from the amplifier enters the two comparators which will compare the current values 1.40 and 1.50 mA. The output voltage from the comparators will either be 0 or 1 when it is passed through an OR-gate. We desire an output of 0 from both comparators; since the input current value should be between the two current values that are being compared. The FET switch

[1]Master-Apex does not manufacture the housing for their bearings, hence, these are special order items.

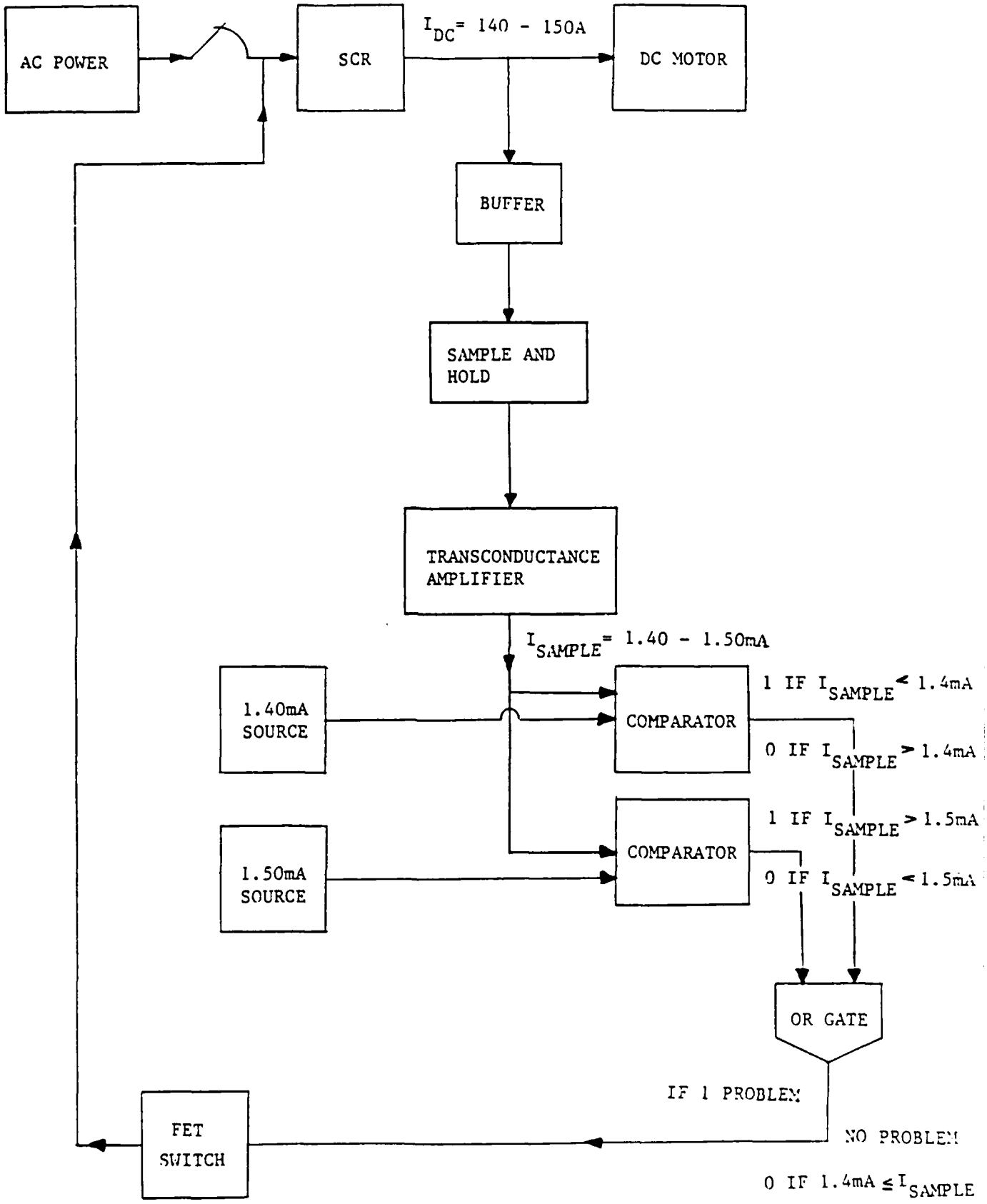

Figure 2.12 An Electrical System to Detect Change in Load Current of the Contraves Motor

will be turned on by a gate voltage of 0, and if one of the outputs (of the comparators) is 1, then the FET switch will be turned off. This signals that there is a problem with the value of the input current (the change in input current occurs when there is metal-to-metal contact between the shaft and the bearing). When the change in load current is detected by this system, the FET switch turns off, the gate of the SCR will not trigger, and the supply will be isolated from running the test apparatus [18].

Roller Bearings

The test apparatus is equipped with three roller bearings to compensate for the thrust loads imposed on the system. The thrust loads are predicted to be very small and almost negligible for our application. But, since it is our intention to eventually test the gears at higher K-factors, cylindrical roller bearings, with the capacity rating to test the gears at 600 K, were selected. The selected bearings have a high radial load capacity and can also tolerate light thrust loads. The bearings, which are manufactured by SKF Industries, are types NUP205EC and NUP207EC. For the one inch shaft, type NUP205EC was chosen. This bearing has the following design data:

inner diameter:	0.9843 in
outer diameter:	2.0472 in
length:	0.5906 in
radial load capacity:	6,440 lbs
calculated thrust load capacity:	72 lbs (for oil lubrication) and 42 lbs (for grease lubrication)
speed limit when grease lubricated:	11,000 rpm
speed limit when oil lubricated:	14,000 rpm
calculated average service life:	493,630 hrs
weight:	0.31 lbs
cost per bearing:	$39.72

For the 1.375 inch shaft, type *NUP207EC* was chosen. This bearing has the following design data:

inner diameter:	1.3780 in
outer diameter:	2.8346 in
length:	0.6693 in
radial load capacity:	10,900 lbs
calculated thrust load capacity:	186 lbs (for oil lubrication) and 124 lbs (for grease lubrication)
speed limit when grease lubricated:	8500 rpm
speed limit when oil lubricated:	10,000 rpm
calculated average service life:	1.679×10^7 hrs
weight:	0.68 lbs
cost per bearing:	$35.57

2.2.2.4. Shaft Couplings. The primary purpose of the shaft couplings is to join the drive section shafts to the test section shafts. Also, the couplings provide the means to isolate the drive section vibrationally from the test section of the Four Square Gear Tester. The general requirements the couplings should meet are as follows:

1) They must possess a low degree of dynamic imbalance to minimize extraneous vibrations; and a high degree of stiffness to minimize shaft bending.

2) The coupling must have the desired operating speed and torque rating.

3) They must compensate for angular and parallel misalignment of the shaft (if the shafts are aligned accurately, the couplings can be fairly rigid and need not have high misalignment capability).

4) The installation and removal of the couplings should be quick and easy; since the test and drive gears will be periodically removed and replaced.

5) They should be lightweight and hence, prevent any sizeable increase in the bearing loads and the lateral deflection of the shafts.

6) The couplings should require no special lubrication and must have an appreciable service life.

Following a survey of various types couplings commercially available, the specifications listed below were chosen:

1. operating speed: 9000 rpm
2. torque rating: 301.11 in-lbs
3. bore size range: 1.3755 to 1.3756 in
4. angular misalignment range: 0.25 to 0.50 deg
5. parallel misalignment range: 0.02 to 0.07 in
6. service life: 10,000 to 20,000 hrs

Based on these requirements Rexnord Thomas Flexible Shaft Couplings were selected. Flexible couplings were chosen for the following reasons:

1) They can be used to connect shafts subjected to both parallel and angular misalignment.
2) They are especially designed for high speed operations.
3) Since they consist of no rubbing or frictional surfaces, they require no lubrication.

The following calculation was made to determine the torque rating of the coupling. The torque rating is given by [21]

$$T_1 = (\text{safety factor})\ T$$

where T (applied shaft torque) = 301.11 in-lbs. In order to assign a value for the safety factor, the following assumptions were made: 1) The gear testing is intermittent in nature; and 2) Each test is to be run for an hour. On the basis of these assumptions, the factor of safety was taken as unity. Thus $T_1 = T = 301.11$ in-lbs.

Based on the calculated torque and the parallel and angular deformation of the shaft, Rexnord Style CC (size 100) Couplings were selected. The Rexnord couplings are flexible disc couplings that use

metal discs to transmit the motion and torque. These couplings not only accommodate angular and parallel misalignment but also provide free end float (or flexibility in the axial direction). Figure 2.13 shows a schematic of the Rexnord coupling. The mounting of the Rexnord coupling is quick and easy in the sense that it could be slipped onto the shaft end and fastened via set screws. Its riveted construction, its machined center members, and its aluminum components make these couplings torsionally rigid and lightweight. The Rexnord coupling has the following design data:

1. weight: 19.6 oz
2. allowable bore range: 1.374 to 1.376 in
3. maximum torque capacity: 700 in-lbs
4. maximum operating speed: 25,000 rpm
5. maximum parallel misalignment: 0.02 in
6. maximum angular misalignment: 0.5 deg
7. free end float: $\mp$ 0.031 in
8. torsional rigidity: 0.00066 milliradians/oz-inch (a 300 in-lb applied torque on the shaft results in a coupling torsional deflection of 0.182 deg)

The service life of these couplings are indefinite as long as one does not go beyond the catalog torque and misalignment values. They require no lubrication or dynamic balancing (during the course of personal correspondence, Rexnord engineers felt that special balancing of these couplings will not be necessary since the operating speed is way below 12,000 rpm). The price per coupling is $452.20.

2.2.2.5. Gear Mounts. The following symbols defined below are used in the calculations for this section.

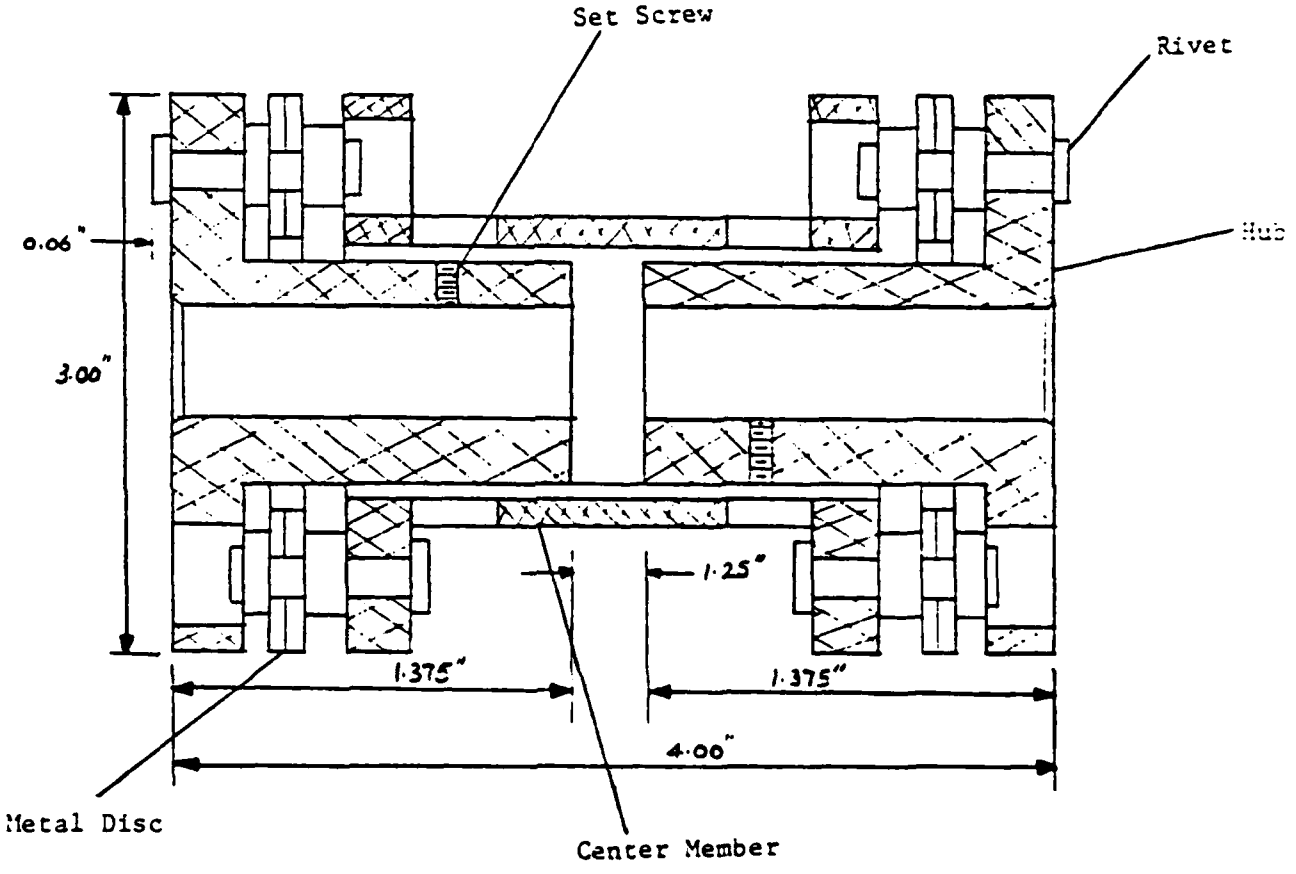

Figure 2.13 Rexnord Flexible Shaft Coupling

a — inner radius of gear
a = 1.348 in

b — outer radius of gear
b = 1.942 in

E — Youngs Modulus of steel
30×10^6 psi [6]

P — internal pressure due to shrink fitting

u — radial expansion

U — radial interference

ν — Poissons ratio for steel
$\nu = 0.3$ [6]

ς — mass density of steel
$\varsigma = 7.253 \times 10^{-4}$ lb-sec^2/in^4 [8]

ω — angular velocity
$\omega = 942.478$ rad/sec

The purpose of the gear mounts is to fasten the gears onto the shafts. The general requirements the mounts should meet are as follows:

1) They must be dynamically balanced to minimize extraneous vibrations.

2) The gear mounts must keep the level of gear expansion to a minimum and hence, prevent additional stresses on the mating tooth surfaces.

3) They must have the desired operating speed and torque rating.

4) The installation and removal of the mounts should be quick and easy; since the test and drive gears will be periodically removed and replaced.

5) The mounts should be lightweight to prevent any sizable increase in bearing loads and the lateral deflection of the shafts.

6) They should require no special lubrication and must have an appreciable service life.

A survey of various types of mounts commercially available led to the following specifictions:

1. operating speed: 9000 rpm
2. torque rating: 301.11 in-lbs
3. allowable gear diameter expansion: 0.001 to 0.002 in
4. service life: 10,000 to 20,000 hrs

Based on these requirements Ringfeder Gear Mounts were selected. These mounts provide an adjustable and releasable mechanical shrink fit without any of the problems associated with shrink fitting. The other advantages of using these mounts are as follows:

1) They are especially designed for high speed operations; and are able to transmit high torques.
2) They keep gear diameter expansion to a minimum.
3) They require no special lubrication.
4) They are easy to install and remove.
5) They are not affected by dynamic or shock loads.
6) They require no shaft keyways or splines.

The following calculations provide an approximation of the radial expansion of the gear that results in shrink fitting the gear onto a bushing.

Gear Expansion

One method of mounting the gear on the shaft is to shrink fit the gear onto a bushing (see Figure 2.14) and then mount this unit on the shaft via keyways or splines. The radial expansion, u, of the gear subjected to an internal pressure, p (due to shrink fit), is given by [6]

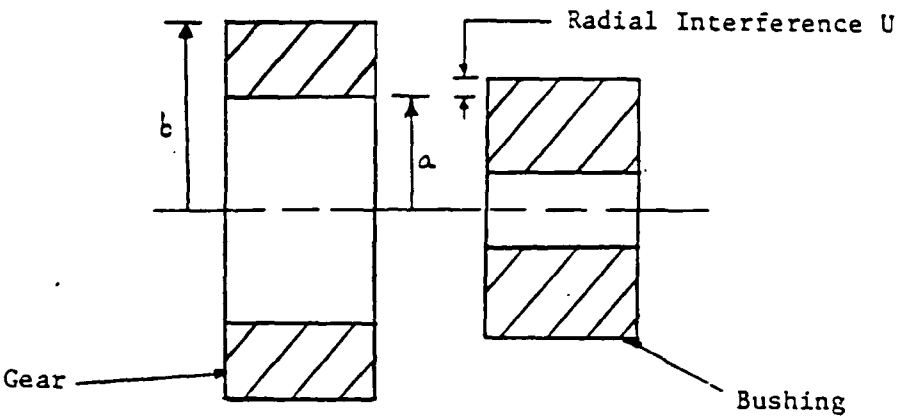

(a) before assembly

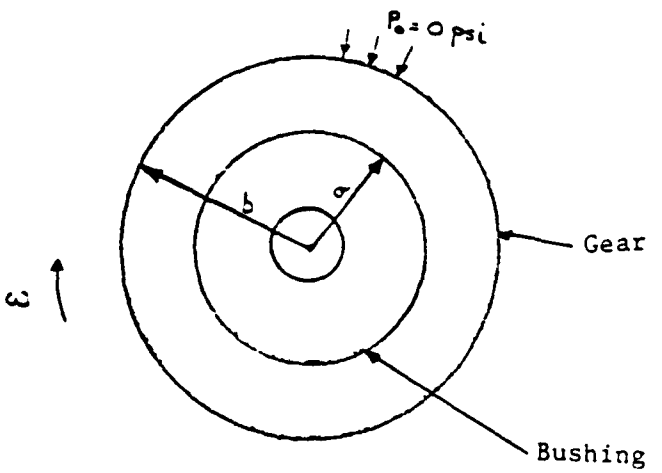

(b) after assembly

Figure 2.14 Shrink Fitting

$$u = \frac{2a^2pb}{E(b^2-a^2)} + \frac{\zeta\omega^2 b}{E}\left(\frac{3+\nu}{8}\right)\left\{(a^2+b^2)(1-\nu) + a^2(1+\nu) - \left(\frac{1-\nu^2}{3+\nu}\right)b^2\right\}$$

$$= \frac{2(1.348)^2\ (p)\ (1.942)}{(30\times10^6)((1.942)^2-(1.348)^2)} + \frac{(7.253\times10^{-4})(942.478)^2(1.942)}{30\times10^6}\left(\frac{3+0.3}{8}\right)$$

$$\left\{((1.348)^2 + (1.942)^2)(1-0.3) + (1.348)^2(1+0.3) - \frac{(1-(0.3)^2)}{(3+0.3)}(1.942)^2\right\}$$

$$= 1.203 \times 10^{-7}\ p + 9.0 \times 10^{-5}$$

where ω is the angular velocity of the unit and internal presure, p, is related to the initial radial interference, U, by [6]

$$U = \frac{ap}{E}\left\{\frac{(b^2+a^2)}{(b^2-a^2)} + 1\right\} + \frac{a\zeta\omega^2}{4E}\left\{(1-\nu)a^2 + (3+\nu)b^2\right\}$$

$$U = \frac{(1.348)p}{(30\times10^6)}\left\{\frac{(1.942)^2 + (1.348)^2}{(1.942)^2 - (1.348)^2} + 1\right\} + \frac{1.348\ (7.253\times10^{-4})(942.478)^2}{4\ (30\times10^6)}$$

$$\left\{(1-0.3)(1.348)^2 + (3+0.3)(1.942)^2\right\}$$

Assigning a value of 0.002 in to U and solving for the internal pressure results in p = 10,955 psi. Substituting this value for p into the equation for radial expansion results in $u = 1.405 \times 10^{-3}$ in. To determine at what speed the shrink fit becomes completely ineffective, we set p = 0 in the radial interference equation and solve for ω. In doing so, we find $\omega = 4231.226$ rad/sec or 673.421 cycles/sec. This value is, of course, far above the operating speed of the test apparatus.

Based on these calculations, Ringfeder Gear Mounts were selected. These mounts are frictional locking devices that offer all the advantages of a shrink fit but none of its problems. The fact that they can provide an adjustable and releasable shrink fit is of great importance to our application. The schematic of the gear mount is shown in Figure 2.15. As shown, the mount consists of a locking element, clamp plate, and bushing. The locking element, in turn, consists of an inner and outer tapered

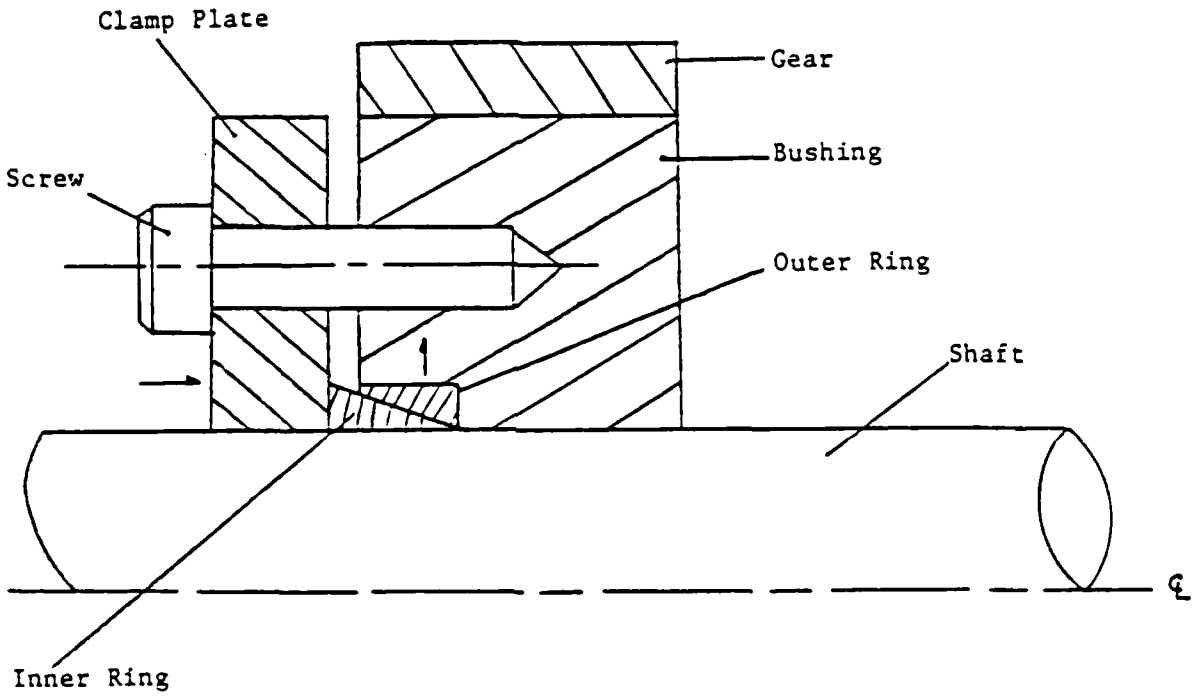

Figure 2.15 Gear Mount and Ringfeder Locking Element

ring. When each of the clamp plate screws are tightened, it exerts an axial force on the ring. This force generates radial clamping pressures on the shaft and bushing bore, providing a frictional connection and hence, transmitting the required torque to the gear.

The locking element is made of aluminum and has a torque capacity of 1510 in-lbs. The radial expansion of the gear as a result of the radial force on the locking element is approximately 1.2×10^{-3} in [25]. The weight and price of the locking element are 0.0312 lbs and $4.00, respectively. Unlike the locking element, the bushing and clamp plate are special order items. The complete drawings of the bushing and clamp plate are provided in Appendix B. To ensure safe operation of the gear/mount unit, it was important to select a material for the bushing that has a thermal expansion coefficient, α, which is greater than that of the gear material. The material selected for the bushing is AISI C1045 steel. The thermal expansion coefficient of this material at 250°F (estimated operating temperature of the gear set) is 7.94×10^{-6}/°F [6].

2.2.2.6. Shafts. The symbols defined below are used in the calculations for this section.

A	solid shaft cross-sectional area $A = 1.485$ in^2
A_o	hollow shaft cross-sectional area
C_m	numerical combined shock and fatigue factor applied to the computed bending stress, σ $C_m = 1.5$ (for steady loads) [9]
C_t	the corresponding factor to be applied to the computed shear stress, τ $C_t = 1.0$ (for steady loads) [9]
d	shaft diameter $d = 1.375$ in

E	Youngs Modulus of steel $E = 30 \times 10^6$ psi [6]
f	natural frequency
F_n	tooth load $F_n = 177.94$ lbs (see Low Friction Bearings)
G	shear modulus of steel $G = 11.5 \times 10^6$ psi [9]
g	gravitational constant $g = 386$ in/sec^2
I	moment of inertia for a solid shaft
I_o	moment of inertia for a hollow shaft
J	polar moment of inertia for a solid shaft
J_o	polar moment of inertia for a hollow shaft
k	spring constant
K	stress concentration factor
L	length of shaft $L = 8.5$ in
M	bending moment
m	mass per unit length $m = 0.415$ lb m/in
n	mode number
r	shaft radius $r = 0.6875$
T	applied shaft torque $T = 301.11$ in-lbs
y	shaft lateral deflection
ϕ	angular deformation of shaft
θ	slope
τ	shear stress
σ	bending stress
ς	mass density of 1045 steel $\varsigma = 0.28$ lb m/in^3 [8]

The primary purpose of the shafts is to transmit the power from the motor to the gears. The general requirements the shafts should meet are:

1) They should be dynamically balanced to minimize extraneous vibrations; and provide center-to-center accuracy to minimize parallel and angular misalignments.

2) The required finish and tolerance levels of the shafts must be compatible to the levels accepted by the couplings, bearings, and gear mounts.

3) The shafts must possess a very low runout (runout is the deviation of the shaft diameter over its length).

4) They must be torsionally rigid to prevent torsional vibrations that influence gear action and cause premature bearing wear.

Based on these requirements and following a survey of various types of shafts, the following specifications were selected:

1. precision ground 1045 steel shafts
2. tolerance range: 1.3745 to 1.3755 in
3. runout: 0.001 to 0.002 in overall shaft length
4. finish range: 10 to 16 micro-inches RMS
5. shaft size: 1.375 in
6. shaft speed: 9000 rpm

Based on these specifications, Centrall Centerless Grinding Company's precision ground 1045 steel shafts were selected. The reasons for the selection of precision ground shafts are the following:

1) They are most suitable for high speed applications. In particular, they provide center-to-center accuracy and can be dynamically balanced to minimize extraneous vibration.

2) A very smooth finish is easy to obtain on a ground shaft.

3) The shaft runout can be kept to a minimum.

4) They have sufficient torsional rigidity.

The following calculations pertain to both drive and test section shafts, since these shafts are identical in size and property. In those areas where the calculations differ significantly, it will be so noted.

Torsional Stiffness

A shaft that permits excessive angular displacement may contribute to vibrations (both torsional and lateral), affect gear action, and cause premature bearing wear or failure [6]. Therefore, it was extremely important to select a shaft with high torsional rigidity. The angular deformation of the shaft due to torque T is given by [9]

$$\phi = \frac{TL}{JG} = \frac{(301.11)(8.5)}{(J)(11.5 \times 10^6)}$$

where the polar moment of inertia, J, for a solid shaft is given by [9]

$$J = \frac{\pi(r)^4}{2} = \frac{\pi(0.6875)^4}{2} = 0.3509 \text{ in}^4$$

Hence, $\phi = 6.3421 \times 10^{-4}$ radians or 0.0363 degrees. Although no standard torsional deflection has ever been established for different shaft applications, it has become standard practice to limit the torsional deflection for transmission shafting to one degree in a length of 20 times the shaft diameter or [6]

$$1.0 \text{ deg } \frac{L}{(20)(d)} = 1.0 \text{ deg } \frac{8.5}{(20)(1.375)} = 0.309 \text{ deg}$$

Since this value is greater than the calculated value, the shaft is sufficiently rigid [6]

Lateral Deflection

In order to determine shaft deformation due to the gear tooth load

F_n, consider Figure Figure 2.16. Here we treat the shaft as a beam. Assuming F_n acts at the center of the beam and neglecting the weight of the shaft, gear, and gear mount, the maximum deflection of the shaft is [9]

$$y_{max} = \frac{F_n L^3}{48 EI} = \frac{(177.94)(8.5)^3}{(48)(30 \times 10^6)(I)}$$

where the shaft moment of inertia, I, is determined by [9]

$$I = \frac{\pi(0.6875)^4}{4} = 0.1755 \text{ in}^4$$

Hence, $y_{max} = 4.3250 \times 10^{-4}$ inches. The slope at the ends of the shaft is given by [9]

$$\theta = \frac{F_n L^2}{16 EI} = \frac{(177.94)(8.5)^2}{16\ (30 \times 10^6)(0.1755)}$$

$$= 1.5264 \times 10^{-4} \text{ rad } (8.7456 \times 10^{-3} \text{ deg})$$

Net Clearance

To check if this value for the slope will not cause the shaft to rub against the inner surface of the air bearing during operation, consider Figures 2.17 and 2.18, where ID (inner diameter of the bearing) = 1.3760 in, OD (outer diameter of the bearing) = 2.1255 in, L (bearing length) = 1.375 in, D (maximum shaft diameter) = 1.3755 in, and θ = 8.7456×10^{-3} deg. Note that the initial clearance between the shaft and the inner bearing surface is 0.00025 in. An exaggerated picture of the shaft bending inside the bearing during operation is shown in Figure 2.18. The net clearance, x, between the shaft and the inner surface of the bearing is given by

$$x = (\frac{ID}{2}) - \frac{D}{2} (\frac{1}{\cos \theta}) - (\frac{L}{2}) \tan \theta$$

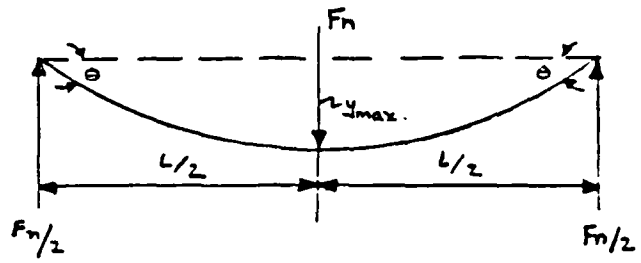

Figure 2.16 Shaft Deformation due to Gear Tooth Load, F_n

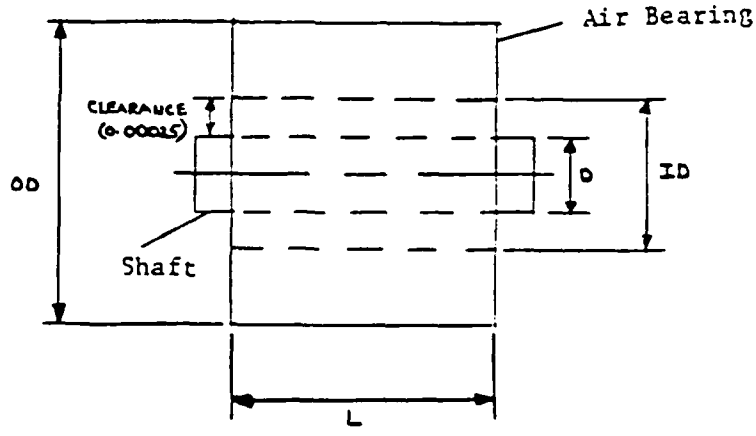

Figure 2.17 Clearance (no load on shaft)

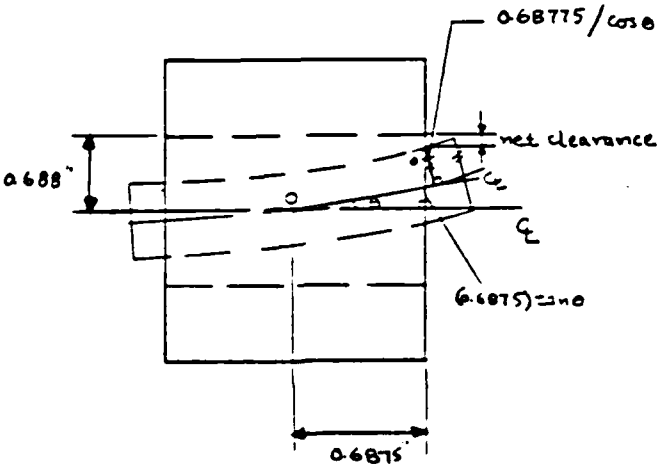

Figure 2.18 Net Clearance (load on shaft)

Substituting the given values, $x = +1.4506 \times 10^{-4}$ in. Since the calculated value for x is positive, the shaft will not make contact with the bearing inner surface during operation and hence, prevent bearing wear.

Maximum Static Shearing Stress

For rotating shafts, the bending stress varies continuously from maximum tension to maximum compression [9]. To compensate for the harmful effects of load fluctuation, the ASME (American Society of Mechanical Engineers) code for the design of transmission shafting was employed. The code makes the proper allowance for load fluctuations by inserting the constants C_m and C_t into the maximum shear theory of failure as follows [9]:

$$\tau_{max} = \sqrt{(\frac{C_m \sigma}{2})^2 + (C_t \tau)^2}$$

where τ_{max} = maximum shear stress. The bending stress, σ, is given by [9]

$$\sigma = \frac{32 M}{\pi d^3} = \frac{32 M}{\pi (1.375)^3}$$

where the bending moment, M, is given by [9]

$$M = F_n (\frac{L}{2}) = 177.94 (\frac{8.5}{2}) = 756.245 \text{ in-lbs}$$

Hence, $\sigma = 2963.155$ psi. The shear stress, τ, is determined by [9]

$$\tau = \frac{Tr}{J} = \frac{(301.11)(0.6875)}{0.3509} = 589.949 \text{ in-lbs}$$

Substituting the values for σ and τ into the ASME code yields $\tau_{max} = 2299.337$ psi. The yield and tensile strength of 1045 steel is 90,000 and 103,000 psi, respectively. Note that the calculated maximum shear stress is significantly less than half the material yield strength ($\sigma_{ys}/2$).

Shaft Natural Frequency

The following calculations were made to determine the natural frequency of the shaft in bending for three different end conditions. The end conditions were carefully selected to resemble what might occur during actual operation. Assuming that the shaft behaves like a uniform beam, the first arrangement considered was a simply supported beam, as shown in Figure 2.19. The natural frequency of this system is given by [19]

$$f_n = \frac{1}{2\pi}\left(\frac{n\pi}{L}\right)^2\sqrt{\frac{EI}{\zeta A}} = \frac{1}{2\pi}\left(\frac{n\pi}{8.5}\right)^2\sqrt{\frac{(30 \times 10^6)(0.1755)}{(0.28)(1.485)}}$$

For n = 1, f_1 = 77.364 cycles/sec; for n = 2, f_2 = 309.456 cycles/sec, and for n = 3, f_3 = 696.276 cycles/sec. Since the natural frequency in mode 1 is less than the operating speed of the shaft (150 cycles/sec), it is of vital importance that the shaft speed pass mode 1 within a fraction of a second to avoid large vibrations.

The second arrangement considered was a uniform beam with fixed ends (as shown in Figure 2.20). The natural frequency of this system is given by [20]

$$f_n = \frac{1}{2\pi}\left(\frac{\mu_n}{L}\right)^2\sqrt{\frac{EI}{\zeta A}}$$

$$= \frac{1}{2\pi}\left(\frac{\mu_n}{8.5}\right)^2\sqrt{\frac{(30 \times 10^6)(0.1755)}{(0.28)(1.485)}}$$

For n = 1, μ_1 = 4.730 [20], for n = 2, μ_2 = 7.853 [20], and for n = 3, μ_3 = 10.966 [20]. Hence, the corresponding natural frequencies are f_1 = 175.373 cycles/sec, f_2 = 483.404 cycles/sec, and f_3 = 942.617 cycles/sec. Note that the calculated frequency values are above the operating speed of the shaft.

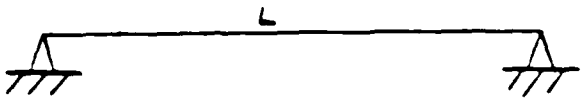

Figure 2.19 Simply Supported

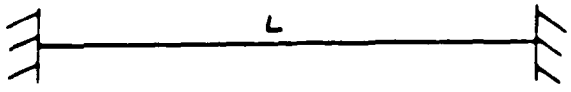

Figure 2.20 Fixed-Fixed

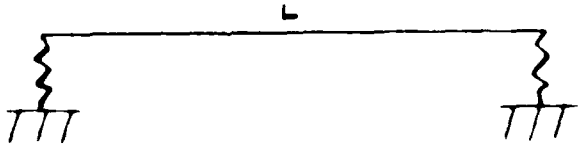

Figure 2.21 Spring Supported

The final arrangement that was considered is shown in Figure 2.21. Here, the ends of the beam are supported by linear springs with spring constant k. Neglecting the beam stiffness and assuming small oscillations, the frequencies of this two-degree of freedom system are determined by [19]

$$\omega_{1,2}^2 = \frac{1}{2}\left(\frac{2k}{m} + \frac{kL^2}{2J} \mp \sqrt{\left(\frac{2k}{m} + \frac{kL^2}{2J}\right)^2 - \frac{4k^2L^2}{mJ}}\right)$$

$$= \frac{1}{2}\left(\frac{2k}{0.415} + \frac{k(8.5)^2}{2(0.3509)} \mp \sqrt{\left[\frac{2k}{0.415} + \frac{k(8.5)^2}{2(0.3509)}\right]^2 - \frac{4k^2(8.5)^2}{(0.415)(0.3509)}}\right)$$

Assuming k = 10,000 lb-in, ω_1 = 219.528 rad/sec and ω_2 = 1014.64 rad/sec. Dividing both ω_1 and ω_2 by a factor of 2π we obtain the natural frequencies f_1 = (34.938 cycles/sec) and f_2 = (161.485 cycles/sec). Again, since f_1 is less than 150 cycles/sec, it is imperative that the shaft speed pass mode 1 within a fraction of a second to avoid large vibrations.

Shaft Critical Speed

The shaft critical speed is another phenomenon that deserves consideration. Rotating shafts also become dynamically unstable at their critical speeds and large vibrations can develop [9]. The equation for finding this speed is as follows [9]:

$$f_1 = \frac{1}{2\pi}\sqrt{\frac{g(W_1y_1 + W_2y_2 + \ldots)}{(W_1y_1^2 + W_2y_2^2 + \ldots)}}$$

where W_1, W_2, etc., are the weights of the rotating bodies, and y_1, y_2, etc., represent the respective static deflections of the weights. The rotating bodies on the drive and test section shafts are the gears and their mounts. The combined weight, W, of the gear and its mount is

approximately 3 lbs and it acts at the center of the shaft. The respective maximum static deflection, y, of the 3 lb weight is 7.290×10^{-6} in. Hence, the above equaton reduces to:

$$f = \frac{1}{2\pi}\sqrt{\frac{g(Wy)}{Wy^2}} = \frac{1}{2\pi}\sqrt{\frac{386(3)(7.290 \times 10^{-6})}{(3)(7.290 \times 10^{-6})^2}} = 1158.111 \text{ cycles/sec}$$

Note that the normal operating speed of the shaft (150 cycles/sec) is significantly below the calculated critical speed, hence, safe operation.

Deflection of the Drive Section Shaft of Non-Uniform Diameter

The following calculations determine the angular and lateral deformation of the non-uniform drive section shaft that transmits the power from the motor to the gears. As shown in Figure 2.22, this shaft is supported by roller bearings and the length of the shaft between the bearings is 9.050 in. The angular deformation, ϕ, of the shaft is given by [13]

$$\phi = \left(\frac{T}{G}\right)\left(\frac{L_1}{J_1} + \frac{L_2}{J_2}\right)$$

where $L_1 = 5.716$ in, $L_2 = 3.334$ in, J_1 (polar moment of inertia of the one inch section) $= 0.09817$ in^4, and J_2 (polar moment of inertia of the 1.375 in section) $= 0.3509$ in^4. Substituting these values and the value for T and G into the above equation yields, $\phi = 1.773 \times 10^{-3}$ rad or 0.102 deg. As a check on the shaft torsional rigidity the rule of limiting the torsional deflection to one degree in a length of 20 times the shaft diameter is again applied. For the one inch section:

$$1 \text{ deg } \frac{(5.716)}{(20)(1)} = 0.286 \text{ deg}$$

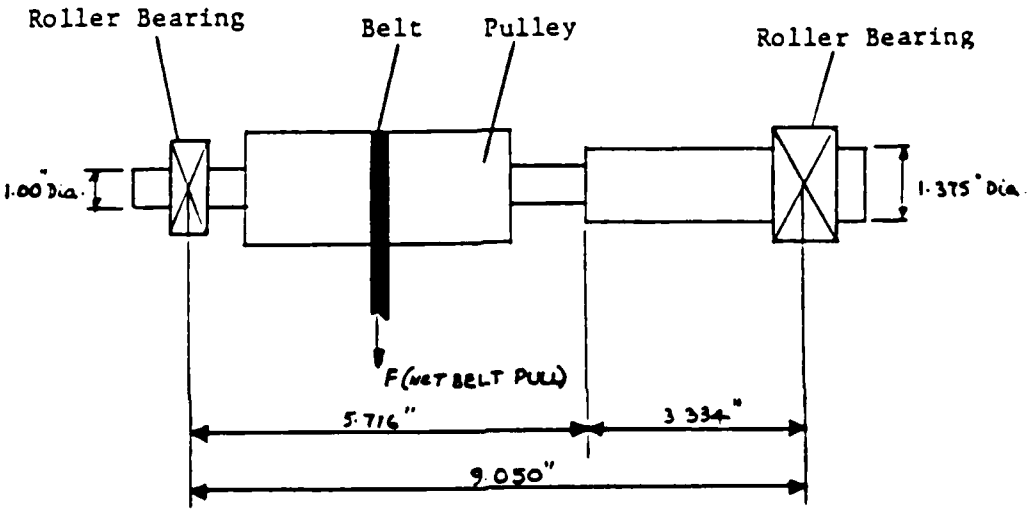

Figure 2.22 Non-Uniform Shaft

For the 1.375 in section:

$$1 \text{ deg } \frac{3.334}{(20)(1.375)} = 0.121 \text{ deg}$$

Since the calculated torsional deflection is less than the above values, the non-uniform drive shaft is sufficiently rigid.

The lateral deformation of the non-uniform shaft is the direct result of the net belt pull of the speed increaser. The net belt pull is 262.96 lb (see Pulleys and Belts) and it acts at point C (see Figure 2.23). Treating the shaft as a non-uniform beam, the deflection, y and slope, θ at points A, B, C, and E were determined using the method of integration [13] and the following boundary conditions:

1) $x = 0;\ y_A = 0$

2) $z = 0;\ y_B = 0$

3) $x = 2.858;\ y_1 = y_2$ and $\theta_1 = \theta_2$

4) $x = 5.716\ (z = 3.334);\ y_2 = y_3$ and $\theta_2 = \theta_3$

Hence,

$y_A = 0;\ \theta_A = 3.863 \times 10^{-6}$ rad or 0.0221 deg

$y_B = 0;\ \theta_B = 1.564 \times 10^{-3}$ rad or 0.0896 deg

$y_C = 1.579 \times 10^{-3}$ in; $\theta_C = 8.852 \times 10^{-6}$ rad or 0.0507 deg

$y_E = 5.315 \times 10^{-3}$ in; $\theta_E = 1.652 \times 10^{-3}$ rad or 0.0946 deg

From static analysis the reactions at A and B were found to be 179.920 lbs and 83.038 lbs, respectively. Note that point E (the point at which the cross-sectional area increases) suffers the largest deflection. Even so this value is far below the misalignment capability of the selected shaft coupling. The maximum parallel misalignment of the coupling is 0.02 in.

It is well known that shafts with an abrupt change in the diameter of its cross-section suffers high stresses at the point of discontinuity

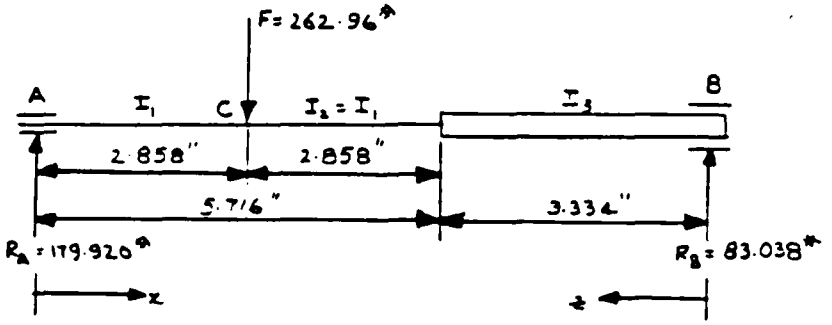

Figure 2.23 Non-Uniform Shaft

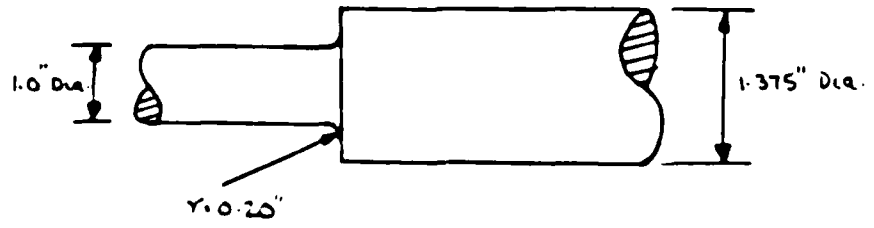

Figure 2.24 Fillet Radius

hence, it is important to determine these stresses. As shown in Figure 2.24, a fillet radius of 0.20 in was selected to reduce the high stresses at point E. The maximum shear stress at this point is determined by [13]

$$\tau_{max} = K \left(\frac{Tr}{J}\right) = 1.2 \left(\frac{(301.11)\ r}{J}\right)$$

where K = 1.2 [9], J (polar moment of inertia of the smaller shaft) = 0.09817 in^4, and r (radius of the smaller shaft) = 0.5 in. Therefore, τ_{max} = 1840.338 psi. A higher value for the maximum shear stress was achieved when the ASME code for the design of transmission shafting was used. In particular, τ_{max} was found to be 2803.339 in-lbs. In any case, both the calculated values are far below the yield strength of the shaft material ($\sigma_{ys}/2$ = 45,000 psi).

The Mounting of Strain Gages and Slip Ring

In order to accommodate the leads from the strain gages to the slip ring, one of the test section shafts is made with a 3/8 in internal bore over its whole length (the overall length of the shaft is 13.875 in, as shown in Figure 2.25). The leads are brought into the shaft through a 1/8 in radial hole bored through the shaft diameter. Since we now have a hollow shaft, the area and inertias of the shaft change. The moment of inertia, I_o, is given by [9]

$$I_o = \frac{\pi}{4} (r^4 - r_o^4)$$

where r_o (radius of the hole) = 0.1875 in. Hence, I_o = 0.1745 in^4. The polar moment of inertia, J_o, is determined by [9]

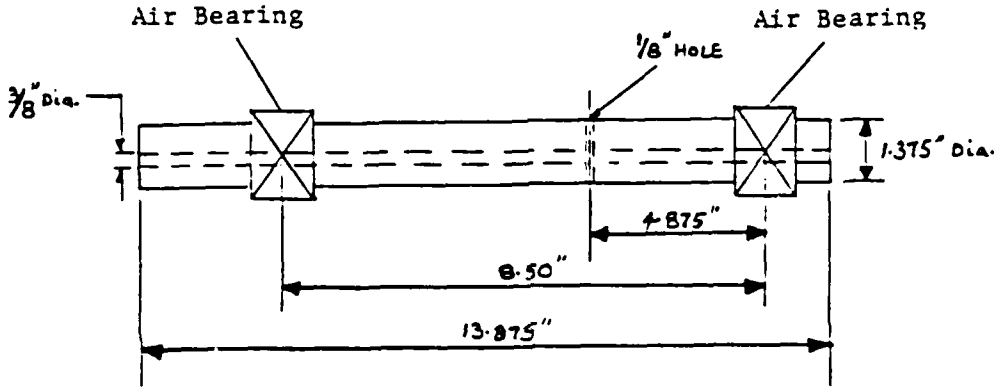

Figure 2.25 Mounting of Strain Rosettes and Slip Ring

$$J_o = \frac{\pi}{2} (r^4 - r_o^4)$$

$$= \frac{\pi}{2} \{(0.6875)^4 - (0.1875)^4\}$$

$$= 0.3490 \text{ in}^4.$$

The shaft cross-sectional area, A_o, is 1.3744 in^2. Note that these values are very close to the values calculated for the solid shaft. In fact, the following data shows that a 3/8 in internal bore has little or no effect on the shaft operation. It is, as though, the hollow shaft is behaving very much like the solid shaft. Following the same procedures as for the solid shaft:

The angular deformation, $\phi = 6.3774 \times 10^{-4}$ rad or 0.03653 deg

The lateral deformation, $y = 4.3490 \times 10^{-4}$ in

The slope, $\theta = 1.5349 \times 10^{-4}$ rad or 8.7947×10^{-3} deg

The natural frequencies for:

The simply supported case: $f_1 = 80.183$ cycles/sec

$f_2 = 320.739$ cycles/sec

$f_3 = 721.663$ cycles/sec

The fixed case: $f_1 = 181.766$ cycles/sec

$f_2 = 501.029$ cycles/sec

$f_3 = 976.986$ cycles/sec

Spring attached case (for k = 10,000 lb/in):

$f_1 = 36.284$ cycles/sec

$f_2 = 161.947$ cycles/sec

When determining the shear stress it is important to take into consideration the 1/8 in transverse hole in the shaft. For a d_o/d ratio of 0.091 (where d_o = diameter of the hole and d = shaft diameter), the

stress concentration factor, K, for torsional loading is 1.86 [9] and the shear stress is given by [9]

$$\tau = 1.86\ (\frac{Tr}{J_o}) = 1.86\ (\frac{(301.11)(0.6875)}{0.3490}) = 1103.279 \text{ psi}$$

Applying the ASME code, the maximum shear stress, $\tau_{max} = 5257.031$ psi. The stress concentration factor for bending is 2.3 [9] and the bending stress is given by [9]

$$\sigma = 2.3\ (\frac{Mr}{I_o}) = 2.3\ \ (\frac{(756.245)(0.6875)}{0.1745}) = 6852.793 \text{ psi}$$

Based on these calculations, Centrall shafts were selected. The Centrall 1045 steel shafts are case hardened and chrome plated to provide corrosion and fatigue resistance. The Centrall shaft has a tolerance range of 1.3745 to 1.3755 in, shaft finish of 10 to 16 micro-inches RMS, and a runout of 0.0005 inches per foot. In order to keep the shaft runout to a minimum and therefore prevent shaft "wobble" during high speeds, Centrall engineers have recommended that shaft length not exceed three feet. More bearings have to be employed, in the event the shaft length has to exceed three feet. The weight and price per inch of shaft are 0.420 lb and $2.20, respectively.

2.2.3. Lubrication System

This section provides a description of the selected lubrication system and the basis for its selection. The main components of the lubrication system along with the drive section of the gear tester will be placed in an acoustically isolated chamber. Therefore, unlike the previous section, noise plays a minor role in the selection of the system components.

The purpose of the lubrication system is to cool and lubricate the mating teeth surfaces of the drive and test gears. Due to the specific requirements of this particular design (Four Square Tester), we have narrowed down the general considerations, which have to be taken into account in the selection of the lubrication system, to the following:

1) Uniformity: The application of the lubricant should be made in a manner that assures complete and uniform distribution between the frictional surfaces. The volume of the lubricant applied is also an important criterion. Excessive amount of lubricant at the tooth mesh will create additional heat (in addition to frictional heat) because of its rapid expulsion from the mesh [11,26].

2) Viscosity: The viscosity of the lubricant plays an important role in the selection of the lubrication system. Since the gear-teeth contact areas are relatively small, the contact unit pressures are comparatively high. It is therefore important to provide a film of lubricant of sufficient strength to withstand the localized pressure during the period of tooth contact. The length of time the lubricant must withstand these local stresses is governed by the pitch-line velocity of the gear set, and hence, when the speeds are high, the gear-tooth contact time is short and the loads are usually light. As a result, a lubricant of a relatively low viscosity can be used [12].

3) Centralized System: A centralized lube system is most practical economically. A lubrication system with a central station consisting of a reservoir and pump can simultaneously serve both the test and drive gears.

4) Automatic and Continuous: A sufficient amount of lubricant must be continuously supplied to the gear surface to sustain an adequate minimum film thickness and maintain safe temperature levels (in well-designed aerospace gears, the temperature rise of the gear body over the incoming oil temperature ought not to exceed 45°F [10]). One form of gear wear, due to inadequate lubrication, is gear scoring, which is especially found in heavily-loaded and fast-running gears. The frictional heat developed in the intra-tooth region of these gears can be severe enough to vaporize the oil film in this region. The break down of the oil film results in metal-to-metal contact of the mating teeth surfaces which in turn leads to welding and radial tearing of the surfaces. This radial tearing action is better known as scoring. A mild extreme pressure (EP) lubricant will often prevent this type of failure because of its ability to prevent welding [10,26].

An automatic system is more accurate, in the sense that frequency and volume rate of lube application can be controlled.

Based on the above considerations and following a survey of various types of lubrication systems commercially available, the following specifications were selected:

1. an oil lubrication system with spray nozzles of the atomizing type.
2. spray nozzles with desired volume rate and spray pattern.
3. a central reservoir with a capacity to hold 2 to 3 quarts of oil.
4. SAE 90 oil (this oil type is most suitable for helicopter gear boxes where extreme-pressure properties are required. The maximum viscosity rating of this oil at 210°F is 120 SUS (Saybolt Universal Seconds). It is estimated that our operating oil temperature will not exceed the 200°F [10].
5. a pump large enough to force oil to the gears.
6. adjustability of the pump stroke (to regulate the amount of oil sprayed onto the gears).
7. a source of air at 50 to 100 psi.

Based on these specifications a Farval Single Line Pressure-Spray Lubrication system was selected. A pressure-spray lubrication system was selected for the following primary reasons:

1) Pressure-spray lubrication is one of the most effective methods of distributing the lubricant uniformly over frictional surfaces of high speed gears.
2) The application of the oil spray can be done [illegible] and continuously.
3) The combination of a centralized system [illegible] of the pump stroke makes the pressure [illegible] system the most efficient and cost [illegible] lubricating high speed gears

The purchased matching components of [illegible] are the following:

AD-A181 902 THE DESIGN OF A FOUR SQUARE GEAR TESTER FOR NOISE AND 2/2
VIBRATION MEASUREME (U) PENNSYLVANIA STATE UNIV STATE
COLLEGE APPLIED RESEARCH LAB S V VILANILAM ET AL
UNCLASSIFIED DEC 86 ARL/PSU/TR-87-002 F/G 14/2 NL

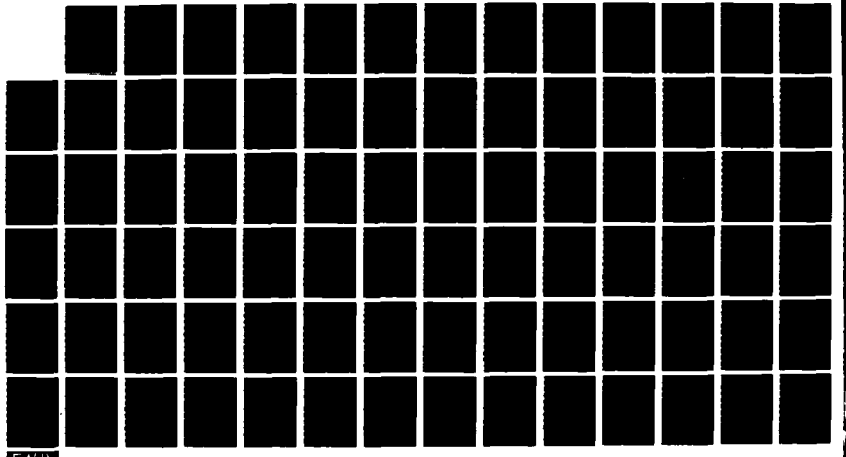

END

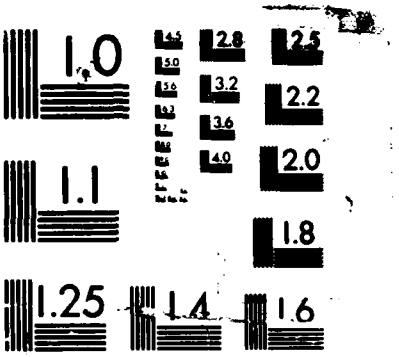

MICROCOPY RESOLUTION TEST CHART

1) A central reservoir with the capacity to store and provide oil to the gears for approximately 16 hours of continuous operation of the tester.

2) A pump large enough to force oil to the gears.

3) A pressure gauge to monitor the outlet pressure of the pump and to prevent hazardous over pressuring of the system.

4) A timer that allows the appropriate oil application frequency and interval of discharge.

5) Spray nozzles with the desired volume rate and spray pattern.

6) Valves and manifolds to direct and meter the flow of oil and air.

7) Air regulators, filters, and lubricators to provide clean and dry air to the pump and maintain smooth and safe operation.

8) The appropriate piping large enough to carry the required volume of oil and air from the pump to the gears at a safe unit pressure.

The Farval Single Line Pressure-Spray Lubrication system is an automatic and quasi-continuous spraying system with the following desirable features:

1) The lubricant is supplied to the gears from a central source that consists of an oil reservoir, pneumatic pump, pressure gauge, and rupture pressure disk indicator. The oil reservoir is mounted on the pump and the oil is fed into the pump via gravitational forces (gravity feed). The reservoir has a transparent plastic body (hence, eliminating the need for an oil level indicator) and a capacity to hold 2.5 quarts of oil. The reservoir is filled from the top through an oil fill cap and filter screen.

   The Farval pneumatic pump has an helical spring attached to its piston. A minimum air pressure of 50 psi is needed to compress the pump spring and activate the piston. The forward thrust of the piston sends a pulse of oil to the spray nozzles. The discharge capacity of the pump is between 0.015 and 0.068 cubic inches per stroke (Farval engineers have suggested an initial setting of 0.068 cubic inches per stroke). The pump also consists of an indicator stem with an adjustment screw that allows the regulation of the pump stroke. The total lube quantity discharged can be increased or decreased by adjusting the pump stroke. The frequency of the stroke is regulated by a non-adjustable cam type timer that allows one pump stroke every four seconds. To monitor the pump output oil pressure,

a pressure gauge, with a 3000 psi capacity, and a rupture pressure disc indicator are attached at the pump outlet. The rupture pressure disc indicator acts as a relief valve. In the event the pump output pressure exceeds 3000 psi, the 3/8 in rupture disc will burst, but will allow the lubricant to continue its flow.

2) The cam type non-adjustable timer allows an interval of oil and air discharge (from the nozzles) of 2.0 seconds (i.e., lube is continuously applied to the gears for 2.0 secs). It has a fixed "on" and "off" time of 2.0 seconds. The voltage rating of the timer is 120 V at 60 hz.

3) The design of the Farval spray nozzle is such that the viscosity of the lubricant cannot exceed 2000 SUS, the volume of lube discharge per cycle is 0.005 cubic inches, and the spray pattern takes the form of a cone with an approximate cone angle of 18 degrees (see Figure 2.26). The volume rate of the nozzle can be determined by multiplying the volume of spray by the frequency of application. Since the frequency of oil application is 0.25 cycles per second, the

$$\text{volume rate of spray per nozzle} = (0.005)(0.25) = 1.25 \times 10^{-3} \text{ in}^3/\text{sec}$$

or 4.340×10^{-5} ft^3/min. For two nozzles the volume rate of spray is 8.681×10^{-5} ft^3/min. At this volume rate of lube discharge, a 2.5 quart reservoir will supply oil to the nozzles for approximately 16 hours. Figure 2.26 also shows the angle and distance at which the spray nozzles should be positioned relative to the gears. The maximum working pressure of the nozzle is 500 psi.

4) The timer is connected to a three way solenoid pneumatic valve. The main functions of the valve are to cycle the pump and blow the lubricant from the spray nozzles. The Farval solenoid valve has a maximum operating pressure of 150 psi and a voltage rating of 120 V at 60 Hz. At this voltage, the valve in-rush current and holding current are 0.12 amps and 0.09 amps, respectively. The Farval manifold acts as a splitter valve. In other words, the oil flow into the manifold is divided equally among the nozzles.

5) The air line filter will allow an airflow of 200 SCFM (Standard Cubic Feet per Minute) and tolerate air pressures up to 150 psi. The maximum operating temperature of the 40 μ porous bronze filter is 120°F. The air line regulator, with pressure gauge, will allow an airflow of 400 SCFM at a maximum pressure of 400 psi. The lubrication system has two of these regulators to allow independent control of air discharge to the nozzles and pump. The Farval air line lubricator is able to withstand a maximum air pressure of 150 psi and a maximum temperature of 120°F.

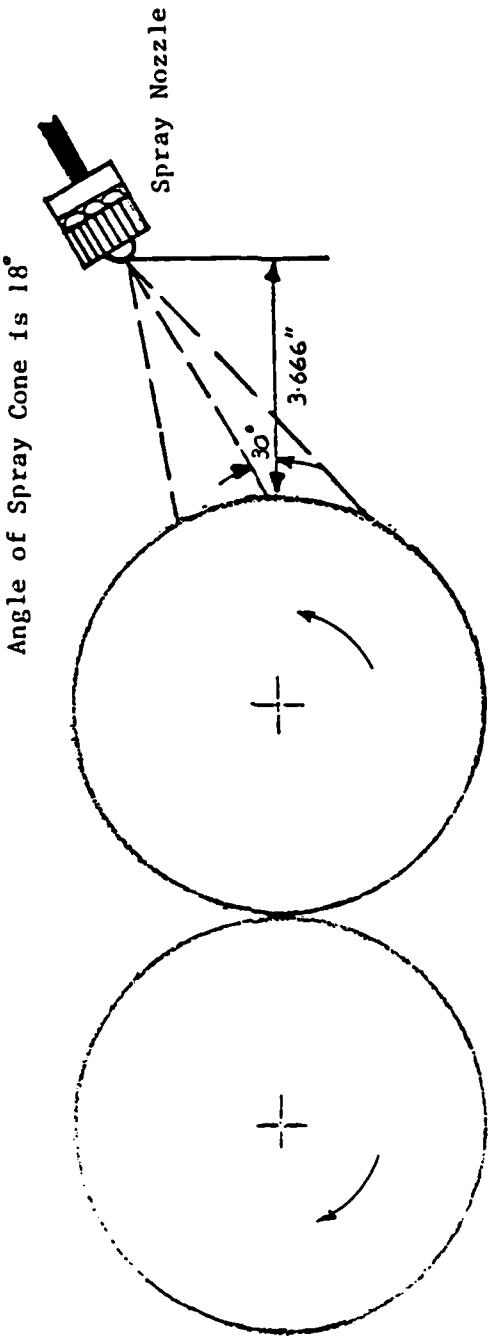

Figure 2.26 Spray Pattern of Farval Spray Nozzle

6) The Farval piping includes medium and low pressure hoses, hose couplings and unions, street and anchor elbows (used for connecting pipe-to-pipe, for adding branch lines, or for changing lube line direction), and line strainers (to remove foreign particles from oil lines). The medium pressure hose has a synthetic rubber casing and wire braid reinforcement. It has a working pressure of 2,750 psi, a burst pressure of 11,000 psi, minimum bend radius of 4 in, and a temperature range of -40 to +200°F. The low pressure hose has a synthetic rubber casing with cotton braid reinforcement. It has a working and burst pressure of 500 and 2000 psi, respecitvely, a minimum bend radius of 3 in, and an operating temperature range of -40 to +200°F. The street elbows are zinc plated with a maximum working pressure of 3500 psi. The anchor elbows are also zinc plated but with a maximum working pressure of 6000 psi. The Farval wire mesh screen type line strainer can tolerate oil viscosities up to 2000 SUS and can withstand up to 5000 psi working pressure.

A schematic of the Farval automatic pressure-spray lubrication system is shown in Figure 2.27. As shown, air supply at 50 to 100 psi enters an air filter. The filtered air then enters a three way solenoid valve which is connected to a timer. The timer controls the valve which will do two things, cycle and pump and blow the lubricant from the spray nozzles. Once the air leaves the valve it enters the air regulators. The system is supplied with two regulators to independently control the discharge of air to the pump and nozzles. Air from regulator 1 directly enters the spray nozzles. Air from regulator 2 first enters an air lubricator and then enters the pump. When air pressure is applied to the pump a piston moves against a spring and forces a measured amount of lubricant out of the pump. This lubricant is forced into the splitter valve (manifold) where it is atomized by the air flow through that nozzle and sprayed onto the gear. The excess oil in the manifold is fed back into reservoir through the oil return line. When the "on" period of 2.0 seconds is over, the solenoid valve relieves the pressure from the pump. This allows the piston in the pump to reset itself. The air valve also stops the air flow through the spray nozzles.

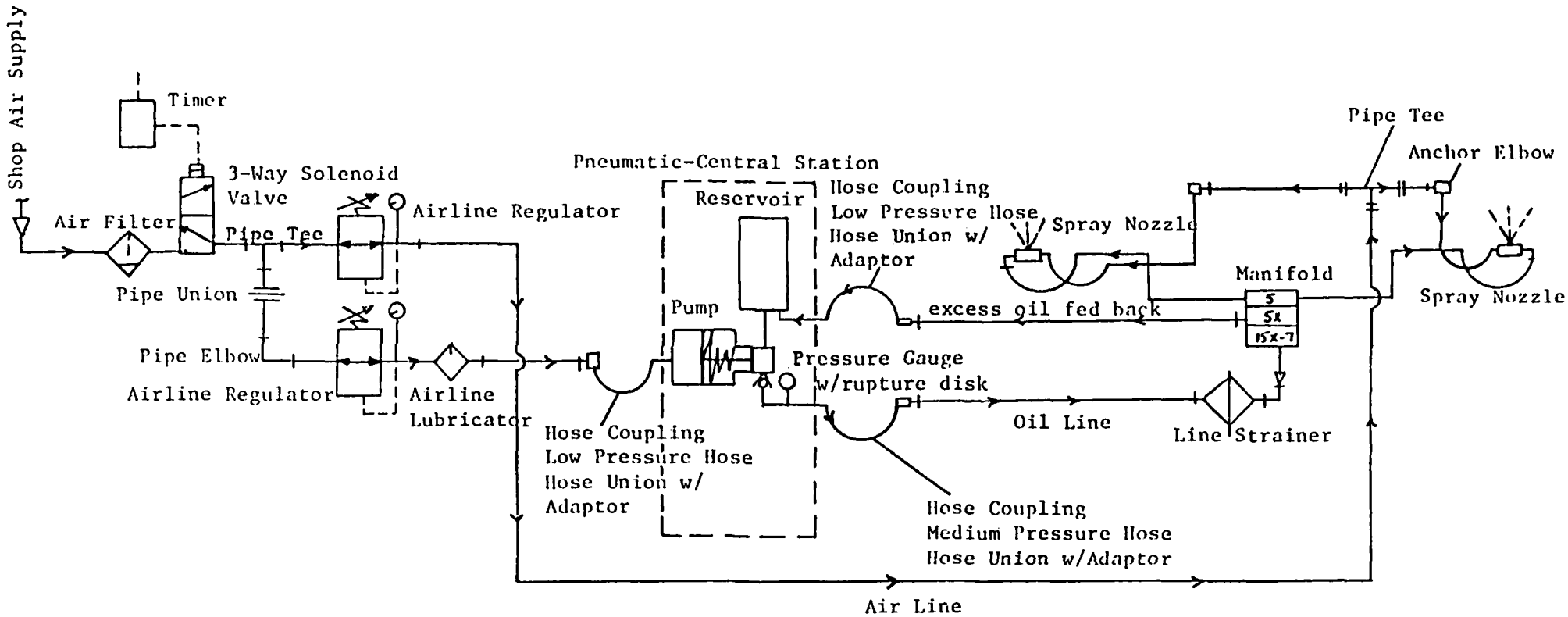

Figure 2.27 Farval Lubrication System

Since the system is not equipped to recirculate the oil, the used oil will be collected in an oil pan located at the bottom of the test and drive section of the gear box. The pans will be periodically removed and emptied. The total cost of the Farval lubrication system is approximately $1290.75. There will be some 1/4 in and 3/8 in outer diameter tubing required. The cost of the tubing is $0.45 and $0.75 per foot, respectively.

3.0 INSTRUMENTATION

This section provides a brief description of the instrumentation system selected to monitor speed, vibration, noise, and torque. This instrumentation system consists of:

1) A high precision tachometer-generator for recording shaft speed.

2) An accelerometer to measure shaft vibration.

3) A hydrophone to measure gear noise.

4) Strain rosettes coupled with a slip ring to measure shaft torsional strain and bending.

The following paragraphs will describe the individual components in the order listed above:

Tachometer-Generator

In order to monitor the shaft speed, a high precision tachometer-generator was purchased along with the selected Contraves motor system. This particular tachometer enables the experimenter to achieve the desired 0.1% long term shaft speed stability. The tachometer is temperature compensated, possesses a ripple of 0.5%, and has an extremely linear voltage-speed relationship throughout its entire speed range, providing accurate regulation for shaft velocity feedback. The output variations due to temperature and ripple are held to a minimum. It also features a two-pole construction with antifriction ball bearings, and a totally enclosed non-ventilated steel frame. The tachometer weighs 35 lbs.

Accelerometer

The accelerometer selected to measure shaft vibration is a Bruel & Kjaer piezoelectric transducer that has the following desirable features:

1) It offers excellent immunity to temperature transients and acoustic noise. The temperature transient sensitivity is $\frac{16 \text{ ft } s^{-2}}{°C}$ for 3 Hz (lower limiting frequency) and 20 dB/decade.

2) It has an ambient temperature range of -101 to 482°F.

3) The frequency response is relatively flat and within the range of interest. The relative response of this accelerometer is +2 dB at 25 KHz.

4) It has a charge sensitivity of $\frac{0.09627 \text{ pC } s^2}{\text{ft}}$ (or 3.1 pC/g).

5) It has a mounted resonance of 55 KHz.

6) It is lightweight (0.00528 lbs) and small in size. The dimensions of the Bruel and Kjaer accelerometer is given in Figure 3.1.

7) It has an acoustic sensitivity of $\frac{0.129 \text{ ft}}{s^2}$ (It must be noted that the acoustic sensitivity is specified as the equivalent acceleration given by a 154 dB sound pressure level which is 2 to 100 Hz).

8) The mounting of the Bruel and Kjaer accelerometer is fairly simple. One accurate method to mount the accelerometer onto the test section shaft is shown in Figure 3.2. Here, a 10-21 UNF steel stud is used to screw the accelerometer onto the shaft. To accommodate the stud, it is necessary to drill a transverse hole, 0.1575 in in depth, into the shaft. The optimum torque for tightening the stud is 15 in-lbs. For improved mounting stiffness a thin film of silicon grease should be applied to the base of the accelerometer before screwing it down onto the shaft.

Along with the accelerometer a Bruel & Kjaer charge amplifier was also selected to condition the signal before input into an analyzer. This particular amplifier was selected for its low noise characteristics and selectable low and high frequency cutoffs. The cost of the accelerometer with charge amplifier is $2916.00.

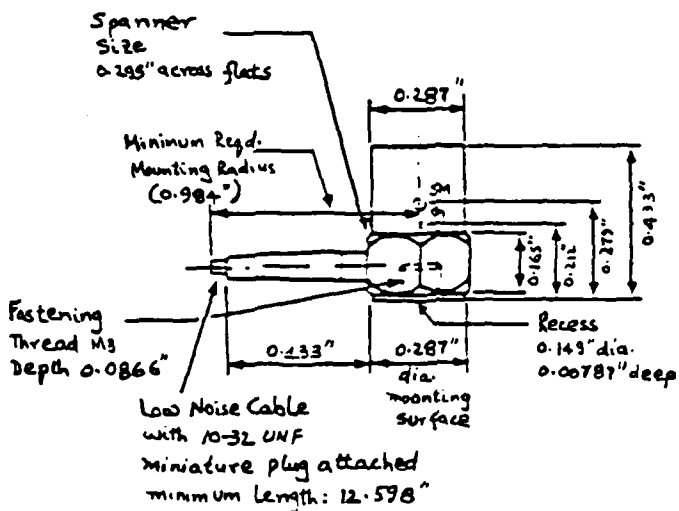

Figure 3.1 Bruel and Kjaer Accelerometer

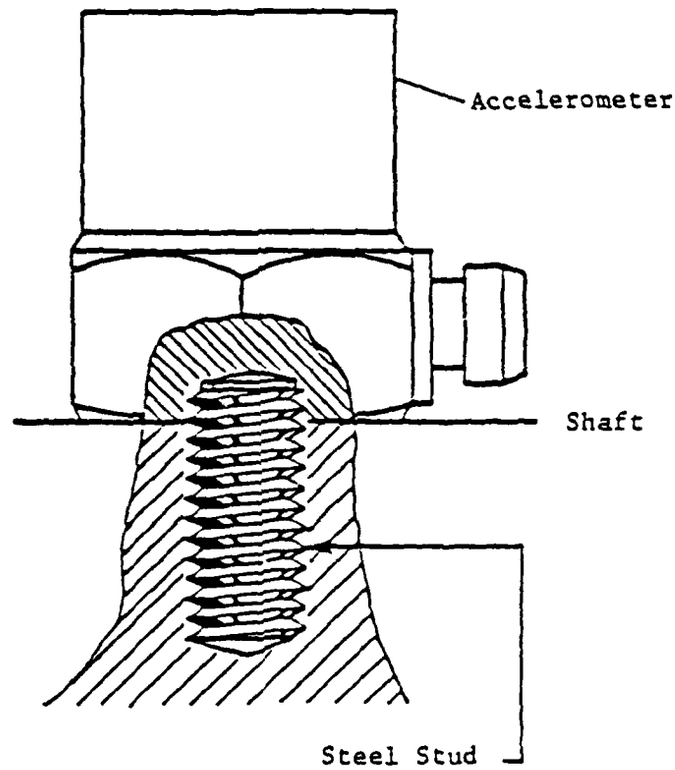

Figure 3.2 Mounting of Bruel and Kjaer Accelerometer

Hydrophone

Because of the severe environmental conditions inside the test section gear box, a hydrophone was selected (as opposed to a microphone) to measure the gear noise. The selected Bruel and Kjaer hydrophone has the following desirable features:

1) It is oil resistant.

2) Its frequency response in air, as shown in Figure 3.3, is 0.1 Hz to 15 KHz (-3 dB), 25 KHz (-5 dB).

3) The operating temperature range of the hydrophone is -40 to 248°F.

4) The dynamic range in air is 74 to 226 dB re 20 μPa (2 Hz to 25K Hz).

5) Its sensitivity change with temperature:

$$\text{charge} \leq + 0.017 \text{ dB/°F}$$
$$\text{voltage} \leq - 0.017 \text{ dB/°F}$$

6) It is lightweight (0.374 lb with cable) and small in size. The dimensions of the hydrophone are provided in Figure 3.4.

7) Because of its size, the hydrophone can be dropped from the ceiling of the test gear box to pick up the noise emitted from the gear mesh region.

Along with the hydrophone a charge amplifier is needed to condition the signal before input into the analyzer. The charge amplifier selected for the accelerometer can be employed for this purpose. The cost of the hydrophone alone is $952.00.

Strain Rosettes and Slip Ring

In order to measure the shaft torsional strain and bending, strain rosettes and a slip ring were selected. The strain rosettes are installed diametrically opposed on the shaft (with the 3/8 in axial hole; see Shafts) of the test section gear box. The leads of the rosettes are

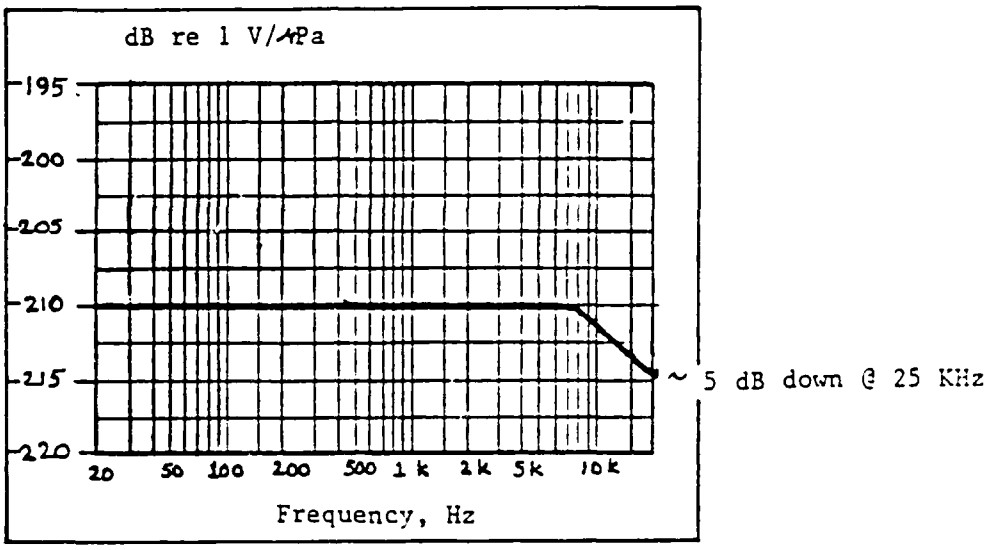

Figure 3.3 Frequency Response in Air of Bruel and Kjaer Hydrophone

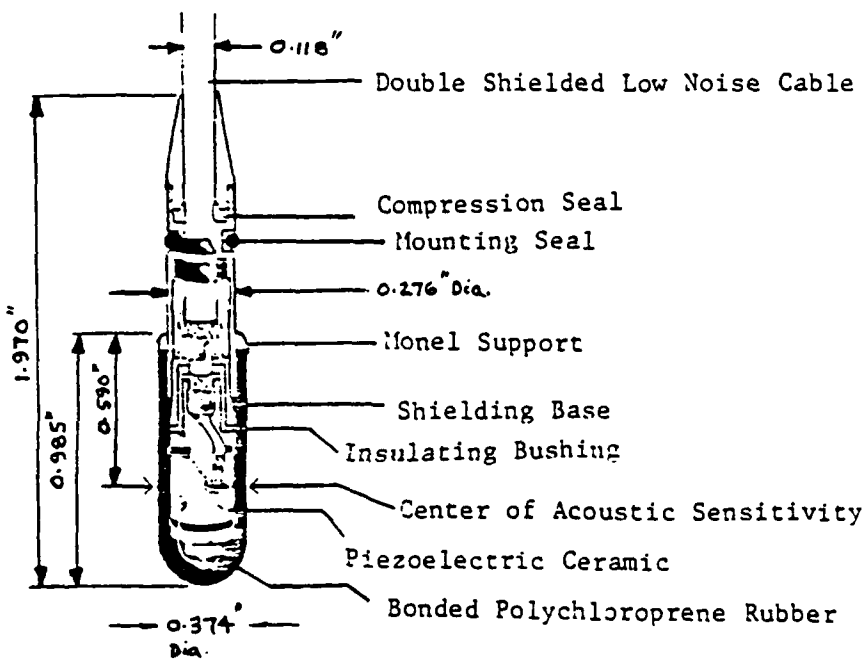

Figure 3.4 Bruel and Kjaer Hydrophone

brought through the axial hole and wired to the slip ring which is mounted on the end of the shaft. The selected gages, manufactured by Micro-Measuremetns Group, are three element 45 deg rosettes that are designed to measure both torque variations and bending. In addition, the gages have the following desirable characteristics:

1) They have a strain range of $\pm$ 5%.

2) The fatigue life of these gages is greater than 10^5 cycles at a strain level of $\pm$ 1500 x 10^{-6}.

3) They are self-temperature compensated and have a temperature range of -100 to +400°F.

4) They are designed for quick and easy installation. The lead wires are directly soldered to the copper-coated solder tabs of the gages.

5) The gage resistance is 350 $\pm$ 0.4%.

The price of each three-element 45 deg rosette is $95.00. The selected slip ring is manufactured by IEC Corporation. The maximum operating speed of the slip ring is 7000 rpm. But, with the proper freon cooling, it can exceed its maximum operating limit. The slip ring is mounted on the end of the shaft via steel studs (similar to the technique used to mount the accelerometer). It is equipped with 8 rings (4 for bending and 4 for torsion) to accommodate the leads from the strain gages. The price of the IEC slip ring is $1550.00.

3.1. Electrooptical Techniques

In order to accommodate the non-intrusive electrooptical techniques, such as, Laser Doppler Velocimetry (LDV) and Laser Doppler Vibrometry (LDV), the test section gear box is equipped with 4 plexiglass

viewports. These viewports allow beams from coherent laser sources to be inserted at the point (gear mesh region) where certain measurements are specified.

4.0 ASSEMBLY DRAWINGS

This section provides the drawings for the Four Square Gear Tester. The front, top, and side view of the test section are shown on the following pages. This section also provides the top and side view of the drive section.

The drawings are done to 1/2 scale and the dimensions are in inches.

NO.	PART	DRWG NO.
1	SHAFT	—
2	AIR BEARING HOUSING	—
3	TEST SECTION HOUSING	HC100 SP100 SP100 SP100
4	"O" RING GROOVE	OR100
5	GEAR	—
6	CLAMP PLATE	CP400
7	OIL PAN	OPS 500 OIE 500 OIB 500
8	HOLE FOR STRAIN GAGE LEADS	—
9	VIEW PORT	VP 600 OR 600
10	OIL SPRAY	—
11	SPRAY NOZZLE	—

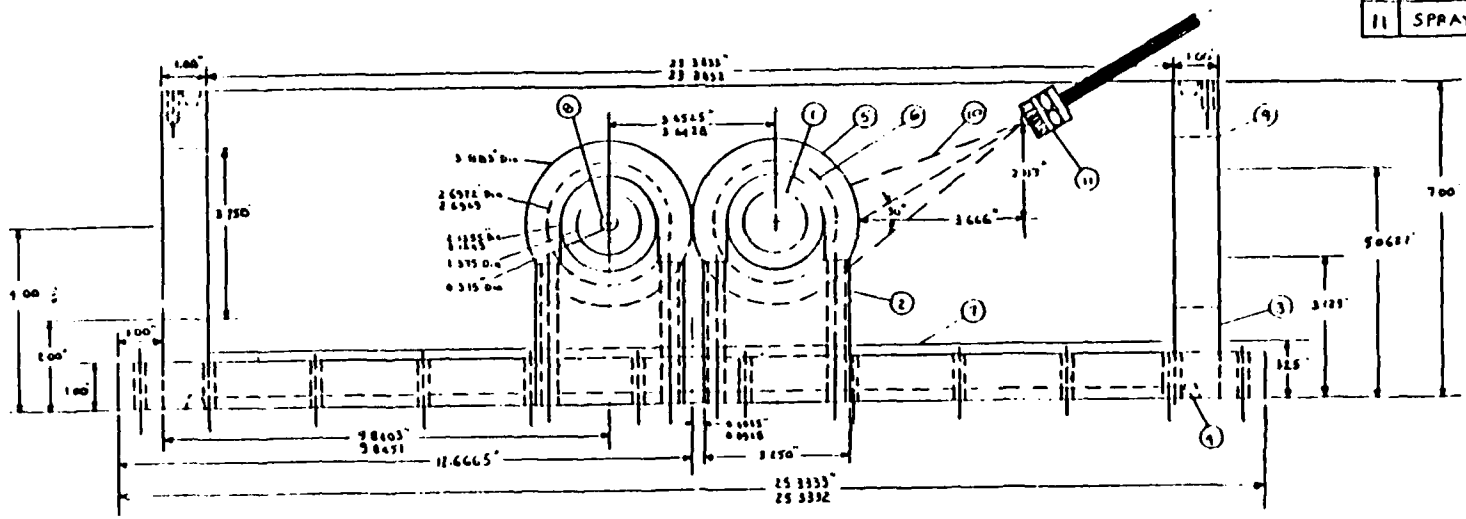

1 THE COVER PLATE WILL HAVE TO BE DRILLED TO ACCOMMODATE THE SPRAY NOZZLE.

TITLE: FOUR SQUARE GEAR TESTER

PART: TEST SECTION, FRONT VIEW

SCALE: 1/1

DATE: 10/25/85

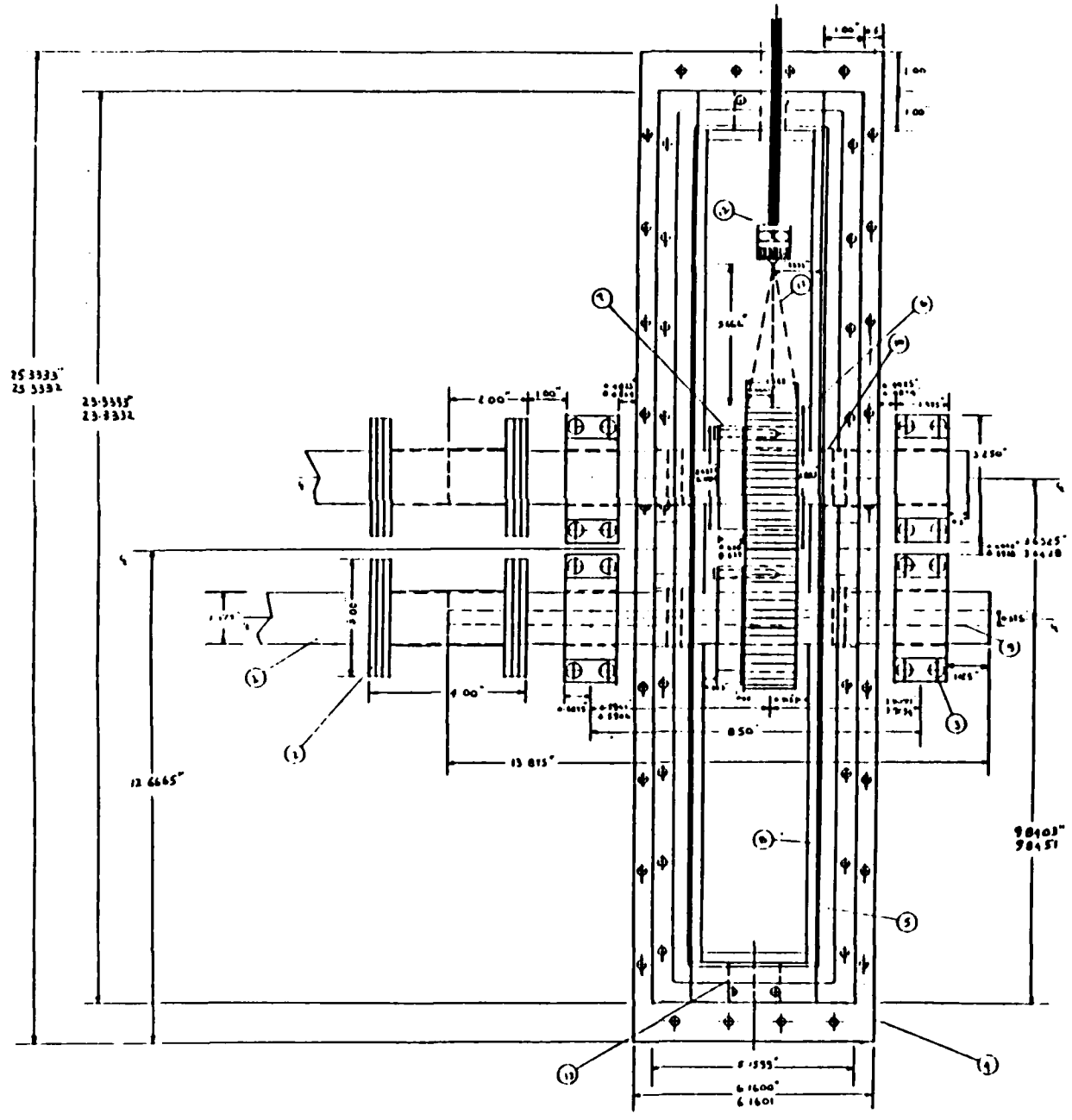

NO.	PART	DRWG. NO.
1	SHAFT	—
2	FLEXIBLE DISC COUPLING	—
3	AIR BEARING HOUSING	—
4	TEST SECTION HOUSING	HC 100 SP 100 E 100 DP 100
5	"O" RING GROOVE	OG 200
6	GEAR	—
7	CLAMP PLATE	CP 400
8	OIL PAN	OPS 500 OPC 500 OPB 500
9	HOLE FOR STRAIN GAGE LEADS	—
10	ACOUSTIC SEAL	—
11	OIL SPRAY	—
12	SPRAY NOZZLE	—
13	VIEW PORT	VP 600 041 00

TITLE	FOUR INCH SPACE WATER
PART	TEST SECTION, TOP VIEW
SCALE	FL
DATE	10/23/81
DRAWN BY	Frederick V. Hanlon

NO.	PART	DRWG NO
1	SHAFT	—
2	FLEXIPLE DISC COUPLING	—
3	AIR BEARING HOUSING	—
4	TEST SECTION HOUSING	HC 100 SP 100 EP 100 BP 100
5	"O" RING GROOVE	C6L00
6	GEAR	—
7	CLAMP PLATE	CP400
8	OIL PAN	OPS 500 OPB 500 OPB 500
9	WELL FOR STRAIN GAGE LEADS	—
10	ACOUSTIC SEAL	—
11	VIEW PORT	VP600 OVP 600

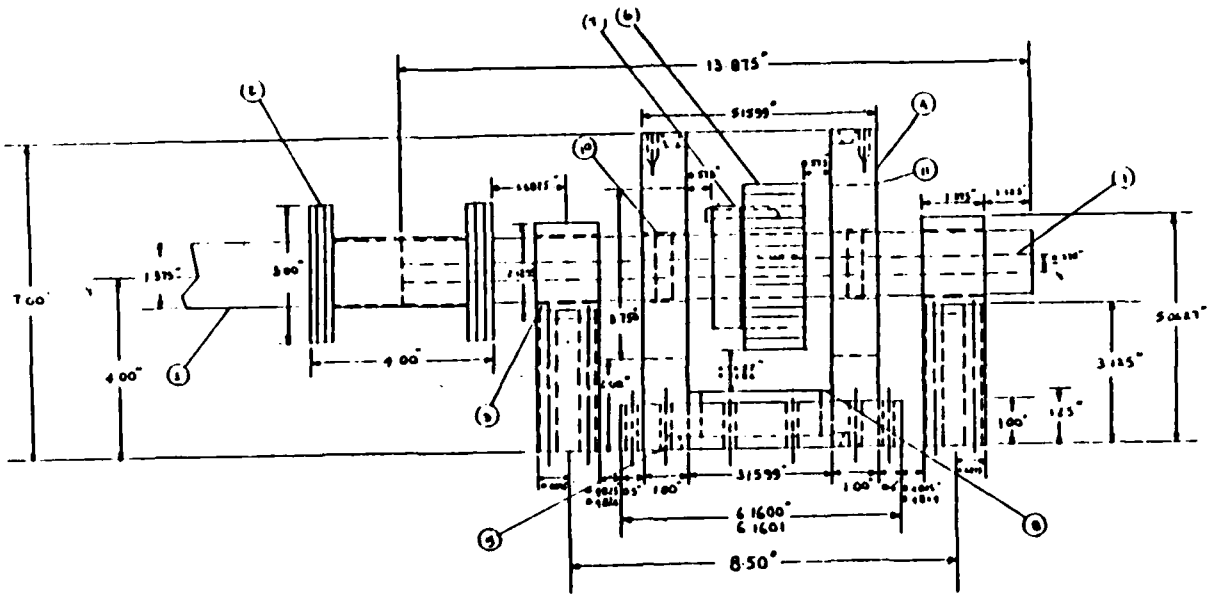

TITLE: 8mm SQUARE GEAR TESTER

PART: TEST SECTION, LEFT SIDE VIEW

SCALE: 1/2

DATE: 12/29/89

DRAWN BY: Samuel Hamilton

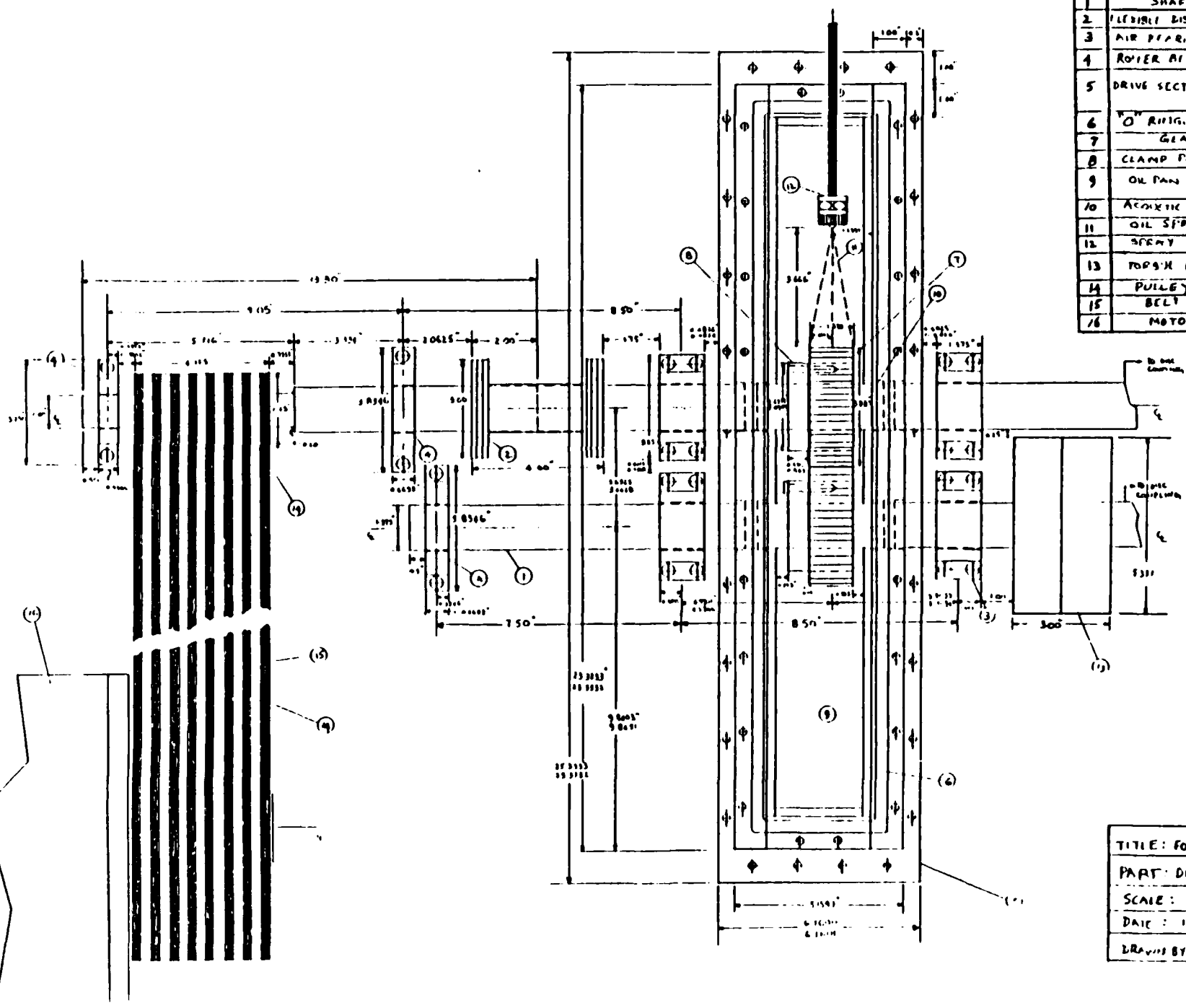

No	PART	REMARKS No.
1	SHAFT	—
2	FLEXIBLE BISC COUPLING	—
3	AIR BEARING HOUSING	—
4	ROLLER BEARING HOUSING	—
5	DRIVE SECTION HOUSING	
6	"O" RING, GLAND NUT	
7	GEAR	—
8	CLAMP PLATE	
9	OIL PAN	
10	ACOUSTIC SEAL	—
11	OIL SPRAY	—
12	SPRAY NOZZLE	—
13	TORQUE FLANGE	—
14	PULLEY	
15	BELT	—
16	MOTOR	—

TITLE:	FOUR SQUARE GEAR TESTER
PART:	DRIVE SECTION, TOP VIEW
SCALE:	1/2
DATE:	10/27/86
DRAWN BY:	Santosh Vilanilam

NO.	PART	DRWG. NO.
1	SHAFT	—
2	FLEXIBLE DISC COUPLING	—
3	AIR BEARING HOUSING	—
4	ROLLER BEARING HOUSING	—
5	DRIVE SECTION HOUSING	HC100 SP100 EP100 BF100
6	"O" RING GROOVE	>>>>>
7	GEAR	—
8	CLAMP PLATE	CP400
9	OIL PAN	OPS100 OPH100 OPB100
10	ACOUSTIC SEAL	—
11	TORQUE FLANGE	—
12	PULLEY	P600
13	BELT	—

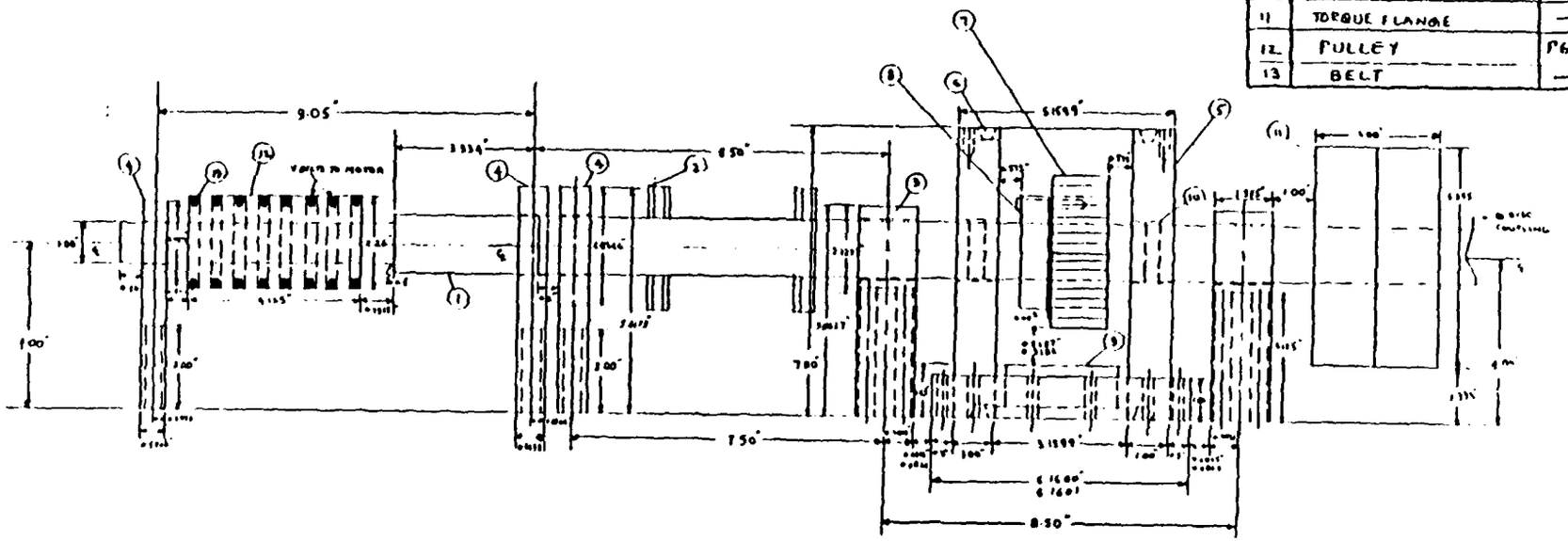

TITLE	FOUR SQUIRE HARMONIC
	BASIC SECTIONAL SIDE VIEW
SCALE	½
DATE	10/12/96
DRAWN BY	[illegible]

5.0 EQUIPMENT LISTS AND COSTS

This section provides the price list for the selected mechanical components, lubrication system, standard instrumentation system, and wide flange beams and steel plates (for the test and drive section stand).

The total cost of the selected mechanical components and lubrication system is $32,384.12. If the cost of the instrumentation system and wide flange beams and steel plates are taken into account, the total expenditure for this project increases to $42,883.99.

The Price List for the Mechanical Components

Description	Company	Part Number	Quantity Required	Unit Price $	Total Price $
Motor					
60 H.P. D.C. shunt-wound electric motor	Contraves Goertz	328AT	1	----	----
Regenerative SCR controller	" "	ADB/F 460.145	1	----	----
Top Mount Drip-Proof Blower	" "	320AT	1	----	----
Tachometer-Generator	" "	XC46 D.C. 100V/1000 rpm	1	----	----
Isolation Transformer in NEMA 1 Enclosure	" "	75KVA 230 V input, 460 V secondary	1	----	----
Floor Mount in NEMA 12 Enclosure with Fan Ventilation. Size 48 x 36 x 16 in	" "	----	1	----	----
Total Cost of the Motor System					20422.00

Description	Company	Part Number	Quantity Required	Unit Price $	Total Price $
Belt-Drive					
Driver Pulley with QD Bushing	Dayco	8-3V80	1	----	80.83
Driven Pulley	"	8-3V2.25	1	----	91.76
V-Belt	"	8-3VX630	8	9.98	79.84
Total Cost of the Belt-Drive					252.43
Air Bearings and Accessories					
Air Bearings	Masten-Apex	AAB-2234-11	12	96.34	1156.08
Air Tank	Compressed Air Products, Inc. (Distributor of Manchester Tanks)	V-2412	1	----	480.00
Air Compressor	Compressed Air Products, Inc. (Distributor of Powerex Compressors)	GI-20	1	----	5904.00
Airline Filter	Compressed Air Products, Inc. (Distributor of Arrow Products)	F329-06	1	----	51.00
Total Cost of the Air Bearings and its Accessories					7591.08

Description	Company	Part Number	Quantity Required	Unit Price $	Total Price $
Roller Bearings					
Cylindrical Roller Bearing for One Inch Shaft	SKF	NUP 205 EC	1	----	39.72
Cylindrical Roller Bearings for 1.375 in Shaft	"	NUP 207 EC	2	35.57	71.14
Total Cost of the Roller Bearings					110.86
Shaft Couplings					
Thomas Flexible Couplings	Rexnord	Style CC Size 100	5	452.20	2261.00
Locking Element (Gear Mount)					
Aluminum Rings	Ringfeder	GSA-1375	4	4.00	16.00
Shafts					
1045 Case Hardened and Chrome Plated	Centrall-Centerless Grinding	----	estimated length (total) = 200 in	2.20	440.00
Total Cost of the Mechanical Components					31093.37

The Price List for the Lubrication System Components

Description	Company	Part Number	Quantity Required	Unit Price $	Total Price $
Pneumatic Central Station (includes pneumatic pump, pressure gauge, reservoir)	Kerry (distributor of Farval products)	TS30-GECXX	1	----	411.00
Cam Timer	"	LE-9721-B	1	----	199.00
3-Way Solenoid Way	"	U-10626-A1	1	----	150.00
Air Line Filter	"	F602-2	1	----	25.00
Air Line Lubricator	"	F606-2	1	----	31.00
Air Line Regulator w/Gauge	"	F119-2G	2	30.10	60.20
Spray Nozzle Assembly	"	U922-B	2	50.00	100.00
Single-Line Manifold w/Cycle Indicator (15XRC-7L, 5X, 5)	"	1001-3-7	1	87.00	87.00
Anchor Elbow	"	U-1927-B	5	5.80	29.00
Low Pressure Hose	"	U-702C	16 ft	2.35	37.60
Hose Coupling	"	U-404B1	3	2.35	7.05
Hose Coupling	"	U-404B2	3	2.95	8.85
Hose Union with Adaptor	"	U-407B2	6	4.35	26.10

Continued.

Description	Company	Part Number	Quantity Required	Unit Price $	Total Price $
Medium Pressure Hose	Kerry (distributor of Farval products)	201200	2 ft	3.05	6.10
Hose Coupling	"	201186	1	----	3.50
Hose Union	"	201188	1	----	4.35
Adaptor	"	U-431-4-4	1	----	1.35
Street Elbow	"	U-1104A	1	----	1.45
Street Elbow	"	U-1104B	4	2.95	11.80
Line Strainer	"	LS-02-106	1	----	32.00
Nipple	"	U-101-A3	1	----	1.45
Nipple	"	U-101-B5	7	2.35	16.45
Bushing	"	U-104-B1	1	----	1.00
Pipe Elbow	"	U-103-B	2	2.90	5.80
Pipe Union	"	U-115-B	1	----	8.10
Pipe Tee	"	U-117-B	2	4.35	8.70

Continued

Description	Company	Part Number	Quantity Required	Unit Price $	Total Price $
Straight Connector	Kerry	U-83-B1	1	----	0.85
Straight Connector	"	U-83-B2	3	1.05	3.15
Straight Connector	"	U-83-D2	6	2.15	12.90
Total Cost of the Lubrication System					1290.75

The Instrumentation Price List

Description	Company	Part Number	Quantity Required	Unit Price $	Total Price $
Tachometer-Generator	Contraves	XC46 (100V/1000 rpm)	1	----	see Motor
Accelerometer	Bruel and Kjaer	4375	1	----	737.00
Hydrophone	"	8130	1	----	952.00
Charge Amplifier	"	2635	2	2179.00	4358.00
Strain Rosettes	Micro-Measurements Group	CEA-06-125UR-350	2	95.00	190.00
Slip Ring	IEC Corp.	IEC-FR-LB	1	----	1550.00
The Total Price of the Standard Acoustic, Strain, and Vibration Instruments					7787

The Price List for the W Beams and Steel Plates

Description	Company	Part Number	Quantity Required	Unit Price $	Total Price $
Wide Flange Beam	Ryerson	W 27 x 146 (length = 96 in)	2	468.49	936.98
"	"	W 27 x 146 (length = 48 in)	2	162.66	325.33
Side Plate (drive section)	"	1/2 x 96 x 24.74	2	131.52	263.04
Side Plate (test section)	"	1/2 x 48 x 24.74	2	70.76	141.52
End Plate (drive section)	"	1/2 x 60 x 24.74	2	85.90	171.81
End Plate (test section)	"	1/2 x 36 x 24.74	2	55.61	111.23
Top Plate (drive section)	"	1/2 x 96 x 60	1	----	314.61
Top plate (test section)	"	1/2 x 48 x 36	1	----	108.35
Vibration Mount	Vibration Eliminator Co., Inc.	OCTLS2	10	34.00	340.00
The Total Price of W Beams, Plates, and Vibration Mounts					2712.87

6.0. CONCLUSIONS

The four square method is perhaps the most effective means of investigating sources of gear noise and vibration. Due to the simplicity of its arrangement, it was possible to design the Four Square Gear Tester with a high degree of accuracy. A substantial effort was made in selecting components with low levels of noise and vibration. Hence, it now appears possible to measure and study gear noise due to dynamic loads and fluid dynamics without being pre-occupied with extraneous noise sources, created by the components, which tend to mask the basic noise and vibration sources in the gears.

The designed test apparatus is strictly for light load testing. The intensity of tooth loading or K-factor should be kept within 70 psi. Therefore, a 10 hp motor can be used to drive the gears, and thus, keep the cost of building the machine to within $25,000 to $30,000. It is important to bear in mind that this design is in the exploratory stage and hence, design changes will have to be made to accommodate unforseen problems.

REFERENCES

1. Pechersky, M. J. Personal Correspondence, 1986.

2. Greeves, C. S. "Gear Noise," Noise Control and Vibration Reduction, June 1974.

3. Shigley, J. E. Mechanical Engineering Design, McGraw-Hill, 1963.

4. Rosen, M. W. "The Noises of Two Spur Gear Transmissions," Navord Report 6569, July 27, 1959.

5. Yuruzume, I., H. Mizutani, and T. Tsubuku. "Transmission Errors and Noise of Spur Gears Having Uneven Tooth Profile Errors," Trans. ASME, J. Mechanical Design, Vol. 101, April 1979.

6. Deutchman, A. D., W. J. Michels, and C. E. Wilson. Machine Design, Theory and Practice, MacMillan, 1975.

7. Hoyt, S. L. ASME Handbook, Metals Properties, McGraw-Hill, 1954.

8. Ross, R. B. Metallic Materials Specification Handbook, E. & F.N. Spon, 1968.

9. Spots, M. F. Design of Machine Elements, Prentice-Hall, 1978.

10. Dudley, D. W. Handbook of Practical Gear Design, McGraw-Hill, 1984.

11. Buckingham, E. Manual of Gear Design, Section Two, Machinery, 1935.

12. Dudley, D. W. Gear Handbook, McGraw-Hill, 1962.

13. Beer, F. P. and E. R. Johnston. Mechanics of Materials, McGraw-Hill, 1981.

14. "1985 Electrical & Electronics Reference Issue," Machine Design, Vol. 57, No. 23, May 30, 1985.

15. Contraves Corporation. Personal Correspondence, 1986.

16. Tempest, M. C. "Air Lubricated Bearings," Bearings, Searching for a Longer Life, Mechanical Engineering, Oct. 17, 1984.

17. Masten Apex Ltd. Personal Correspondence, 1986.

18. Lakhtakia, A. Personal Correspondence, 1986.

19. Tse, F. S., I. E. Morse, and R. T. Hinkle. Mechanical Vibration, Theory and Application, Allyn and Bacon, 1978.

20. Hayek, S. I. Personal Correspondence, 1985.

21. Phelan, R. M. Fundamentals of Mechanical Design, McGraw-Hill, 1970.

22. "1984 Mechanical Drives Reference Issue," Machine Design, Vol. 56, No. 15, June 28, 1984.

23. Dayco Technical Center. Personal Correspondence, 1986.

24. Shigley, J. E. and L. D. Mitchell. Mechanical Engineering Design, 4th Edition, McGraw-Hill, 1983.

25. Ringfeder Corporation. Personal Correspondence, 1986.

26. Gunther, R. C. Lubrication, Chilton Book, 1971.

27. Blodgett, O. W. Design of Weldments, James F. Arc Welding Foundation. 1976.

28. Drago, R. J. and H. J. Nonemaker. "Gear Tooth Surface Fatigue Testing with Full Size Test Specimens," American Helicopter Society, October 1984.

APPENDIX A

Dayco V-Belt Drive

The following page provides the complete drawing of the driven pulley (pitch diameter of 2.25") of the Dayco belt-drive. The shop drawing was provided by the Browning Manufacturing Division of Emerson Electric Company (one of the distributors of Dayco produts). Appendix A also provides a schematic of the Dayco V-belt, and driver pulley and its matching bushing.

DRIVEN PULLEY

O D ECCENTRICITY .012 TIR
FACE RUNOUT .015 TIR

8 STD 36° 3V GROOVES

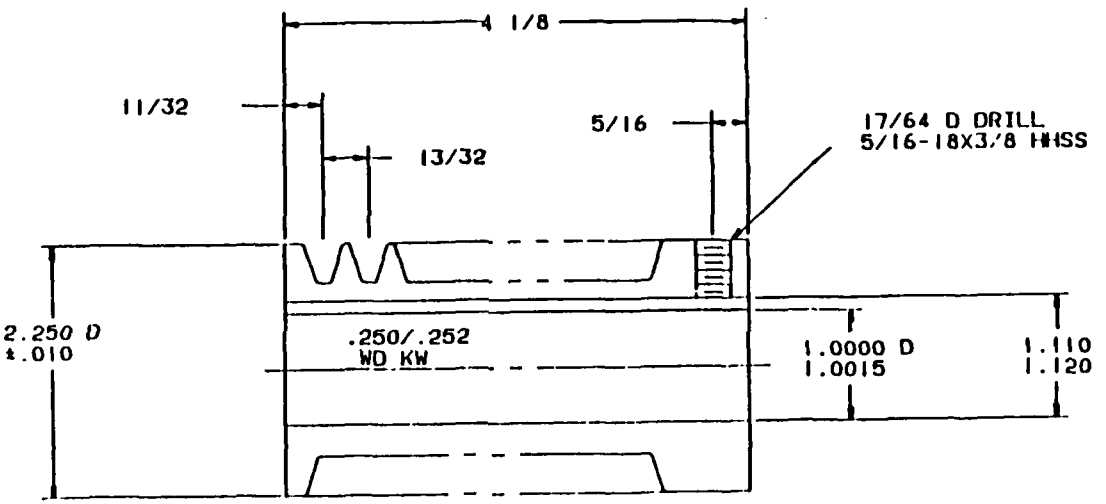

CAD DRAWING--NO MANUAL REVISIONS

MAT'L: 2 1/2 INCH BLOCK X 4 5/16 SAW LG	TOLERANCES UNLESS OTHERWISE SPECIFIED	DATE 7-9-86	A — — — —
	ANGLES ±1/2°	DRAWN DPW	LTR REVISION BY DATE
BALANCE: 1/4 OZ	FRACTIONS ±1/64	CHECK	BROWNING MANUFACTURING DIV. EMERSON ELECTRIC CO. MAYSVILLE, KENTUCKY U.S.A.
FINISH: STD GRAY	ONE PLACE DECIMAL ±.030	APPROVED	2.25 X 8 GR 3V X : SPCL SHEAVE
EST. RGH. WT.	TWO PLACE DECIMAL ±.010	DISTRIBUTION	PENN STATE UNIVERSITY
EST. FIN. WT. 2.6 LB	THREE PLACE DECIMAL ±.005		SCALE FULL SHEET OF
	DO NOT SCALE DRAWING		SK-0 '0986-'6 REV.

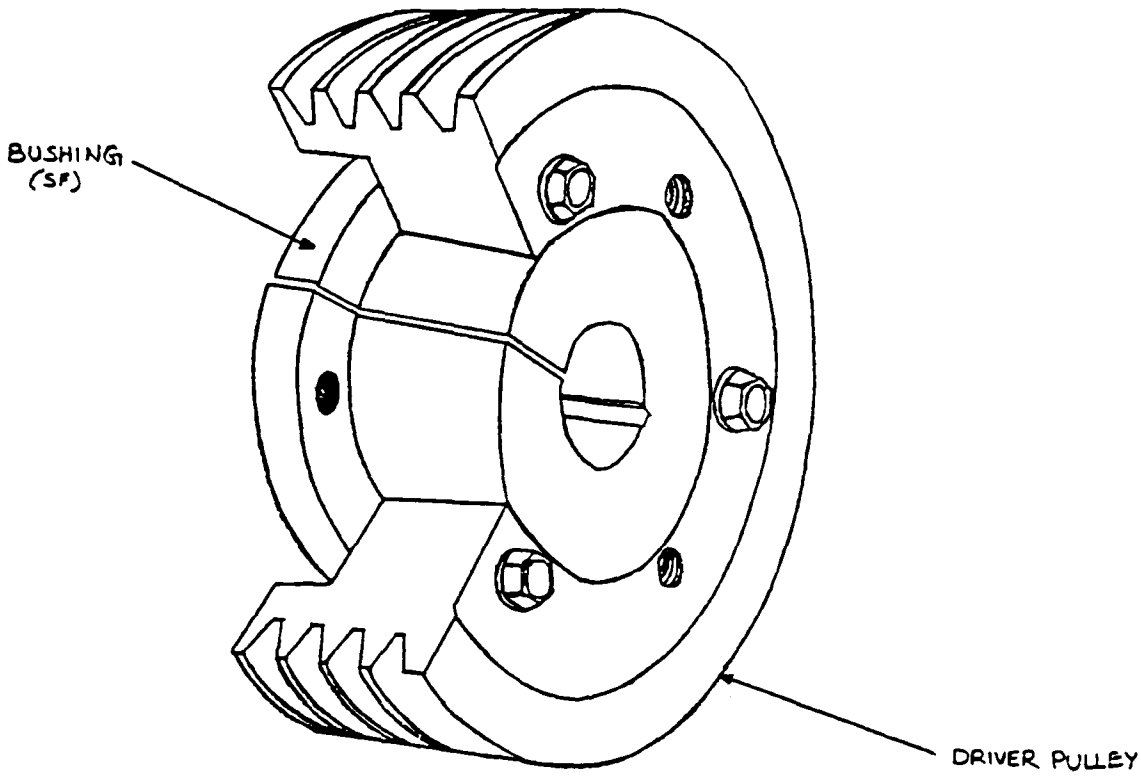

DAYCO POWER-WEDGE PULLEY

8 GROOVES FACE WIDTH = 3-17/32 inches			
PART NUMBER	OUTSIDE DIAMETER (inches)	BUSHING	WEIGHT (lbs) LESS BUSH.
8-3V80	8.0	SF	16.4

DAYCO SF BUSHING

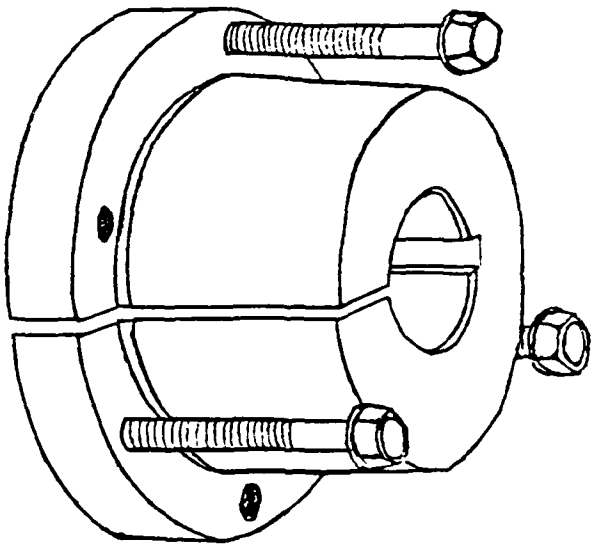

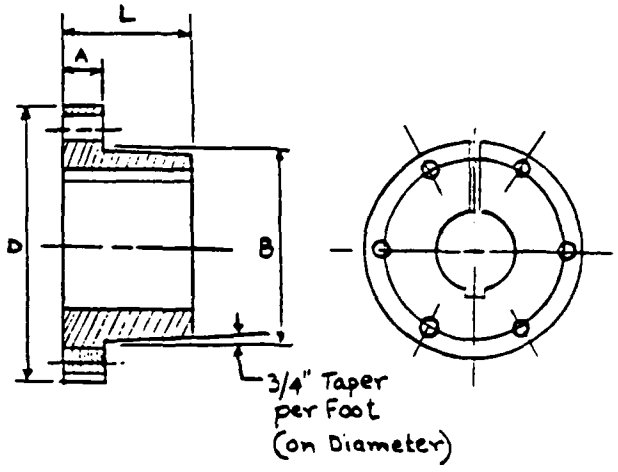

DIMENSIONS IN INCHES

A	B	D	L	BOLT CIRCLE DIAMETER (in)	WEIGHT RANGE (lbs)		NUMBER AND SIZE OF CAP SCREWS REQUIRED
					MAXIMUM BORE (in)	MINIMUM BORE (in)	
5/8	3 1/8	4 5/8	2 1/16	3.88	2.2	5.4	3 (3/8 x 2)

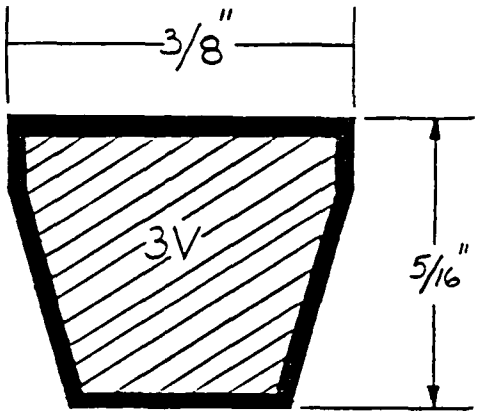

DAYCO POWER-WEDGE COGGED V-BELT

APPENDIX B

Gear Mount

This Appendix consists of the following:

1. Assembly drawings of the gear mount set-up,
2. The complete drawing of the clamp plate; and
3. The complete drawing of the bushing.

GEAR MOUNT

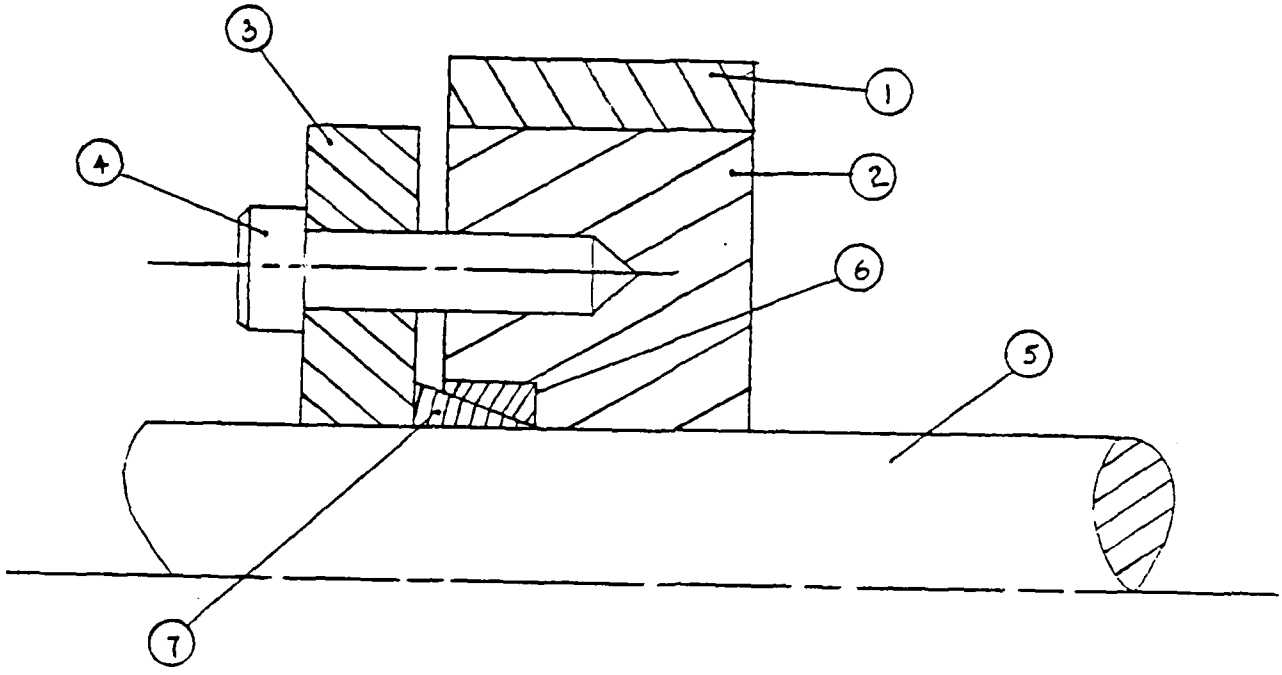

NO.	PART NAME	REQD.	MATERIAL
1	GEAR	—	9310 STEEL
2	BUSHING	1	1045 STEEL
3	CLAMP PLATE	1	1045 STEEL
4	SCREW	3	5/16"-18 UNC GR 8 HH.C.S
5	SHAFT	—	1045 STEEL
6	OUTER RING	1	ALUMINUM
7	INNER RING	1	ALUMINUM

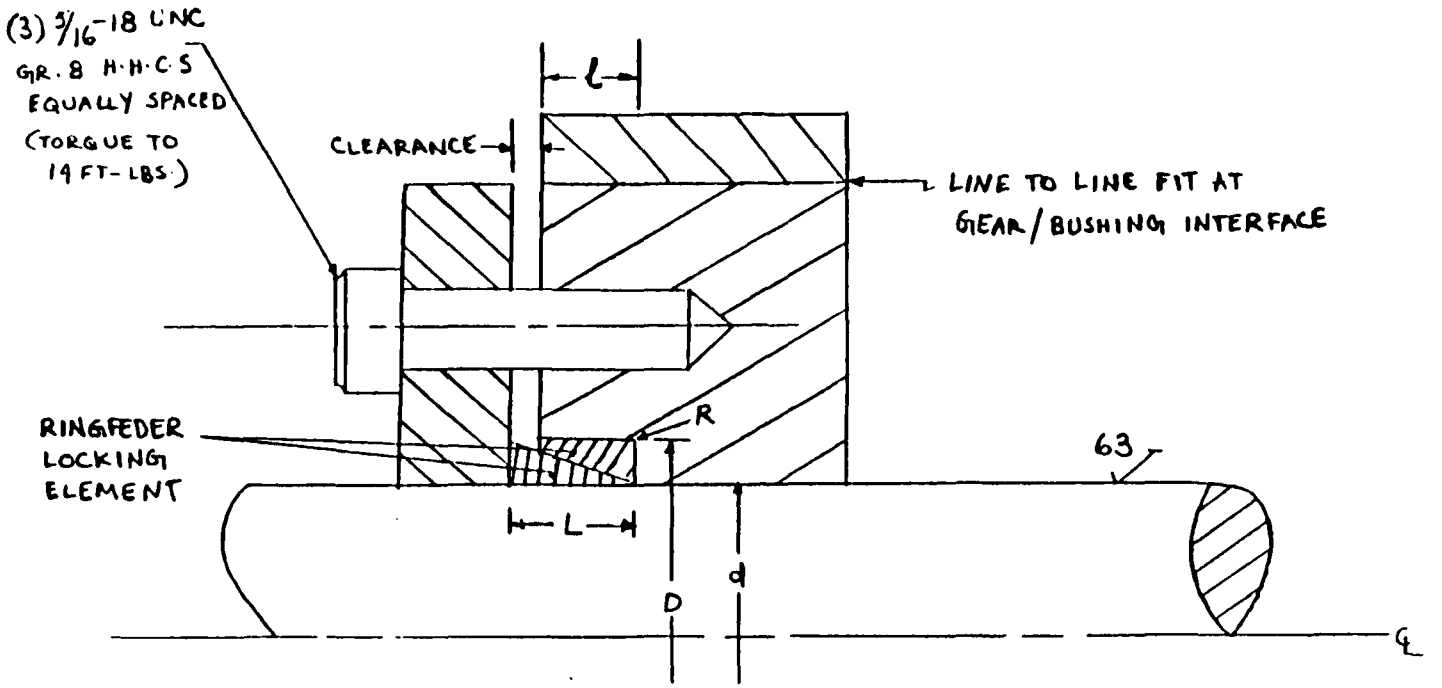

RINGFEDER LOCKING ELEMENT								
SIZE	d (in)	T_1 (in)	D (in)	T_2 (in)	L (in)	l (in)	R (in)	CLEARANCE (in)
GSA-1375	1.375	0 to -.002	1.687	-0 to +.002	0.426	0.376	0.004	0.05

NOTE: (1) d = shaft dia.

T_1 = machining tolerance for shaft (d)

D = counterbore dia.

T_2 = machining tolerance for counterbore (D)

L, l = width dimensions, relaxed state

R = radius of curvature of counterbore

(2) DRAWING NOT TO SCALE

(3) THE LOCKING ELEMENT REQUIRES A SHAFT FINISH OF 63 RMS

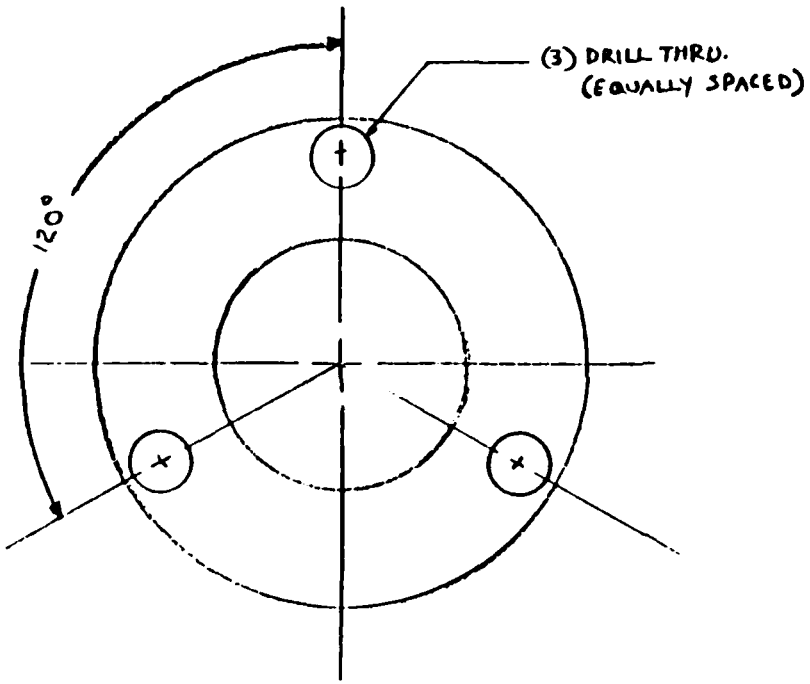

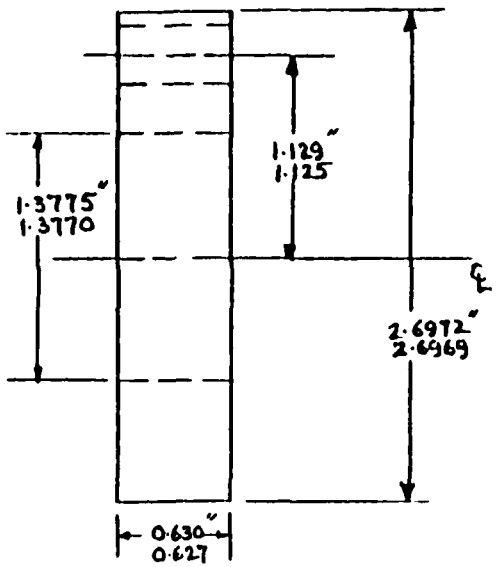

I MATERIAL : 1045 STEEL

II MAX. RUNOUT : 0.003"

TITLE : CLAMP PLATE
DRWG. NO: CP 400
SCALE : FULL
DRAWN BY : Santosh Vishwanath

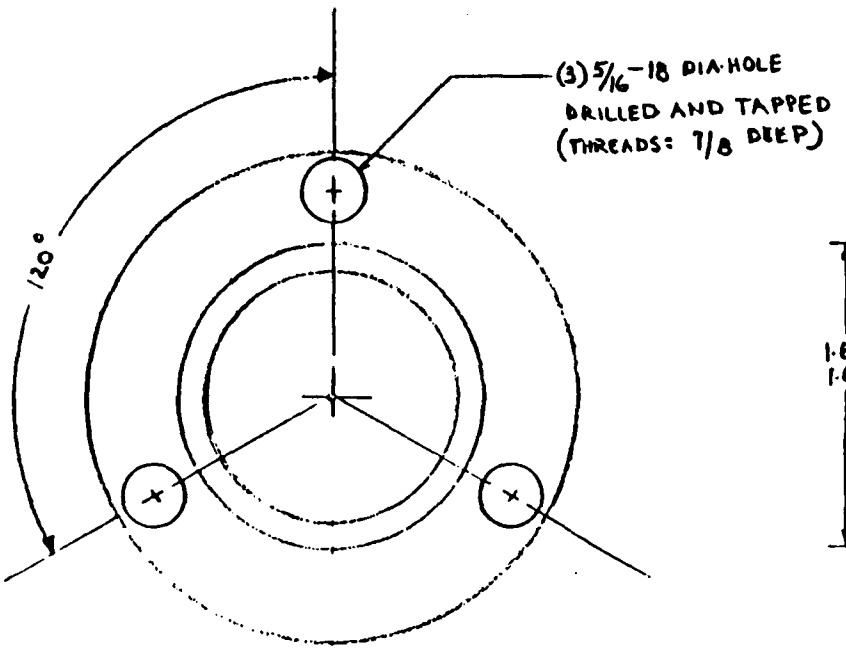

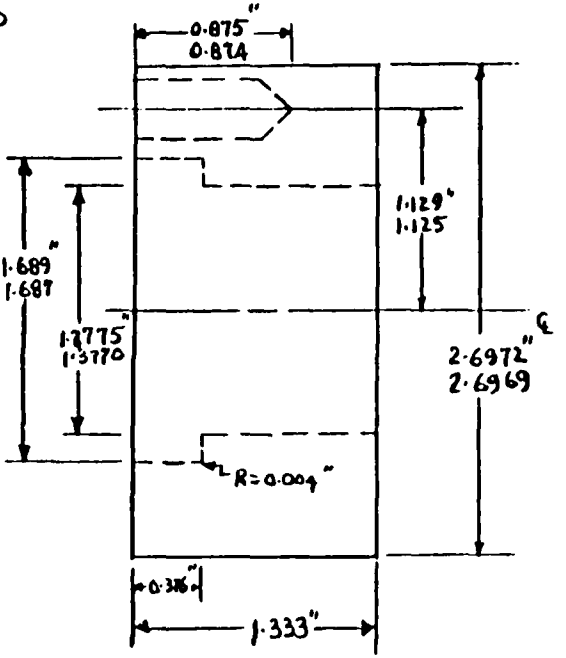

I MATERIAL : 1045 STEEL

II MAX. RUNOUT: 0.003"

TITLE :	BUSHING
DATE :	10/26/86
SCALE :	FULL
DRAWN :	Santosh Vilanilam

APPENDIX C

The Test and Drive Section Housing

The test and drive gears are housed in identical rectangular stainless steel (type 304 L) boxes. These gear boxes are a welded[1] fabrication and mounted on top of their respective steel bases via 1/4 in hexagonal bolts and dowel pins (to hold the boxes in alignment). To observe the gears, the test section housing incorporates plexiglass viewports through which the test gears can be inspected. The viewports also enable the application of non-intrusive electrooptical techniques such as Laser Interferometry and Laser Vibrometry. Each box is equipped with a spray nozzle and oil pan (to collect the spent oil). The oil pan is also a weld fabrication and is located at the base of the housing. The dimensions of the pan are such that it provides a snug fit.

As shown on the following pages, O-rings (1/4 in in diameter) are provided for each box so that the entrance of contaminants is precluded. The O-ring seals also prevent the sprayed oil from escaping the box. O-ring sealing is also found at all viewport locations. Here, the ring grooves are embedded in the plexiglass itself. It is recommended that a 1/8 in O-ring be used at all viewport locations. This Appendix provides the proper groove dimensions (for both the box and plexiglass cover) to hold the rings in place and ensure safe operation. At a later date, a special shaft seal material, that has a rubbing speed of 3240 fpm, will be selected. It is of vital importance that the seal material will not burn

[1]It is advised that inert gas shielded electric arc welding processes be used for best results as no fluxes are involved, thus reducing the danger of oxide trapping.

or get up to ignition temperature; since there will be oil fumes in the gear box and hence, the danger of explosion.

Appendix C also consists of the following:

1) The complete drawings of the test and drive section housing,
2) The complete drawings of the test and drive section oil pan,
3) The complete drawing of the plexiglass cover; and
4) The dowel pin dimensions.

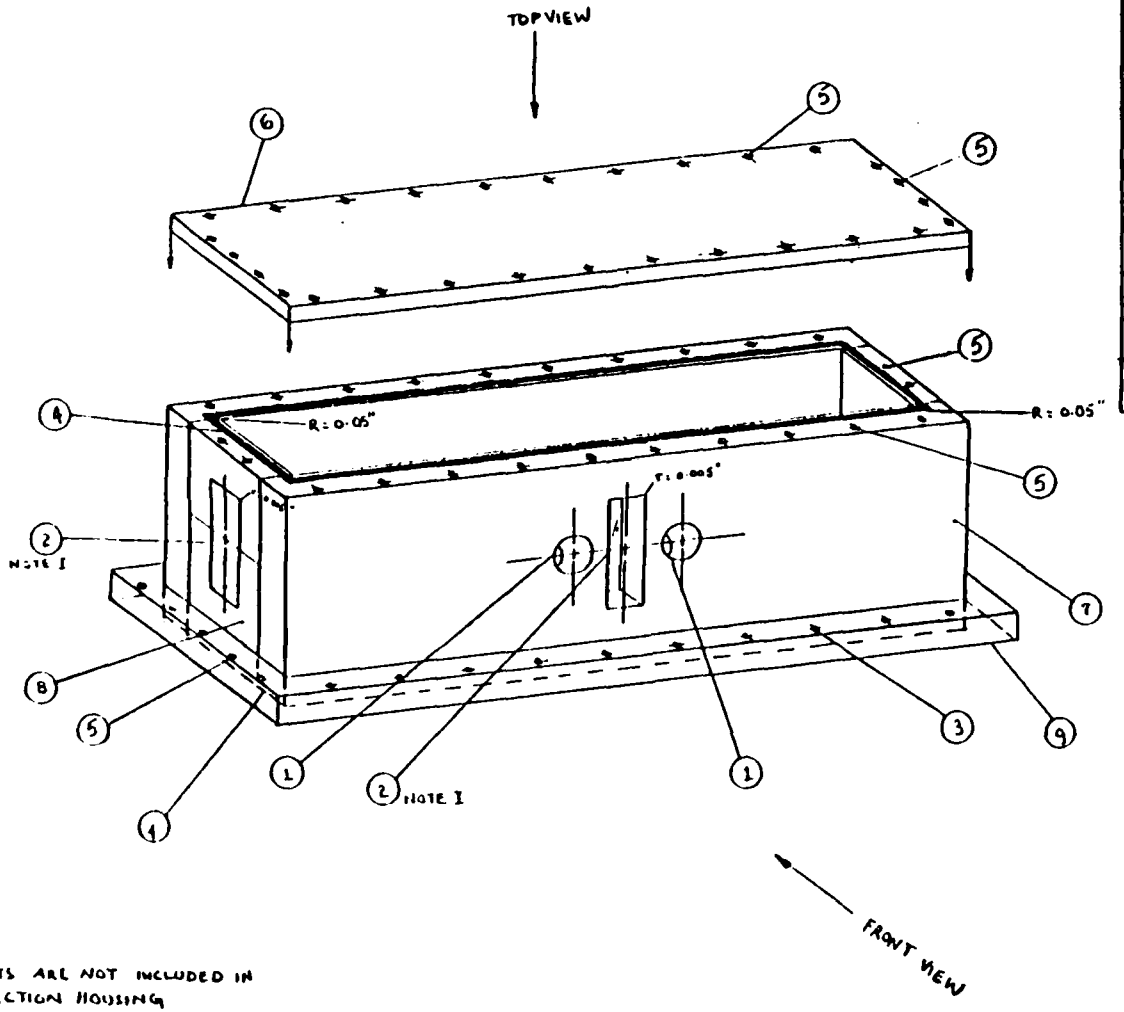

NO	PART	DRNG NO.
1	HOLE FOR SHAFT	—
2	VIEWPORT W/LEADED PLEXIGLASS COVERING	VP600
3	HOLE FOR DOWEL PINS	—
4	"O" RING GROOVE	OG200
5	HOLE FOR BOLTS	—
6	HOUSING COVER	HC100
7	SIDE PLATE	SP100
8	END PLATE	EP100
9	BASE PLATE	BP100

I THE VIEWPORTS ARE NOT INCLUDED IN THE DRIVE SECTION HOUSING

TITLE : DRIVE AND TEST SECTION HOUSING
SCALE : 1/4
MATERIAL : STAINLESS STEEL (TYPE 304L)
DATE : 10/12/86

TITLE:	HOUSING, COVER
SCALE:	1/2
MATERIAL:	304 L AISI STEEL
DATE:	10/17/96
DRAWN BY:	Santosh Vikanjam
DRWG. NO:	HC 100

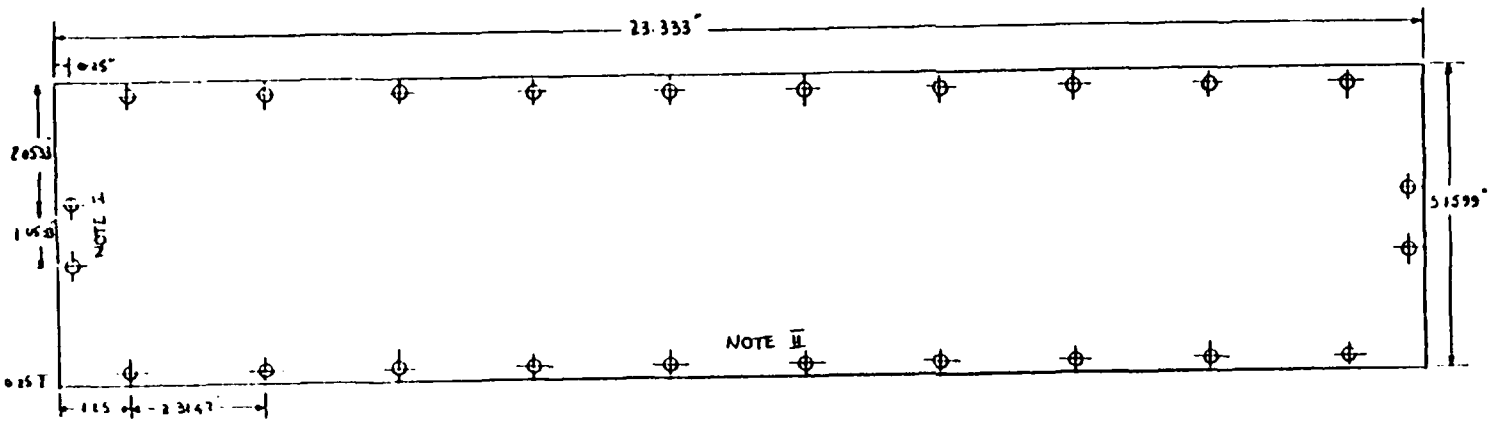

TOP VIEW

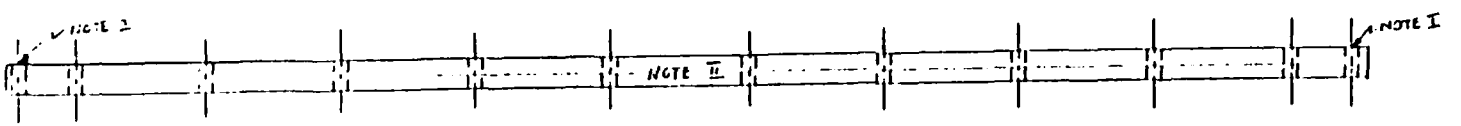

FRONT VIEW

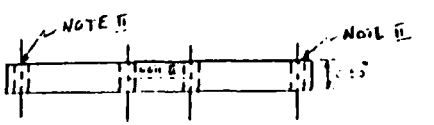

RIGHT SIDE VIEW

I HOLES FOR 1/4" REGULAR HEXAGONAL BOLTS, 1.0553" SPACING OF HOLES

II HOLES FOR 1/4" REGULAR HEXAGONAL BOLTS, 2.3147" SPACING OF HOLES

TITLE :	SIDE PLATE
SCALE :	1/2
MATERIAL :	304 L AISI STEEL
DATE :	10/17/86
DRAWN BY :	Santosh Kulkarni
DRWG NO :	SP 100

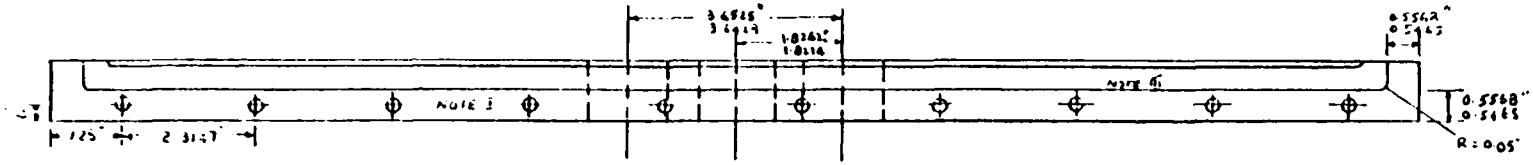

TOP VIEW

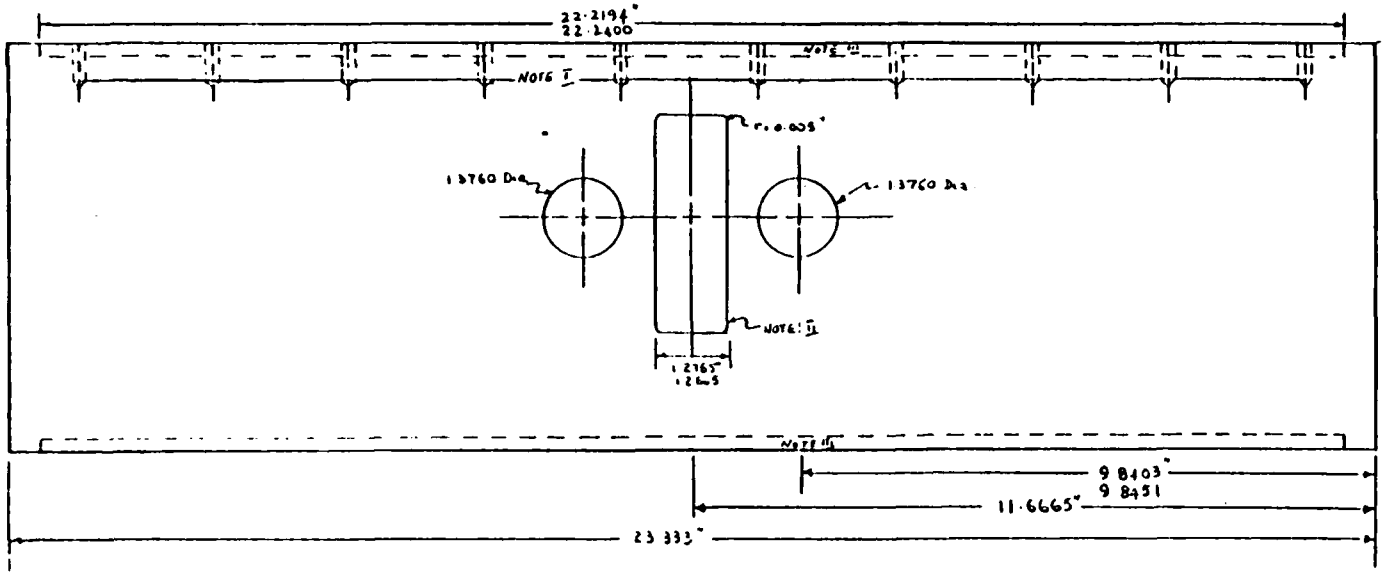

FRONT VIEW

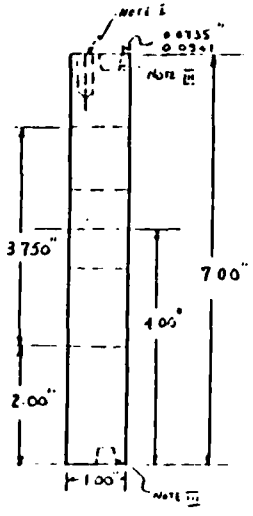

RIGHT SIDE VIEW

I 1/4" - 28 UNF - 2B, 3/4" DEPTH, 2.3147" SPACING OF HOLES

II VIEWPORTS ARE NOT INCLUDED IN THE DRIVE SECTION HOUSING

III "O" RING GROOVE (SEE SEPARATE SHEET FOR DIMENSIONS)

IV TOTAL OF 2 SUCH PLATES ARE REQUIRED

TITLE :	END PLATE
SCALE :	1/2
MATERIAL :	304L AISI STEEL
DATE :	10/17/86
DRAWN BY :	Santosh V. Lalam
DRWG NO :	EP 100

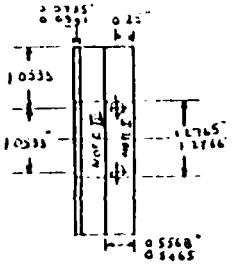

TOP VIEW

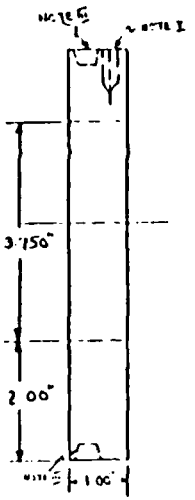

FRONT VIEW

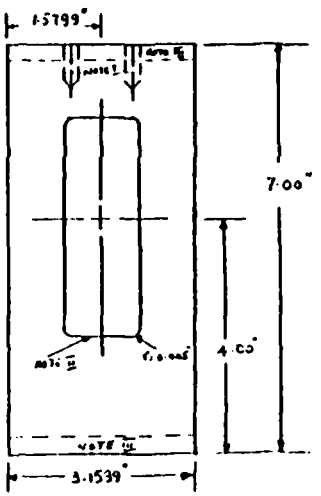

RIGHT SIDE VIEW

I 1/4" - 28 UNF - 2B, 3/4" DEPTH, 1.0533" SPACING OF HOLES

II VIEWPORTS ARE NOT INCLUDED IN THE DRIVE SECTION HOUSING

III "O" RING GROOVE (SEE SEPARATE SHEET FOR DIMENSIONS)

IV TOTAL OF 2 SUCH PLATES ARE REQUIRED

TITLE :	BASE PLATE
SCALE :	½
MATERIAL :	304 L AISI STEEL
DATE :	10/17/86
DRAWN BY :	Santosh Kilani/am
DRWG. NO :	BP 100

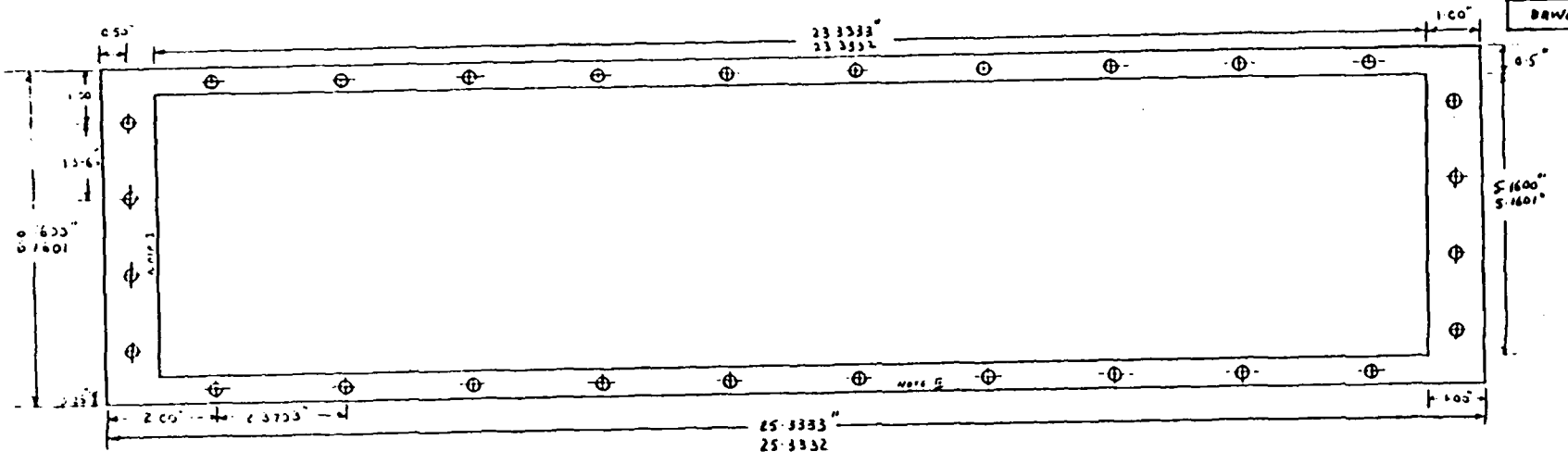

TOP VIEW

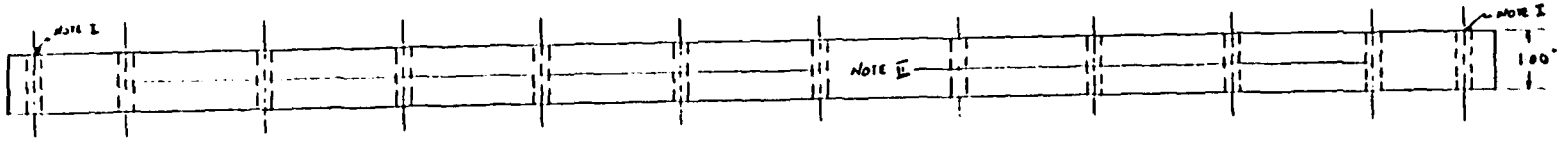

FRONT VIEW

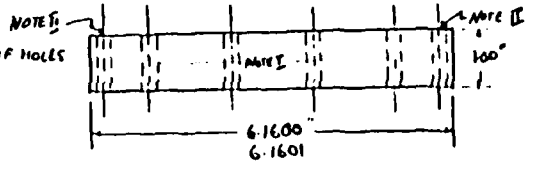

RIGHT SIDE VIEW

I HOLES FOR ¼" REGULAR HEXAGONAL BOLTS, 1.3966" SPACING OF HOLES

II HOLES FOR 1/4" DOWEL PINS, 2.3703" SPACING OF HOLES.

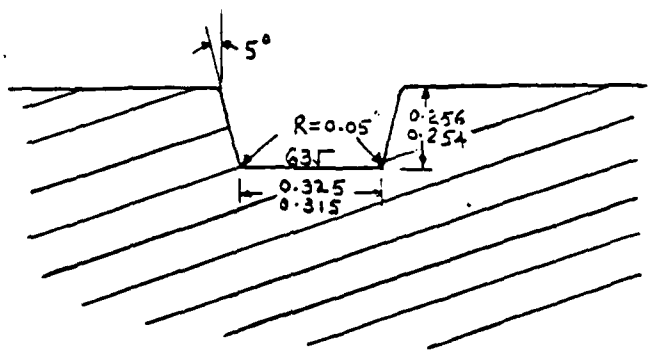

TITLE: "O" RING GROOVE DIMENSIONS FOR TEST AND DRIVE SECTION HOUSING
DATE: 10/12/96
DRAWN BY: Santosh Vijayalam
DRWG. NO: OG 200

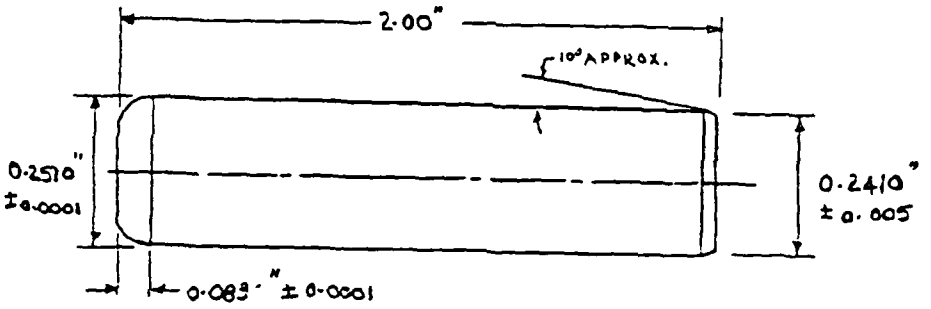

DOWEL PIN DIMENSIONS

TITLE : COVER FOR VIEW PORTS
SCALE : FULL
MATERIAL : LEADED PLEXIGLASS
DATE : 10/17/26
DRAWN BY : Santosh Yilanilam
DRWG. NO : VP 600

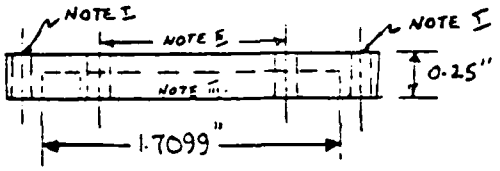

TOP VIEW

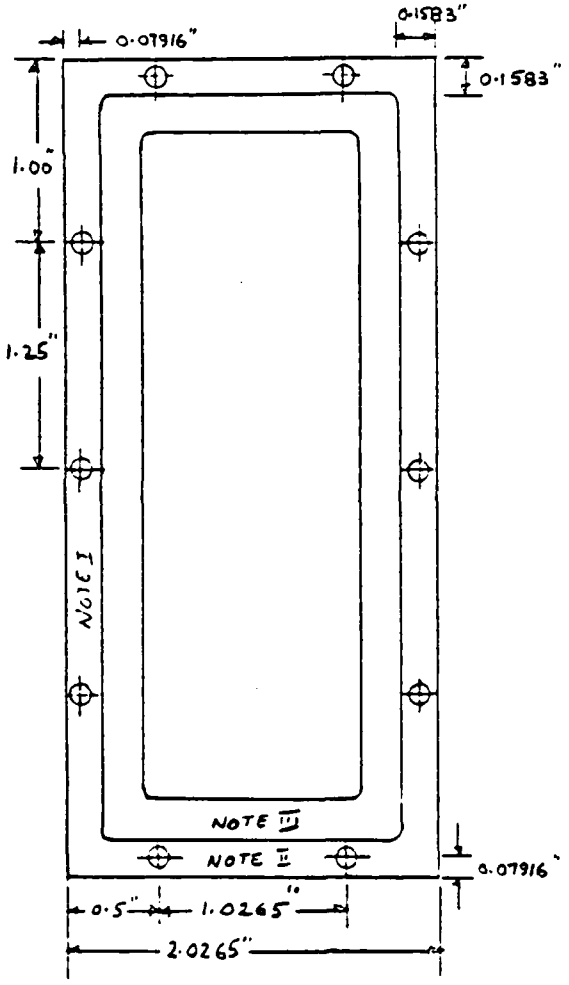

FRONT VIEW

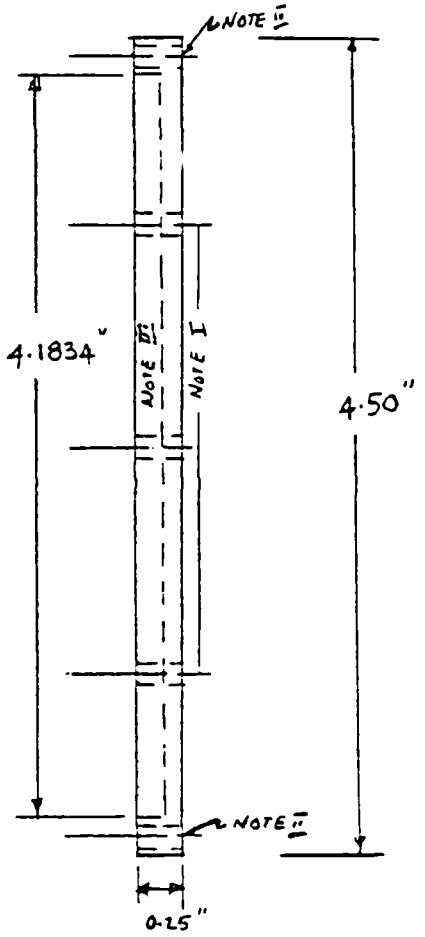

RIGHT SIDE VIEW

I. HOLES FOR 1/8" SCREWS, 1.25" SPACING OF HOLES

II. HOLES FOR 1/8" SCREWS, 1.0265" SPACING OF HOLES

III. "O" RING GROOVE (SEE SEPARATE SHEET FOR DIMENSIONS)

IV TOTAL OF 4 REQUIRED

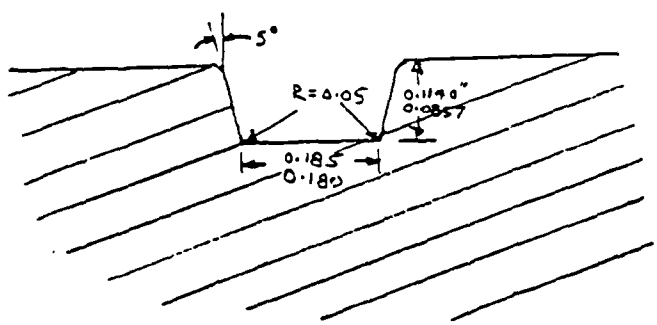

TITLE: "O" RING GROOVE DIMENSIONS FOR VIEWPORT COVERS
DATE: 10/17/80
DRAWN BY: Santosh Vilamilam
DRWG. NO: OG 600

NO	PART	DRW. NO.
1	SIDE PLATE	OPS500
2	END PLATE	OPE510
3	BASE PLATE	OPB500

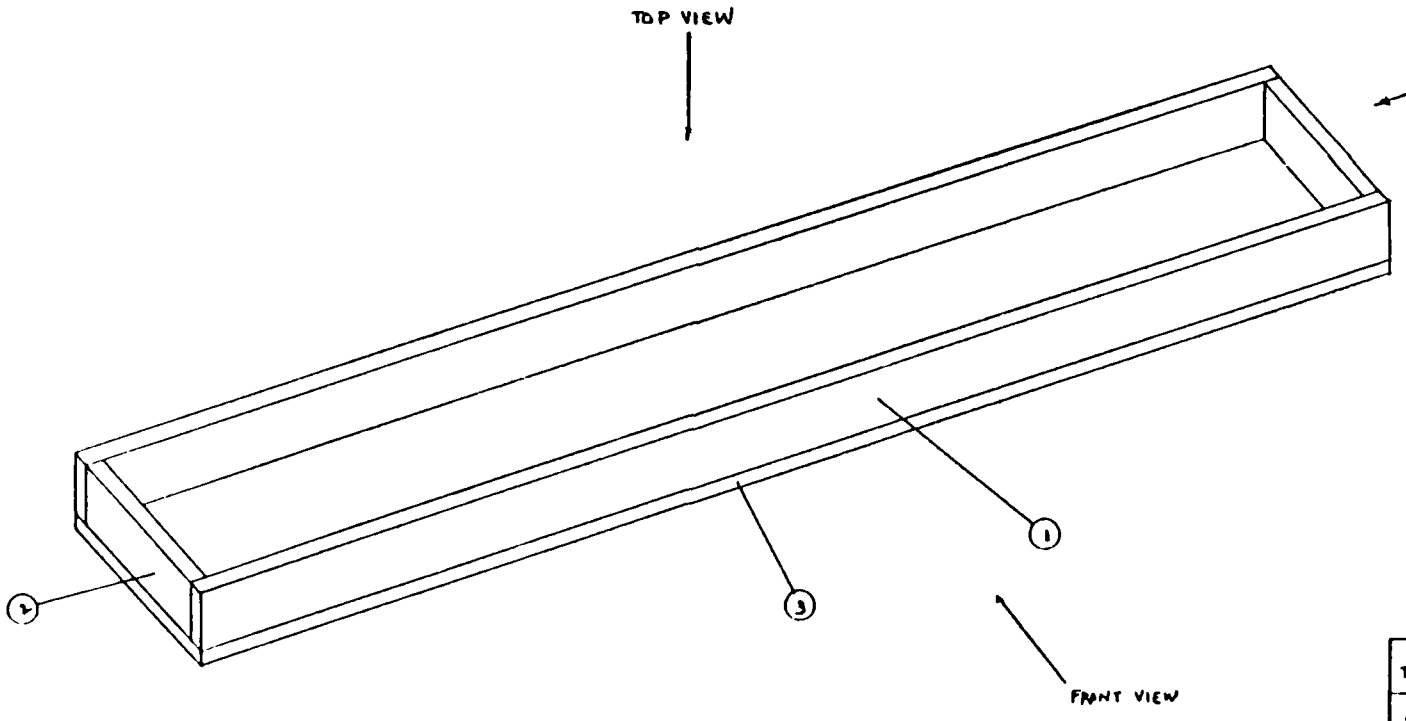

TITLE: DRIVE AND TEST SECTION OIL PAN	
SCALE: 1/2	
MATERIAL: ALUMINUM	
DRAWN BY: Sanjeet Vishwakarma	

TITLE : SIDE PLATE
SCALE : 1/2
MATERIAL : ALUMINUM
DATE : 10/17/86
DRAWN BY: Santosh Vilvanilam
DRWG NO: 015 500

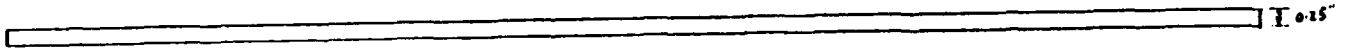

TOP VIEW

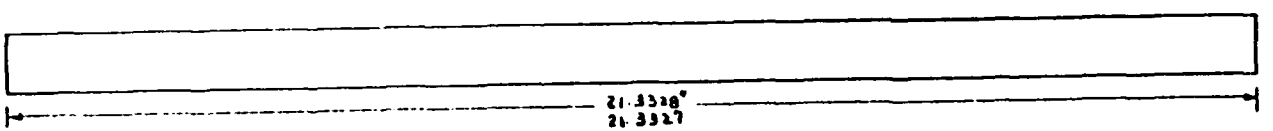

FRONT VIEW

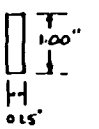

RIGHT SIDE VIEW

NOTE : TOTAL OF 2 SUCH PLATES ARE REQUIRED

TITLE : END PLATE (OIL PAN)
SCALE : 1/1
MATERIAL : ALUMINUM
DATE : 10/17/86
DRAWN BY : Santosh Vilas Jam
DRWG. NO : OPE 500

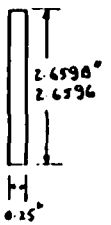

TOP VIEW

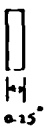

FRONT VIEW

RIGHT SIDE VIEW

NOTE : TOTAL OF 2 SUCH PLATES ARE REQUIRED

TITLE : BASE PLATE (OIL PAN)
SCALE : Y_L
MATERIAL : ALUMINUM
DATE : 10/17/86
DRAWN BY : Santosh Vilgaikam
DRWG. NO : OPB 500

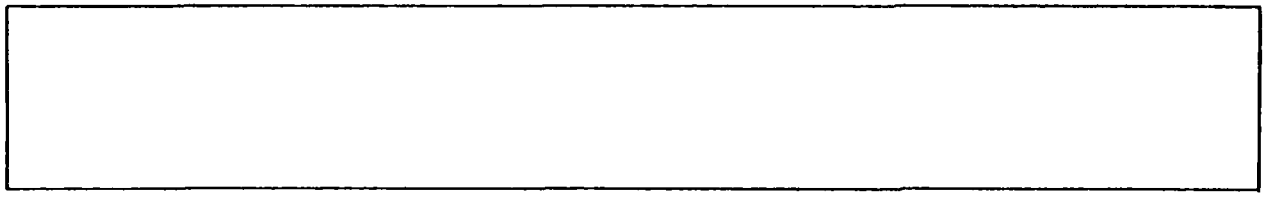

TOP VIEW

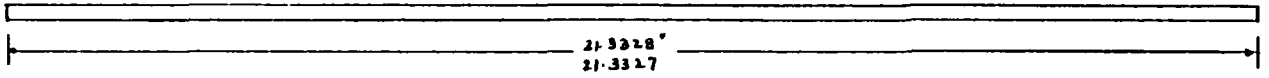

FRONT VIEW

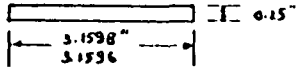

RIGHT SIDE VIEW

APPENDIX D

The Drive and Test Section Stand

The Drive Section Stand

The drive section stand is a fabricated steel frame structure that is designated to support all of the components of the drive section, including the drive motor, drive pulley and belt assembly, and gear casing. Also mounted on top of the support frame structure are the components of the pressure-spray lubrication system (with the exception of the test section spray nozzle) and air bearing accessories, such as, the air compressor and air tank. The steel stand itself is mounted on vibration isolation pads to reduce any cross influence between the stand and other stands within the laboratory.

The drive section stand is a 97 x 61 x 25 in steel stand consisting of parallel wide flange beams which are separated by four cross members that contribute to the total resistance to deflection. The cross members are equally spaced and welded to the beams. Furthermore, rectangular steel plates are welded and bolted to the beams to improve torsional resistance. The drive section stand is designed to accommodate a net load of 5000 lbs (the total weight of the components that make up the drive section is far below this value). Following the procedures outlined in reference 27 the corresponding lateral and torsional deflection of the stand are 0.0096 inches and 0.00177 degrees, respectively. The torsional deflection of the stand was calculated without considering the welded steel plates. The torsional rigidity of the stand is much higher when the beams are boxed in.

Test Section Stand

The test section stand is also a fabricated steel frame structure and supports the test section components. Since, only the test gear box is mounted on top of the stand, the test stand is much smaller than the drive stand. Here again, the stand is mounted on isolation pads to eliminate or reduce cross talk between the stand and other stands within the laboratory. The test stand was also designed to accommodate the proposed electrooptical techniques.

The design of the test stand is very much parallel to the drive stand. It is a 49 x 37 x 25 in steel stand and is composed of parallel W beams and steel cross members. Alike the drive stand, the beams are boxed in for torsional rigidity. The test stand employs W beams of the same designation as the drive stand to support the imposed load. As a result, it was possible to design the stand to accommodate 5000 lbs (the net weight of the test section components is way below this value). The corresponding lateral and torsional deflection of the stand are 0.0048 inches and 0.00177 degrees (not considering the welded plates), respectively.

Leveling Stand for Both Drive and Test Stand

The leveling stand is a welded fabrication that is bolted to the side plates of both the drive and test stand. It was specially designed to accommodate the selected vibration mount shown on the following page. As shown, the spring type mount consists of an all-thread, dual nut, and neoprene acoustical pad. By adjusting the nut it is possible to level the stands to the desired specification and hence, reduce shaft angular and

VIBRATION ELIMINATOR MOUNT

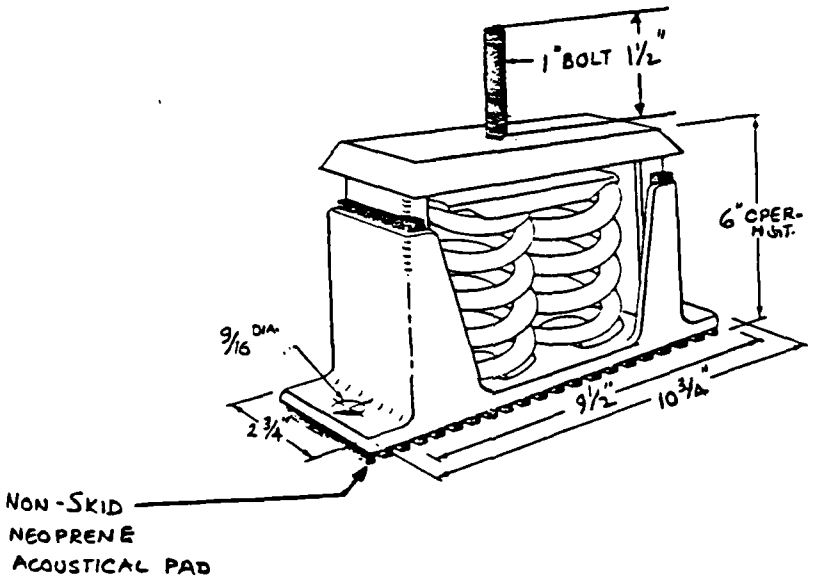

parallel misalignment. This particular mount is designed to support 6000 lbs. The corresponding lateral deflection of the spring is one inch.

The complete drawings of the test and drive section stand and leveling stand are provided in this Appendix. Also provided are the dimensions of the wide flange beam.

NO	PART	DRWG NO.
1	WIDE FLANGE BEAM	W100
2	END PLATE	EP200
3	SIDE PLATE	SP200
4	TOP PLATE	TP200
5	CROSS MEMBER	CM300
6	LEVELING STAND	LS400
7	ALL THREAD	—
8	ISOLATION PAD	—
9.	DUAL NUT	—

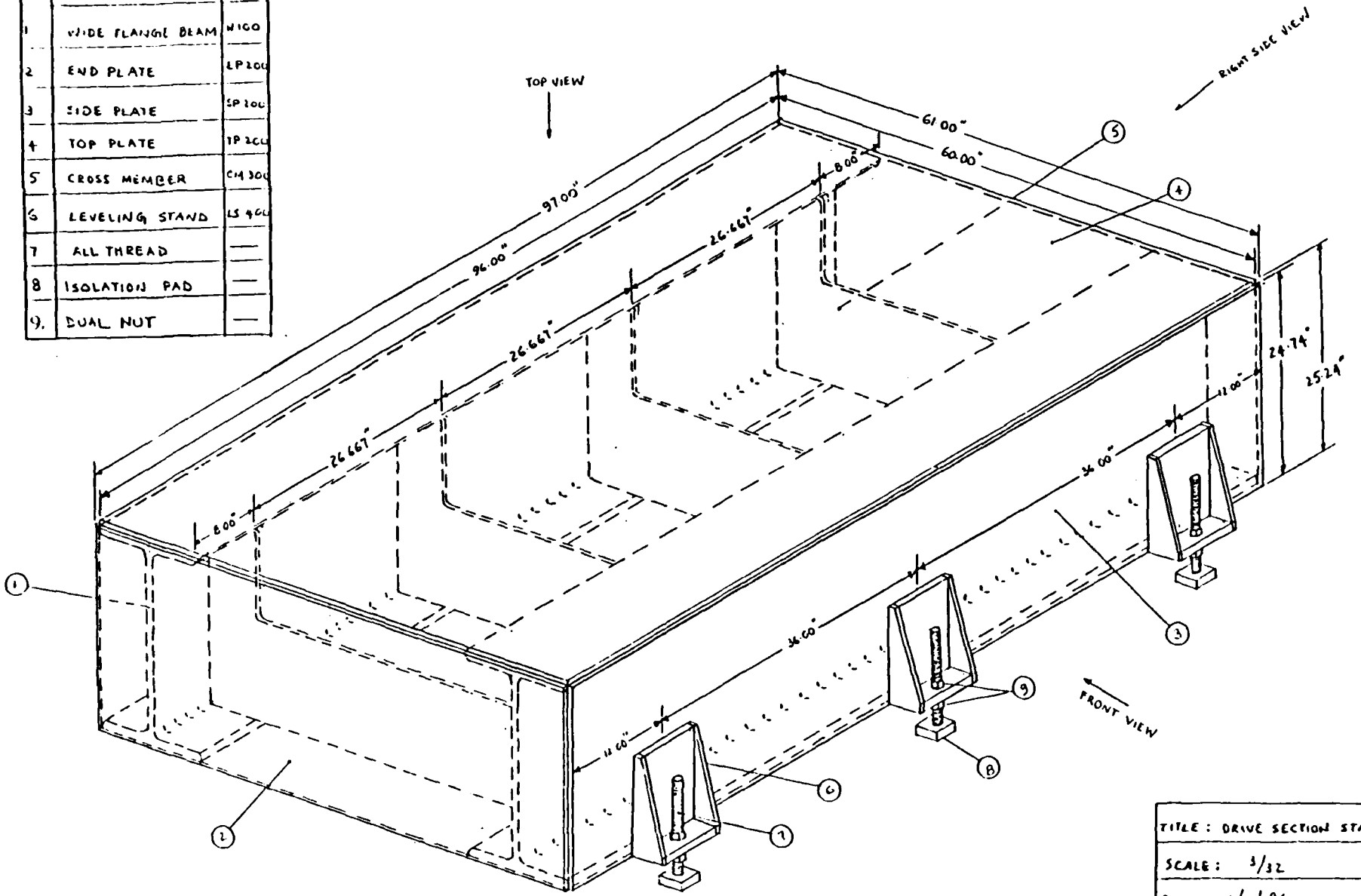

TITLE :	DRIVE SECTION STAND
SCALE :	3/32
DATE :	11/1/86
DRAWN BY :	Santosh Vilvanathan

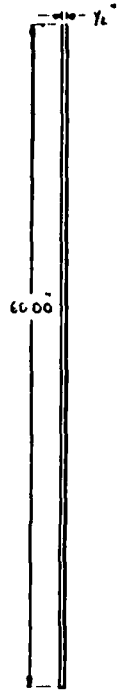

TOP VIEW

FRONT VIEW

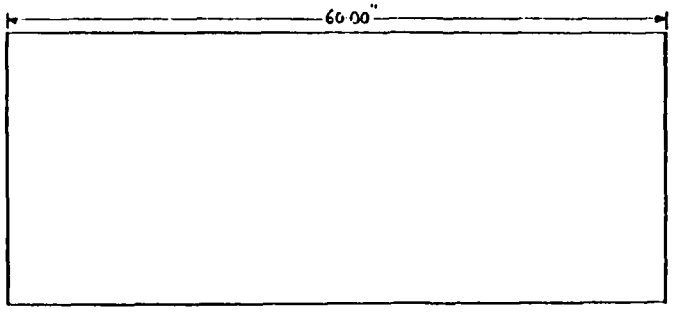

RIGHT SIDE VIEW

I. TOTAL OF 2 SUCH PLATES ARE REQD.

II. THESE PLATES ARE TO BE WELDED TO THE W. BEAMS

III. MATERIAL: CARBON STEEL

TITLE :	END PLATE (D.S. STAIR)
SCALE :	3/32
DATE :	11/2/96
DRAWN BY :	Santosh Vishwakarma
DRWG. NO :	EP 200

148

I. HOLES ARE ½" IN DIA. AND ½" IN DEPTH.

II. MATERIAL: CARBON STEEL

III. TOTAL OF 2 SUCH PLATES ARE REQD.

IV. THESE PLATES ARE TO BE WELDED TO THE W BEAMS.

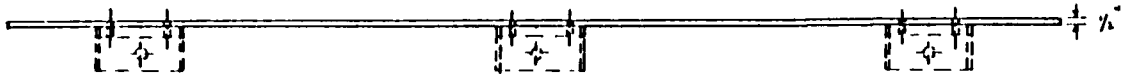

TOP VIEW

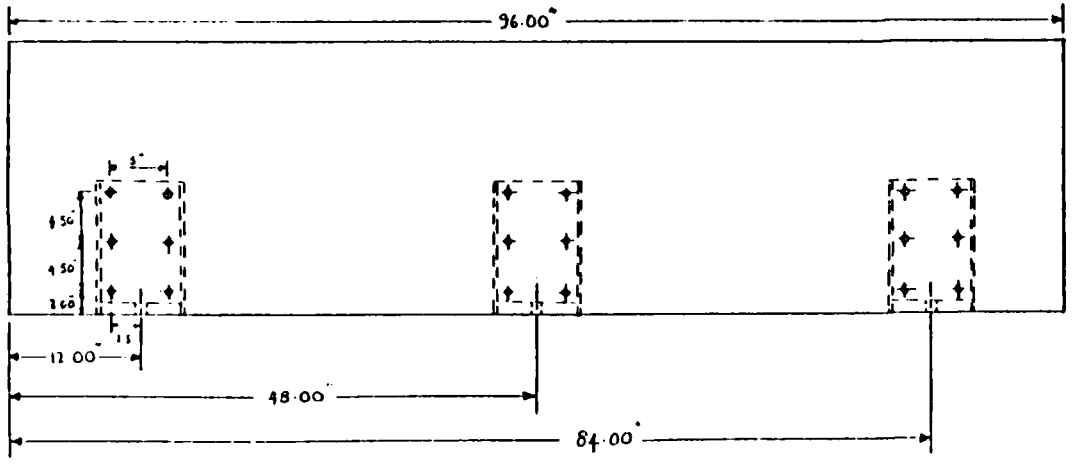

FRONT VIEW

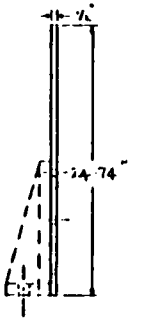

RIGHT SIDE VIEW

TITLE: SIDE PLATE (D.S. STAND)	
SCALE: 3/32	
DATE: 11/2/86	
DRAWN BY: Santos I. Vilgailgan	
DRWG. NO.: SP 200	

TITLE: TOP PLATE (D.S. STAND)	
SCALE: 3/32	
DATE: 11/2/86	
DRAWN BY: Santosh Vilavilam	
DRWG. NO: TP 200	

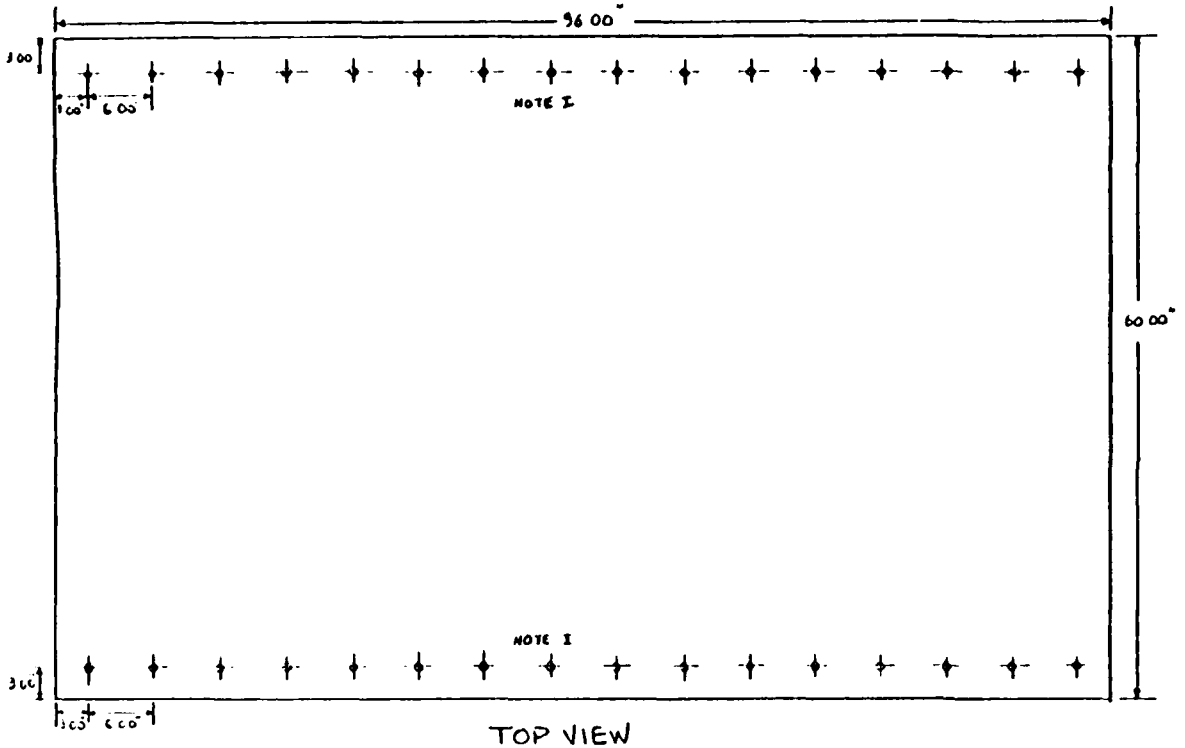

TOP VIEW

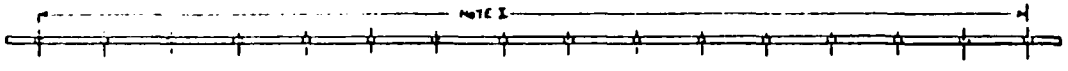

FRONT VIEW

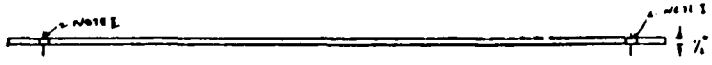

RIGHT SIDE VIEW

I. HOLES FOR ½" BOLTS, 6.00" SPACING OF HOLES.

II. MATERIAL: CARBON STEEL

III. THIS PLATE IS TO BE BOLTED TO W BEAMS.

TITLE: CROSS MEMBER
SCALE: 1/8
DATE: 11/3/86
DRAWN BY: Santosh Vilaniam
DRWG. NO: CM 300

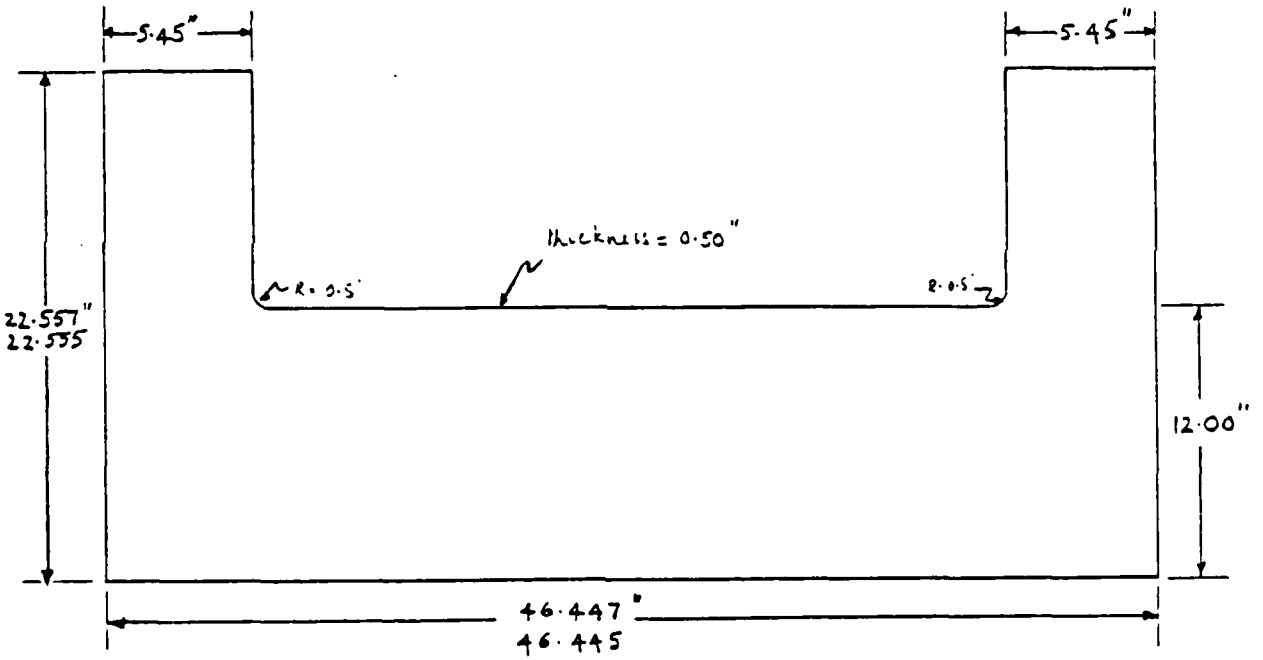

I. 4 SUCH PLATES ARE REQD.

II. THESE PLATES ARE TO BE WELDED TO THE W BEAMS

III. MATERIAL: CARBON STEEL

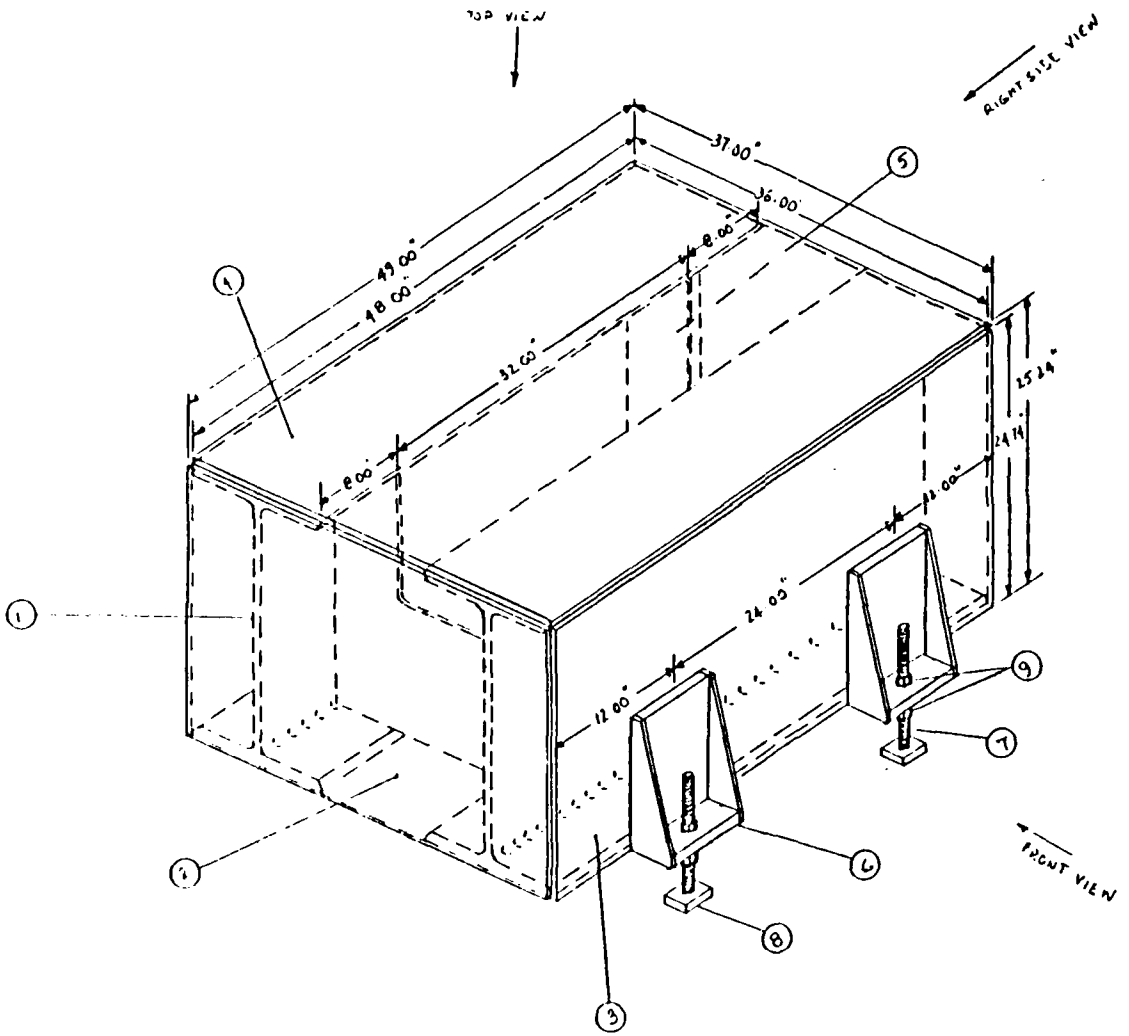

NO	PART	DRWG NO.
1	WIDE FLANGE BEAM	W100
2	END PLATE	EP300
3	SIDE PLATE	SP300
4	TOP PLATE	TP300
5	CROSS MEMBER	CM400
6	LEVELING STAND	LS400
7	ALL THREAD	—
8	ISOLATION PAD	—
9	DUAL NUT	—

TITLE : TEST SECTION STAND

SCALE : 3/32

DATE : 11/3/30

DRAWN BY : Sanford Vaughn

152

TITLE: END PLATE (T.S. STAND)
SCALE: 3/32
DATE: 11/4/86
DRAWN BY: Santosh Vilamjam
DRWG. NO.: EP 300

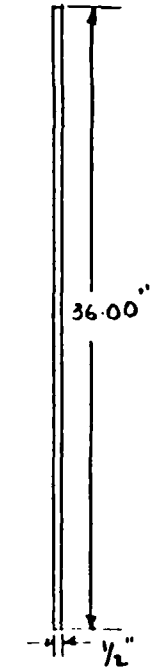

TOP VIEW

I. TOTAL OF 2 SUCH PLATES ARE REQD.

II. THESE PLATES ARE TO BE WELDED TO THE W BEAMS.

III. MATERIAL: CARBON STEEL

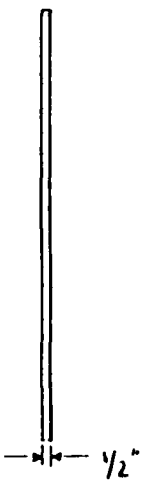

FRONT VIEW

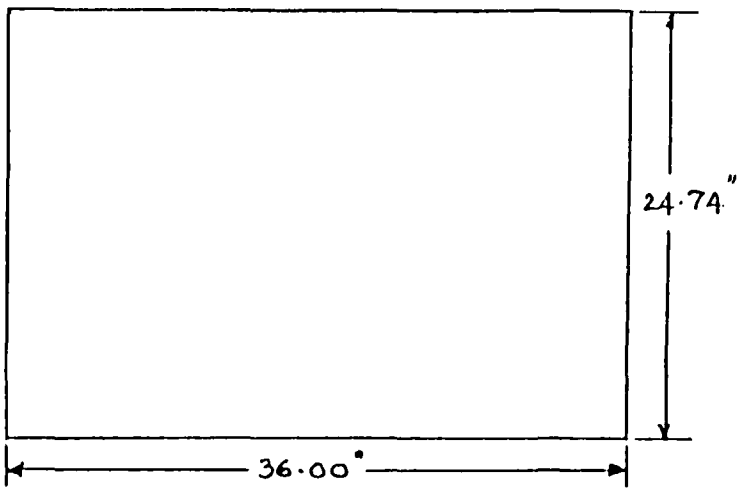

RIGHT SIDE VIEW

TITLE : SIDE PLATE (T.S. STAND)
SCALE : 3/32
DATE : 11/4/86
DRAWN BY : Santosh Vilani/Com
DRWG. NO: SP 300

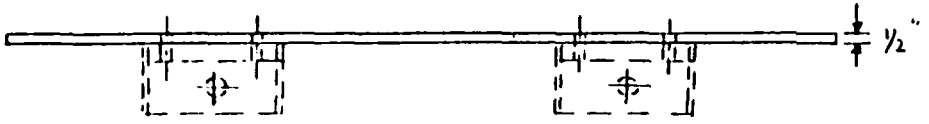

TOP VIEW

I. HOLES ARE ½" IN DIA. AND ½" IN DEPTH

II. MATERIAL : CARBON STEEL

III. TOTAL OF 2 SUCH PLATES ARE REQD.

IV. THESE PLATES ARE TO BE WELDED TO THE W BEAMS

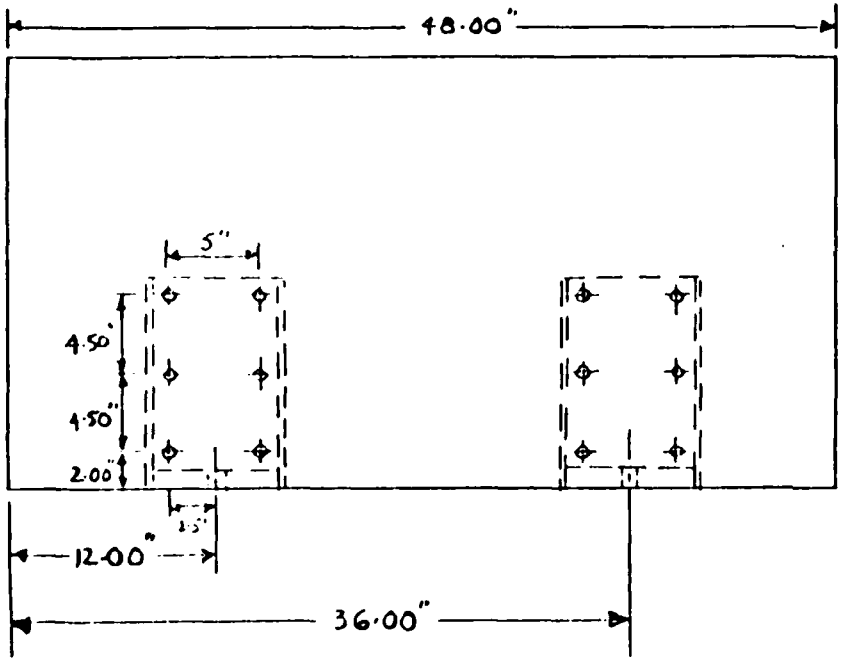

FRONT VIEW

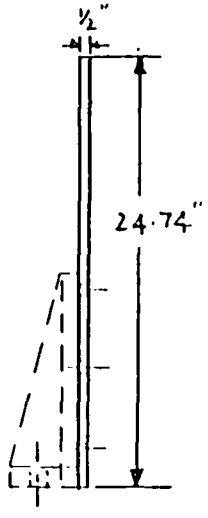

RIGHT SIDE VIEW

TITLE : TOP PLATE (T.S. STAND)
SCALE : 3/32
DATE : 11/4/86
DRAWN BY : Santosh Vilvanilam
DRWG. NO: TP 300

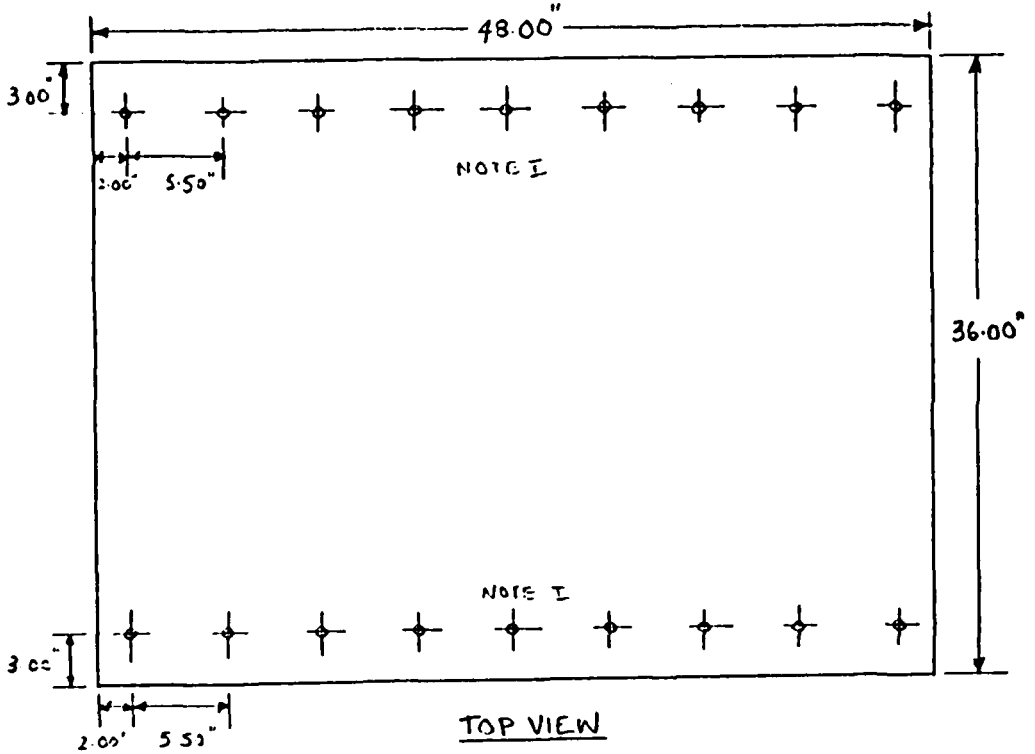

TOP VIEW

I. HOLES FOR ½" BOLTS, 5.50" SPACING OF HOLES

II. MATERIAL : CARBON STEEL

III. THIS PLATE IS TO BOLTED TO THE W BEAMS

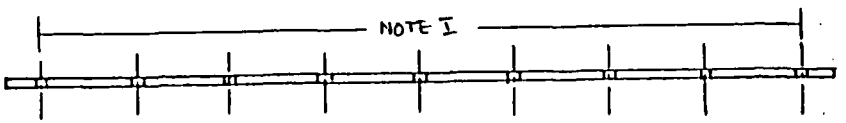

FRONT VIEW

RIGHT SIDE VIEW

TITLE: CROSS MEMBER
SCALE: 1/8
DATE: 11/4/86
DRAWN BY: Santosh Vijayakumar
DRWG. NO: CM 400

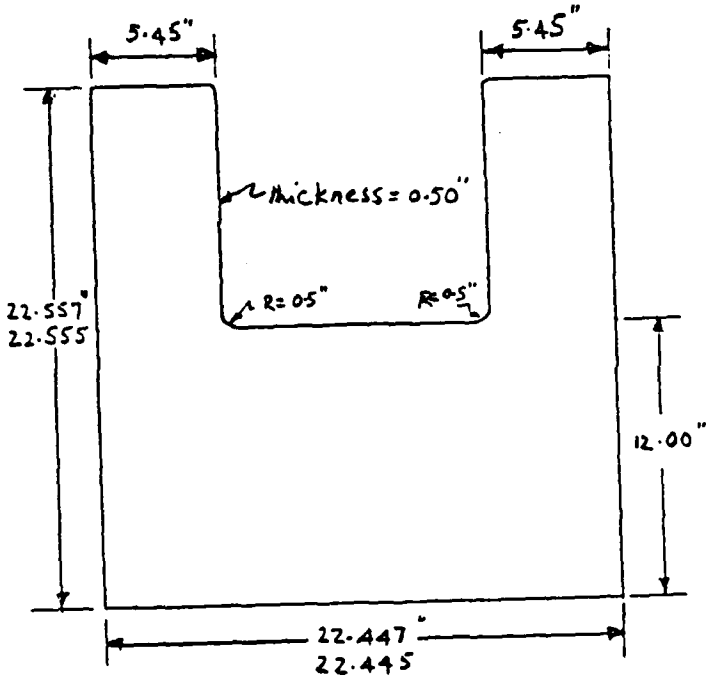

I. 2 SUCH PLATES ARE REQD.

II. THESE PATES ARE TO BE WELDED TO THE W BEAMS

III. MATERIAL: CARBON STEEL

TITLE: WIDE FLANGE BEAM
SCALE: 1/8
DATE: 11/2/86
DRAWN BY: Sa-tosh Kilam/am
DRWG NO: W100

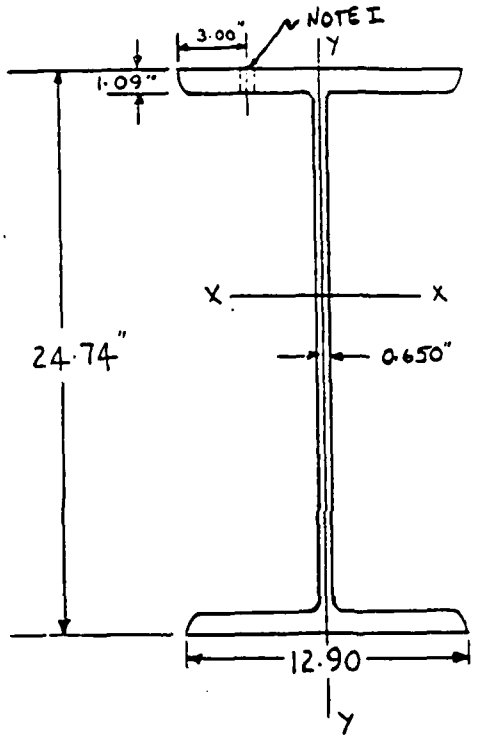

$I_x = 5630\ in^4$

$I_y = 443\ in^4$

AREA = 42.79 in^2

I. HOLE FOR 1/2" BOLT

II. DESIGNATION : W 27 x 46

III. TWO SUCH BEAMS ARE REQD. FOR EACH STAND.

IV. FOR BEAM 2, THE 1/2" HOLE SHOULD BE DRILLED 3" FROM THE FAR RIGHT OF FLANGE

V. LENGTH OF BEAM (DRIVE SECTION) : 96.00"
" " " (TEST SECTION) : 48.00"

NO.	PART	DRWG. NO.
1	BASE PLATE	LSCCO
2	SIDE PLATE	"
3	MID PLATE	"
4	HOLES FOR 1/2" BOLTS	—
5	HOLE FOR 1" ALL THREAD	—

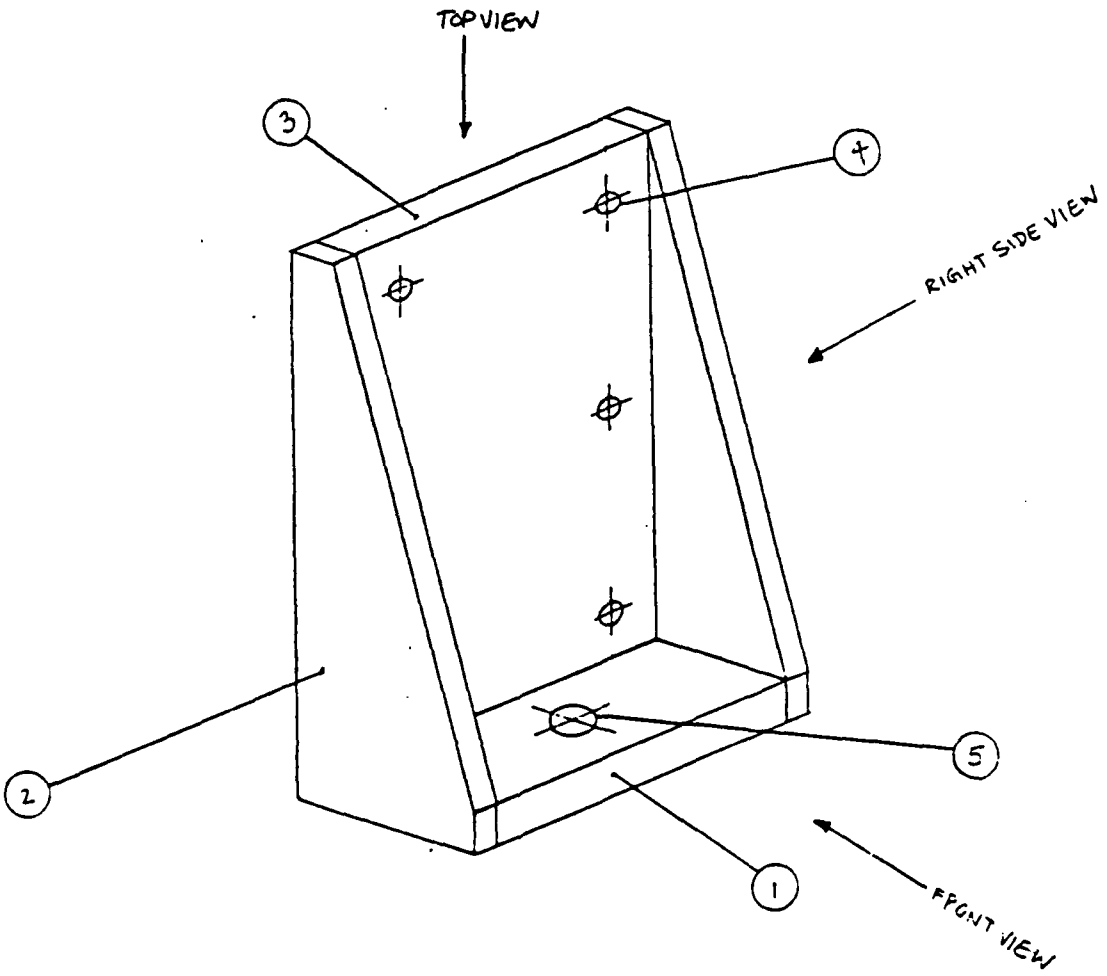

NOTE: TOTAL OF 6 SUCH STANDS ARE REQD. FOR DRIVE SECTION STAND AND A TOTAL OF 4 SUCH STANDS ARE REQD. FOR TEST SECTION STAND

TITLE : LEVELING STAND FOR DRIVE AND TEST STAND
SCALE : 1/4
DATE : 11/2/85
DRAWN BY: Santosh Vemuganti

TITLE: BASE PLATE
SCALE: 1/4
DATE: 11/12/86
DRAWN BY: Santosh Vilamilam
DRWG NO: LS 400

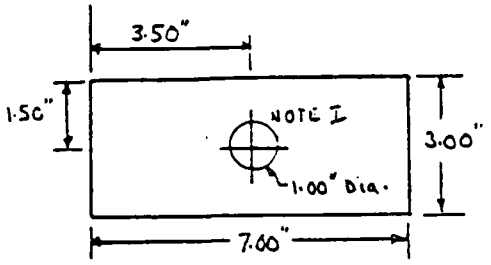

TOP VIEW

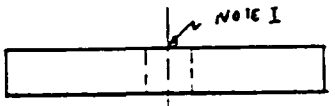

FRONT VIEW

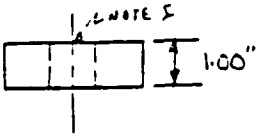

RIGHT SIDE VIEW

I. THREADED HOLE FOR 1" ALL THREAD

II. MATERIAL - CARBON STEEL

TITLE: SIDE PLATE
SCALE: 1/4
DATE: 11/2/86
DRAWN BY: Santosh Yelamanchi
DRWG. NO: LS400

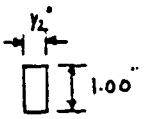

TOP VIEW

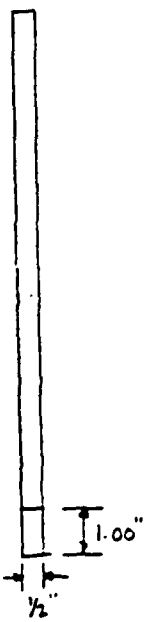

FRONT VIEW

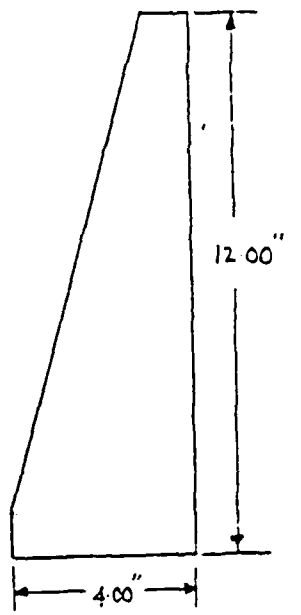

RIGHT SIDE VIEW

I. MATERIAL: CARBON STEEL

II. TWO SUCH PLATES ARE REQD.

TITLE : M.C PLATE
SCALE : 1/4
DATE : 11/2/36
DRAWN BY : Santosh Vijayan
DRWG NO: LS 400

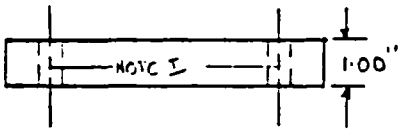

TOP VIEW

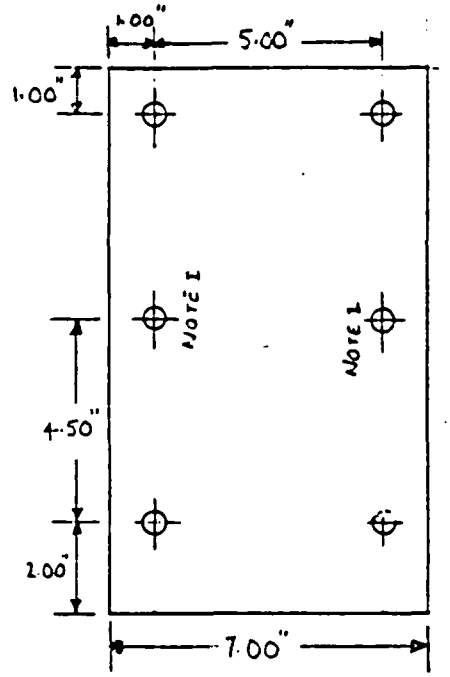

FRONT VIEW

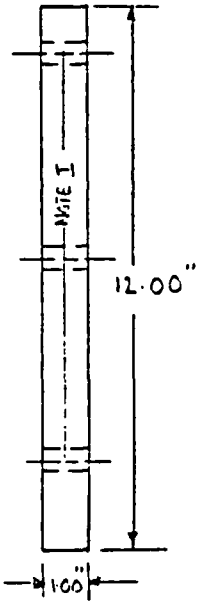

RIGHTSIDE VIEW

I. HOLES FOR 1/2" BOLTS, 4.50" SPACING OF HOLES

II. MATERIAL: CARBON STEEL

APPENDIX E

Block Diagram

This Appendix consists of block diagrams showing the locations of test and drive section components on top of their respective steel stands.

TITLE: BLOCK DIAGRAM SHOWING LOCATIONS OF TEST SECTION COMPONENTS
SCALE: 3/32
DATE: 11/4/86
DRAWN BY: Santosh Vikaiyam

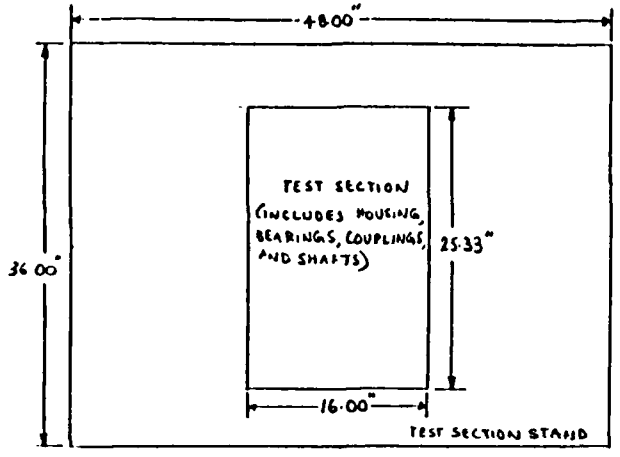

TOP VIEW

TITLE:	BLOCK DIAGRAM SHOWING LOCATIONS OF TEST SECTION COMPONENTS
SCALE:	3/32
DATE:	11/4/86
DRAWN BY:	Santosh Vijaniam

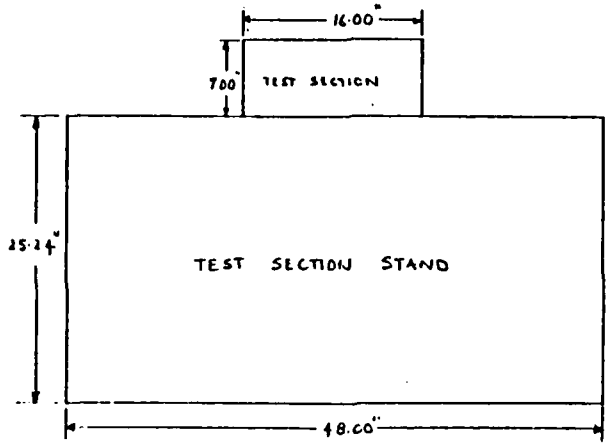

FRONT VIEW

TITLE:	BLOCK DIAGRAM SHOWING LOCATIONS OF DRIVE SECTION COMPONENTS
SCALE:	3/32
DATE:	11/4/86
DRAWN BY:	Santosh Vilanilam

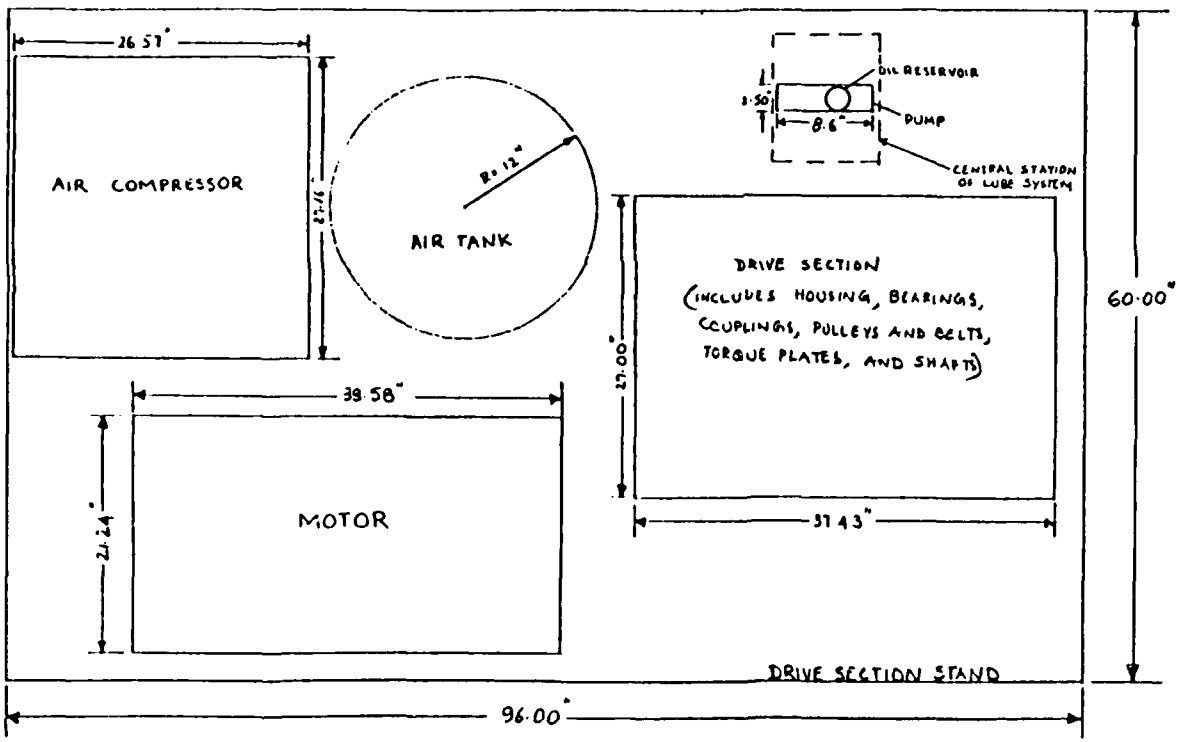

TOP VIEW

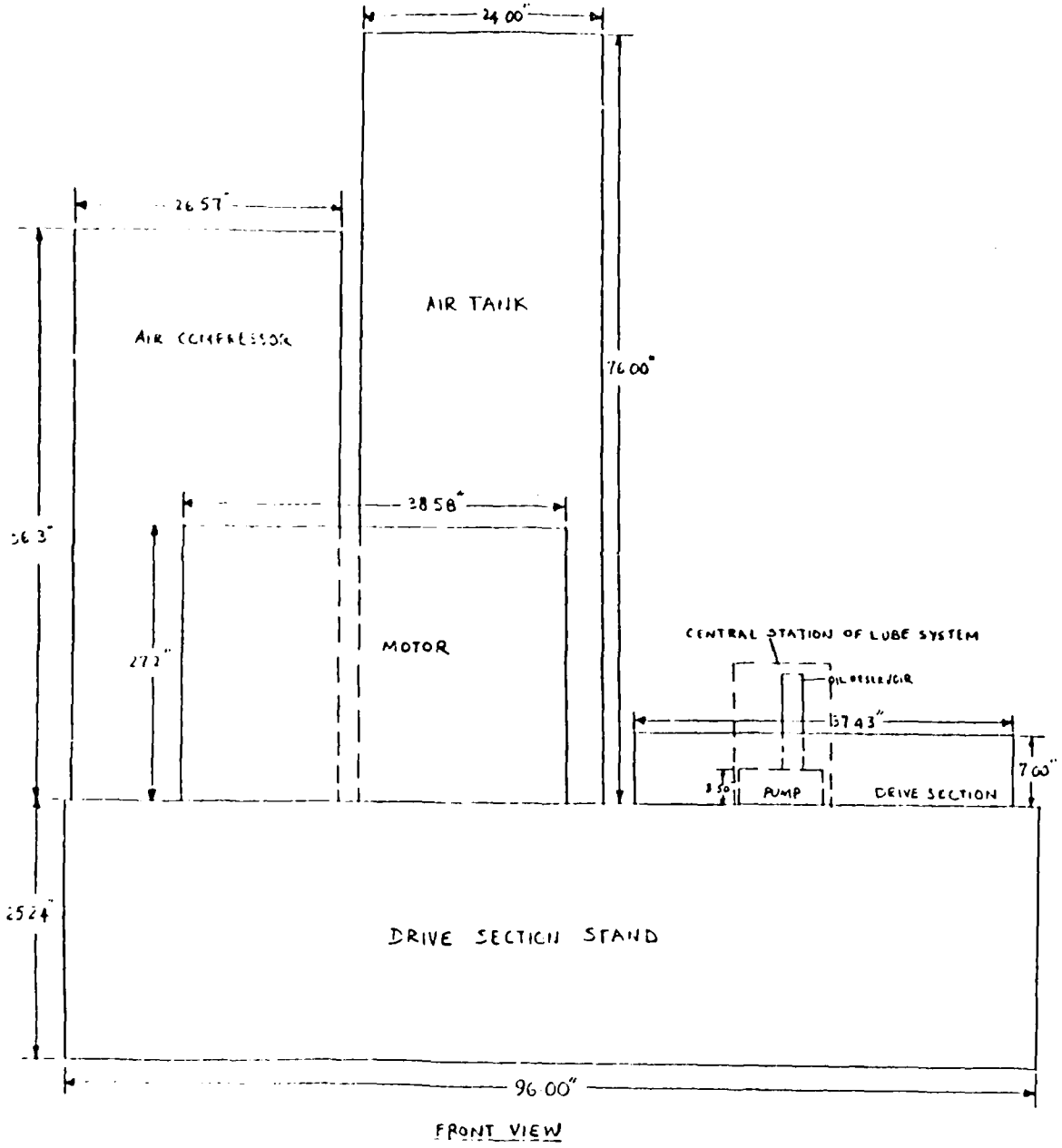

TITLE: BLOCK DIAGRAM SHOWING LOCATIONS OF DRIVE SECTION COMPONENTS
SCALE: 3/32
DATE: 11/4/86
DRAWN BY: Santosh Vilgnilam

END

8-87

DTIC